

Dissertation for Doctor of Philosophy

Compressed Sensing for Support Set Reconstruction:
Information-Theoretic Results and Design of Practical Algorithm

Sangjun Park

School of Electrical Engineering and Computer Science

Gwangju Institute of Science and Technology

2019

박 사 학 위 논 문

압축 센싱을 위한 서포터 셋 복원: 정보
이론적 결과 및 복원 알고리즘 설계

박 상 준

전 기 전 자 컴 퓨 터 공 학 부

광 주 과 학 기 술 원

2019

Compressed Sensing for Support Set Reconstruction: Information-Theoretic Results and Design of Practical Algorithm

Advisor: Heung-No Lee

by

Sangjun Park

School of Electrical Engineering and Computer Science
Gwangju Institute of Science and Technology

A thesis submitted to the faculty of the Gwangju Institute of Science and Technology in partial fulfillment of the requirements for the degree of Doctor of Philosophy in the School of Electrical Engineering and Computer Science

Gwangju, Republic of Korea

May 31, 2019

Approved by



Professor Heung-No Lee

Committee Chair

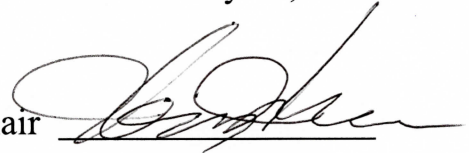
Compressed Sensing for Support Set Reconstruction: Information-Theoretic Results and Design of Practical Algorithm

Sangjun Park

Accepted in partial fulfillment of the requirements
for the degree of Doctor of Philosophy

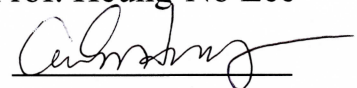
May 31, 2019

Committee Chair



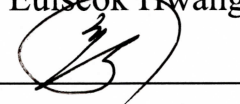
Prof. Heung-No Lee

Committee Member



Prof. Euseok Hwang

Committee Member



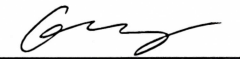
Prof. Jong Won Shin

Committee Member



Dr. Seung-Hun Oh

Committee Member



Prof. Gongguo Tang

Ph.D/EC Sangjun Park, Compressed sensing for support set reconstruction: information-theoretic
20094025 results and design of practical algorithm, School of Electrical Engineering and Computer
Science, 2019. 75p. Advisor: Prof. Heung-No Lee

Abstract

Compressed Sensing (CS) is a new signal acquisition and reconstruction framework which has attracted lots of interests in both the signal processing and the information theory communities. This framework promises to compressively sample a sparse signal via random linear projections at a rate below the Shannon-Nyquist rate, and also indicates this sparse signal can be reliably reconstructed from its compressed samples.

The signal acquisition can be easily done by only conducting matrix-vector multiplications. In contrast, the signal reconstruction can be complicated because the model of the acquisition is an under-determined linear system. However, if the support set of an original sparse vector, i.e., a set of indices corresponding to the nonzero elements in this sparse vector, is given, this under-determined linear system becomes an over-determined system, implying that the signal reconstruction can be easily done using traditional least square methods. Thus, there have been not only several information-theoretic works regarding necessary and sufficient conditions to reliably reconstruct this support set but also several algorithms to reconstruct the support set in practice.

As CS has been applied into various applications such as wireless sensor network (WSN) and magnetic resonance imaging (MRI), the signals of interests are modeled to be jointly sparse vectors, implying that the signals share a single support set. There are two different approaches for sampling these signals. The

first model is called multiple measurement vectors (MMV) with the same sensing matrix in which all of sparse signals are measured via the same sensing matrix. The second model is called MMV with different sensing matrices where different sensing matrices are used to sample each sparse signal. There have been information-theoretic works for MMV with the same sensing matrix in the presence of noise. In contrast, for MMV with different sensing matrices, the information-theoretic work has been only conducted in the absence of noise.

This dissertation mainly focuses on not only an information-theoretic study for a reliable support set reconstruction but also a derivation of a practical algorithm which can reconstruct support set with large variables. In the first part, we aim to provide information-theoretic results regarding the reliable support set reconstruction under noisy MMV with different sensing matrices. We begin to define a decoder, extended from a joint typical decoder proposed in the work of Akcakaya and Tarokh, and define a failure probability that the defined decoder fails to reconstruct the support set. Using mathematical tools such as the Fano's inequality and the Chernoff bound, we develop upper and lower bounds of this failure probability in terms of the sparsity, the ambient dimension, the minimum signal-to-noise ratio, the number of measurement vectors and the number of measurements. These bounds can be used to provide guidelines for determining the system parameters for various applications in CS under noisy MMV with different sensing matrices. We develop asymptotic necessary and sufficient conditions for the reliable support set reconstruction based on these bounds. Using these conditions, we not only show how the usage of the joint sparsity structure can result in benefits on the support set reconstruction but also provide theoretical explanations regarding results which have been only empirically reported in the works of Caione *et al.* and Wu *et al.*. We then compare our sufficient conditions with the other existing sufficient conditions which are obtained for noisy MMV with the same sensing matrix. In a sublinear sparsity regime under some reasonable assumptions, we show that noisy MMV with different sensing matrices may require

fewer measurements for the reliable support set reconstruction, which is an advantage of the usage of different sensing matrices for sampling sparse vectors which have the joint sparsity structure.

In the second part, we aim to propose a fast first-order-type algorithm for support set reconstruction with cheap per-iteration cost. We begin to reformulate the l_0 -norm minimization problem into a mixed integer quadratic programming (MIQP) problem by following the works of Bourguignon *et al.*, where a solution to this MIQP problem is shown to be a support set. We then use an alternating direction method (ADM), recently becoming a popular and powerful method for solving various integer programming (IP) problems studied in the works of Souto and Dinis, Yadav *et al.*, and Takapoui *et al.*, to derive the proposed algorithm. We define two metrics such as a mean square error (MSE) and a support set error (SSE) to evaluate how this proposed algorithm can reconstruct support set properly. We conduct extensive simulations to provide phase transition results, indicating that *i*) our algorithm significantly surpasses other algorithms based on ADM in terms of both MSE and SSE, and *ii*) our algorithm exhibits good MSE and SSE close to those of an optimal decoder that knows support set a prior. Then, we empirically confirm that the computational costs of our algorithm is roughly $O(n^{1.3})$, where n is the ambient dimension.

Notational Conventions

| Notation | Definitions |
|--|--|
| \mathbb{R} | Real numbers |
| \mathbb{R}^N | Space of real valued N dimensional Vectors |
| $\mathbb{R}^{M \times N}$ | Space of real valued $M \times N$ dimensional matrices |
| $\mathbb{P}\{\cdot\}$ | Probability of a given event |
| $\mathbb{E}[\cdot]$ | Expectation of a given random variable |
| $\mathbb{V}[\cdot]$ | Variance of a given random variable |
| \mathcal{S} | Euclidean math letters denotes sets |
| $ \mathcal{S} $ | Cardinality of a given set |
| f | Small bold letters denote vectors |
| F | Capital bold letters denote matrices |
| f (i) | The i^{th} element of a given vector |
| f [$i:l$] | Column vector constructed by collecting elements of a given vector from the i^{th} element to the l^{th} element |
| f _{\mathcal{I}} | Sub-vector formed by the elements of a given vector indexed by a given set |
| F _{\mathcal{I}} | Sub-matrix formed by the columns of a given matrix indexed by a given set |
| F ^{T} | Transpose of a given matrix |
| F ⁻¹ | Inverse of a given matrix |
| F [†] | Pseudo inverse of a given matrix |
| tr[F] | Trace of a given matrix |
| $\lambda_i(\mathbf{F})$ | The i^{th} eigenvalue of a given matrix |
| $f^n(x)$ | The n^{th} derivation of a function f with respect to x |
| $\ \mathbf{x}\ _0$ | l_0 -norm of a given vector |
| $\ \mathbf{x}\ _1$ | l_1 -norm of a given vector |
| 1 _{N} | N -dimensional vector of ones |
| 0 _{N} | N -dimensional vector of zeros |
| I _{N} | The $N \times N$ identity matrix |
| O _{N} | The $N \times N$ matrix of zeros |

List of Contents

| | |
|--|----------|
| Abstract | i |
| Notational Conventions | iv |
| List of Contents | v |
| List of Tables | vii |
| List of Figures | viii |
| Chapter 1: Introduction to Compressed Sensing and Support Set Reconstruction | 1 |
| 1.1 Compressed Sensing | 1 |
| 1.2 Information-Theoretic Problem of Support Set Reconstruction | 2 |
| 1.3 Practical Algorithms for Support Set Reconstruction | 4 |
| 1.4 Motivations | 6 |
| 1.5 Contributions and Outline of this Dissertation | 7 |
| Chapter 2: An Information-Theoretic Study for Joint Sparsity Pattern Recovery with Different Sensing Matrices | 9 |
| 2.1 Introduction | 9 |
| 2.1.1 Information-Theoretic Works for CS with SMV | 10 |
| 2.1.2 Information-Theoretic Works for CS with MMV | 10 |
| 2.1.3 Motivations | 12 |
| 2.1.4 Contributions of Chapter 2 | 13 |
| 2.2 Notations, System Model & Problem Formulation | 14 |
| 2.2.1 Notations | 14 |
| 2.2.2 System Model | 14 |
| 2.2.3 Problem Formulation | 15 |
| 2.3 Main Results | 17 |
| 2.3.1 Sufficient Conditions on M | 17 |
| 2.3.2 Discussions on the Sufficient Conditions | 18 |
| 2.3.3 Necessary Condition on M | 22 |
| 2.4 Relations to the Existing Information-Theoretic Results | 23 |
| 2.4.1 Relations to Noisy MMV with the Same Sensing Matrix [23] | 23 |

| | | |
|---|--|-----------|
| 2.4.2 | Relations to Noisy SMV [12] | 24 |
| 2.5 | Conclusions | 25 |
| 2.6 | Appendices | 26 |
| 2.6.1 | Appendix A: Lemmas 1 and 2 | 26 |
| 2.6.2 | Appendix B: Lemmas 3 and 4 | 30 |
| 2.6.3 | Appendix C: Proofs of Theorems 1, 2, and 3 | 33 |
| 2.6.4 | Appendix D: Proofs of Corollaries 1, 2 and 3 | 36 |
| 2.6.5 | Appendix E: Proofs of Propositions 1 and 2 | 38 |
| Chapter 3: Fast Mixed Integer Quadratic Programming for Sparse Signal Estimation | | 42 |
| 3.1 | Introduction | 42 |
| 3.2 | Alternating Direction Method (ADM) | 44 |
| 3.3 | Sparse Signal Estimation via MIQP Problem | 45 |
| 3.3.1 | Derivation of ADM-MIQP | 46 |
| 3.3.2 | Computation Costs per Iteration | 49 |
| 3.3.3 | Comparison with Work [40] | 49 |
| 3.4 | Simulations Studies | 51 |
| 3.4.1 | Convergence Behaviors of ADM-MIQP | 52 |
| 3.4.2 | Comparison Studies and Discussion | 54 |
| 3.4.3 | An Image Recovery Example | 62 |
| 3.5 | Conclusion | 62 |
| Chapter 4: Conclusions Remarks of this Dissertation | | 64 |
| References | | 65 |
| Curriculum Vitae | | 71 |
| Acknowledgement | | 75 |

List of Tables

| | | |
|-------------|---|----|
| Table 2.4.1 | Sufficient conditions on M for support set reconstruction. | 23 |
| Table 3.3.1 | The pseudo codes of ADM-MIQP. | 48 |

List of Figures

| | | |
|--------------|--|----|
| Figure 3.4.1 | It plots the average MSE of ADM-MIQP depending on the number of iterations. The problem dimension n , the number of measurements m and the sparsity level k are set to be 1024, 307 and 30, respectively. | 53 |
| Figure 3.4.2 | It plots the average SSE of ADM-MIQP depending on the number of iterations. The problem dimension n , the number of measurements m and the sparsity level k are set to be 1024, 307 and 30, respectively. | 53 |
| Figure 3.4.3 | It plots the empirical phase transitions of the ADM-based methods such as ADM-MIQP, MDAL and YALL1, respectively. | 55 |
| Figure 3.4.4 | It plots the average MSEs of ADM-MIQP, MDAL, YALL1 and ORACLE depending on the sparsity level k . The problem dimension n , the number of measurements m and SNR [dB] are set to be 1024, 307 and 35, respectively. | 57 |
| Figure 3.4.5 | It plots the average SSEs of ADM-MIQP, MDAL and YALL1 depending on the sparsity level k . The problem dimension n , the number of measurements m and SNR [dB] are set to be 1024, 307 and 35, respectively. | 57 |
| Figure 3.4.6 | It plots the average running times of ADM-MIQP, MDAL, YALL1 and CPLEX depending on the problem dimension n with $m = \lfloor 0.3n \rfloor$, $k = \lfloor 0.3m \rfloor$ and SNR [dB] = 45. ADM-MIQP, MDAL and YALL1 have the polynomial computational order. | 60 |
| Figure 3.4.7 | It plots the average running times of ADM-MIQP and CPLEX depending on the problem dimension n with $m = \lfloor 0.3n \rfloor$, $k = \lfloor 0.2m \rfloor$ and SNR [dB] = 45. This figure shows that ADM-MIQP is significantly faster than CPLEX. | 60 |
| Figure 3.4.8 | The original grayscale images of size 512×512 are shown in the first row. The images recovered by ADM-MIQP are shown in the second row. The images recovered by MDAL are shown in the third row. Then, the PSNR value of each recovered image is averaged 10 trials at $m = \lfloor 0.15n \rfloor$ and $k = \lfloor 0.05n \rfloor$ | 61 |
| Figure 3.4.9 | The images are corresponding to the part of the original and each recovered airplane images. | 61 |

Chapter 1: Introduction to Compressed Sensing and Support Set Reconstruction

1.1. Compressed Sensing

A conventional signal acquisition and reconstruction framework has been processed under the Shannon-Nyquist sampling theory [1] which was introduced by Shannon at 1940's. This theory suggests that we have to uniformly sample a signal at the Nyquist sampling rate, which is higher than twice the maximum frequency, to reconstruct this signal from the samples. However, the number of samples decided by this theory can be often large; we have to compress the samples before they are stored. As Donoho has stated in his work [2], the most of samples we take have to be discarded to reduce the number of samples before being stored, which is inefficient in the conventional framework.

As a new signal acquisition and reconstruction framework, compressed sensing (CS) was introduced in 2000's by the seminal works of Donoho, Candes, Tao, Romberg, and Baraniuk [2]–[8]. CS aims to remove the inefficiency of the conventional framework by conducting both “sampling” and “compression” simultaneously. This implies that CS allows for the acquisition of signal samples at a rate lower than the Shannon-Nyquist sampling rate. As a result, the signal acquisition time can be reduced and the development of small sensors with good resolution or fast analog-to-digital converters can be possible.

The fundamental reason to directly acquire samples at a rate lower than the Shannon-Nyquist sampling rate is that any signals can be sparsely represented using only a few nonzero elements in some domains [2], [7], [8]. As an example, let consider an image. Definitely, all the elements in this image are almost nonzero. However, a result obtained by applying the wavelet transform to it has a lot of zeros. This is to say that this image can be sparsely represented in the wavelet domain.

We give the definition of a k -sparse vector given by Baranuk [8], which is “*The signal \mathbf{x} is K -sparse if it is a linear combination of only K basis vector; that is, only K of the coefficients in a vector $\Psi^T \mathbf{x}$ are nonzero and $N - K$ are zero, where Ψ is an orthonormal transform of size $N \times N$.*” For simplicity, in this dissertation, we assume that this orthonormal transform is the identity matrix of size $N \times N$. That is, the

interest of signal is K -sparse itself.

CS aims to directly acquire compressed samples of such K -sparse signals without going through the unnecessary stage of getting N samples. Mathematically, a K -sparse vector \mathbf{x} can be sampled to yield an M -dimensional measurement vector \mathbf{y} via a linear system model called noisy single measurement vector (SMV) as follows:

$$\mathbf{y} = \mathbf{F}\mathbf{x} + \mathbf{n} \quad (1)$$

where \mathbf{n} is a noise vector of size $M \times 1$ and \mathbf{F} is a sensing matrix of size $M \times N$ whose rank is assumed to be full. Typically, all the elements of this noise vector are independently and identically distributed (i.i.d) Gaussian with a zero mean and a σ^2 variance, and those of this sensing matrix are also i.i.d. Gaussian with a zero mean and a unit variance.

We investigate how the signal acquisition in CS can be different to the conventional signal acquisition. In the conventional signal acquisition, a signal is uniformly sampled at the Nyquist sampling rate. This can be interpreted that \mathbf{F} in (1) is the identity matrix of size $N \times N$. Thus, each element in \mathbf{y} contains the information regarding the corresponding element in \mathbf{x} . In contrast, in CS, the i^{th} element in \mathbf{y} is obtained by multiplying \mathbf{x} with the i^{th} row vector of \mathbf{F} which is randomly constructed. Thus, each element in \mathbf{y} can include pieces of the whole information on \mathbf{x} . This process is repeated M times where M is smaller than N , implying that both the sampling and the compression are conducted jointly.

1.2. Information-Theoretic Problem of Support Set Reconstruction

The linear system (1) is under-determined, making the signal reconstruction in CS difficult. However, the number of nonzero elements in \mathbf{x} is K . If we know the positions of them in advance, the number of unknowns is reduced to K . For more details, for a given \mathbf{x} , we begin to define its support set as follows:

$$\mathcal{I} := \{i | x(i) \neq 0\} \quad (2)$$

which collects indices corresponding to the nonzero elements in \mathbf{x} . If this set is given in advance, we have

$$\mathbf{y} = \mathbf{F}_{\mathcal{I}}\mathbf{x}_{\mathcal{I}} + \mathbf{n} \quad (3)$$

where $\mathbf{F}_{\mathcal{I}}$ is a sub-matrix of size $M \times K$ constructed by taking columns of \mathbf{F} corresponding to the support set and $\mathbf{x}_{\mathcal{I}}$ is a sub-vector of size $K \times 1$ constructed by taking elements of \mathbf{x} corresponding to the support

set. Since the linear system (3) is over-determined, then we can easily get a solution to (3) as follows:

$$\mathbf{x}_{\mathcal{I}^c} := \mathbf{F}_{\mathcal{I}}^\dagger \mathbf{y} \in \mathbb{R}^k. \quad (4)$$

Once we get this solution, the original K -sparse vector can be finally estimated as follows:

$$\hat{\mathbf{x}} = \begin{cases} \mathbf{x}(i) = 0 & \text{if } i \notin \mathcal{I} \\ \mathbf{x}_{\mathcal{I}} = \mathbf{x}_{\mathcal{I}^c} & \text{o.w.} \end{cases}. \quad (5)$$

Thus, it is interesting to investigate necessary and sufficient conditions for a reliable support set reconstruction. There have been several information-theoretic works [9]–[14] where optimal or sub-optimal decoders for this reliable support set reconstruction are analyzed to examine their necessary and sufficient conditions in both the linear and sublinear sparsity regimes. In [9], Wainwright got the necessary and sufficient conditions for \mathbf{F} in which each row vector is a multivariate Gaussian vector with a zero mean and a covariance matrix. In [10]–[14], the authors obtained these conditions for \mathbf{F} in which all the elements are i.i.d. Gaussian with a zero mean and a unit variance as well. All these works indicate that for the reliable support set reconstruction, we at least take

$$M = \Omega\left(K \log \frac{N}{K}\right) \quad (6)$$

in the sublinear sparsity regime, and

$$M = \Omega(K) \quad (7)$$

in the linear sparsity regime, respectively. These results are to say that the reconstruction can be possible even we obtain the compressed samples (1) at a rate lower than the Shannon-Nyquist sampling rate.

In some applications such as wireless sensor networks (WSNs) and magnetic resonance imaging (MRI), sensors can be distributed to jointly monitor a phenomenon to improve resolutions in their acquired signals. In these applications, the signals of interest can be often assumed to be correlated. There are needs to mathematically describe this correlation because this correlation has to be used during the signal reconstruction for obtaining benefits. For example, we consider a WSN where there are S sensors in a restricted area measuring a phenomenon. Each sensor acquires its own signal, compresses the acquired signal and transmits the compressed signal to a fusion center. After taking all these compressed signals, this fusion center runs an algorithm to jointly decompress them for understanding the phenomenon at the sensor positions. Since the sensors are intentionally distributed in the restricted area, there exist correlations among the acquired signals. During the compression stage, the sensors can exploit the correlation to improve the

compression capability, making them less consume their battery power for transmission operations. The fusion center has to use the correlation to decompress them which are being compressed using the correlation. This example is to indicate that correlations among acquired signals should be not only used in the compression stage but also used in the decompression stage.

In CS, there exists a joint sparsity structure [15]–[21] that is useful to mathematically define the correlation in the above applications. This structure is to indicate that all of signals to be acquired share a common support set, as we will mathematically define in Section 2.1.2.

There are two different models for sampling sparse signals under this joint sparsity structure. The first model is called multiple measurement vectors (MMV) with the same sensing matrix [21]. In this model, all the sparse signals are sampled by the same sensing matrix. In the second model called as MMV with different sensing matrices [17][18], each sparse signal is sampled by its own sensing matrix.

It is interesting to examine how this structure can make impacts on a reliable support set reconstruction. In [22], [23], the authors have obtained the necessary and sufficient conditions in the first model in the presence of noise. In [22], Tang and Nehorai proved that a success probability for this reliable support set reconstruction can grow with the number of sparse vectors whenever each sparse vector is sampled at the rate provided in (6). In [23], when the noise variance is sufficiently small, Jin and Rao showed that for the reliable support set reconstruction, each sparse vector has to be sampled at the following rate:

$$M = \Omega \left(\frac{K \log N}{\min(K, S)} \right) \quad (8)$$

where S is the number of sparse vectors to be sampled. As comparing (6) with (8), we see that the usage of the joint sparsity structure can result in yielding the better sufficient condition (8). In the second model without the presence of noise, Durate *et al.* [24] got necessary and sufficient conditions on the number of measurements, and interpreted that $M = K + 1$ is enough for a reliable support set reconstruction. This interpretation is obvious because a decoder analyzed by them is akin to the l_0 -norm minimization problem which requires a combinatorial search.

1.3. Practical Algorithms for Support Set Reconstruction

The results obtained by conducting information-theoretic studies [9]–[14], [22]–[24] are to say that a

reliable support set reconstruction can be theoretically possible even we take a small number of measurements. It now should be considered how to reconstruct a support set. The most naïve approach is to solve the l_0 -norm minimization problem [6], [7] as follows:

$$\min_{\mathbf{x}} \quad \tau \|\mathbf{x}\|_0 + 2^{-1} \|\mathbf{y} - \mathbf{F}\mathbf{x}\|_2^2 \quad (9)$$

where τ is a positive regularization parameter. It is immediately seen that this problem is equal to

$$\min_{\mathbf{x}} \quad \|\mathbf{x}\|_0 \quad \text{subject to} \quad \|\mathbf{y} - \mathbf{F}\mathbf{x}\|_2^2 \leq \varepsilon \quad (10)$$

where ε is a positive parameter.

Intuitively, solving either (9) and (10) can be interpreted in finding a support set which jointly meets *i*) the number of elements included in this set has to be minimized and *ii*) the data fidelity, i.e., the l_2 -norm part, has to be also sufficiently small. However, this l_0 -norm function in them is non-convex, and discontinues. Moreover, these problems are known to be NP-hard because we have to exhaustively consider all possible support sets, requiring a non-polynomial computational complexity. Thus, for a small value of N , one can solve either (9) and (10). But, for a large value of N , no one can solve them because its computational complexity exponentially grows with N .

Greedy algorithms such iterative hard thresholding (IHT) [25], variants of IHT [26]–[28] are in popular to solve (9). Some of these algorithms have been analyzed. Their sufficient conditions for a reliable support set reconstruction have been provided. Convex algorithms such as smoothed l_0 -norm (SL0) and its variant [29], [30] have been proposed to solve an approximated problem of (9) in which the l_0 -norm function is approximated as a series of convex functions. These algorithms are also proved that they can find a local solution to (9) under some reasonable conditions. Last, mean doubly augmented Lagrangian (MDAL) [31] as a non-convex algorithm has been proposed to solve (9). Although this non-convex algorithm has no theoretical foundation regarding their convergence, it has been empirically shown to yield the better reconstruction performance rather than both the greedy algorithms and the convex algorithms do.

Last, there are other approaches to solve (9). These approaches aim to solve an l_1 -norm minimization problem which is relaxed from (9) by replacing the l_0 -norm function with the l_1 -norm function. The l_1 -norm function is convex and continuous; that is, the l_1 -norm minimization problem is convex. As we will state in Section 3.1, many algorithms have been proposed to solve this problem. Some of them have been

analyzed to prove their global convergence. There have been a lot of theoretical works to link the l_1 -norm minimization problem to (9). But, the aim to solve the l_1 -norm minimization problem is to estimate x itself, not to reconstruct its support set. Thus, this dissertation does not mainly consider the l_1 -norm minimization problem and related algorithms.

1.4. Motivations

CS with noisy MMV with different sensing matrices has been successfully applied in applications such as WSNs [15] and MRI [16]. Empirical results in these applications show benefits facilitated by the joint sparsity structure. However, no theoretic-tool is available to explain fundamental reasons which cause these results. We are motivated to develop a theoretic-tool by conducting an information-theoretic study in which we aim to analyze a sub-optimal decoder for a reliable support set reconstruction under noisy MMV with different sensing matrices.

Next, consider both of the models regarding MMV without the presence of noises. In noiseless MMV with the same sensing matrices, all measurement vectors are obtained through the same sensing matrix, implying that that all the elements of them can be correlated. In contrast, in noiseless MMV with different sensing matrices, each measurement vector is taken using its own sensing matrix. Thus, all the elements of these measurement vectors are uncorrelated because each sensing matrix is randomly and independently constructed. Consider an extreme example in which all sparse vectors to be sampled are the same. In noiseless MMV with the same sensing matrix, all the measurement vectors are also identical. In contrast, those are different in noiseless MMV with different sensing matrices. As we have considered this example, we have an intuition that the usage of different sensing matrices provides more degree of freedoms in all of the measurement vectors rather than the usage of the same sensing matrix does. Is this intuition still valid in the presence of noise? This question motivates us to conduct the study on noisy MMV with different sensing matrices as well.

Last, recently, Bourguignon *et al.* [32] have showed that (9) is reformulated into a mixed integer quadratic programming (MIQP) problem when the interest of signals is bounded. Then, Bertsimas *et al.* [33] have solved this problem using CPLEX [34], a typical solver for integer programming (IP) problems, and shown that a solution obtained by CPLEX is better than that obtained by IHT [25]. However, for a

large value of N , CPLEX cannot be useful because it requires exhaustive approaches [35] to search a feasible space to IP problems, implying that its computational complexity grows exponentially with N . Nowadays, an alternating direction method (ADM) [36], [37], [62] becomes very popular because ADM has been empirically shown to be powerful for finding solutions to IP problems [38]–[40]. Moreover, in [40], it was reported ADM could be greatly faster than a commercial IP method. We hence are motivated to propose a support set reconstruction algorithm based on ADM to solve the reformulated problem of (9).

1.5. Contributions and Outline of this Dissertation

This dissertation is organized as follows. In Chapter 2, we give necessary and sufficient conditions for noisy MMV with different sensing matrices, and give various interpretations on these conditions, which were published in [41]–[45] as follows:

- [41] **Sangjun Park**, Nam Yul Yu, Heung-No Lee, “An Information-Theoretic Study for Joint Sparsity Pat-tern Recovery with Different Sensing Matrices,” *IEEE Trans. Inf. Theory*, vol. 63, no. 9, pp. 5559-5571, May, 2017.
- [42] Heung-No Lee, Junho Lee, **Sangjun Park**, “Signal Acquisition and Method for Distributed Compressive Sensing and Joint Signal Recovery,” application number: 13/250,082, application date: Sep., 30th, 2011, registration number: 8391800, registered date: Mar. 5th, 2013.
- [43] **Sangjun Park** and Heung-No Lee, “Number of Compressed Measurements Needed for Noisy Distribute Compressed Sensing,” *2012 IEEE International Symposium on Information Theory Proceedings*, Cambridge, MA, 2012, pp. 1648-1651
- [44] **Sangjun Park**, Hwanchol Jang and Heung-No Lee, “Study on performance behavior of the compressive sensing measurements for multiple sensor system,” *2011 Conference Record of the Forty Fifth Asilomar Conference on Signals, Systems and Computers (ASILOMAR)*, Pacific Grove, CA, 2011, pp. 1980-1983.
- [45] **Sangjun Park**, Junho Lee and Heung-No Lee, “Per-sensor measurements behavior of compressive sensing system for multiple measurements,” *2010 Conference Record of the Forty Fourth Asilomar Conference on Signals, Systems and Computers*, Pacific Grove, CA, 2010, pp. 240-242.

In Chapter 3, we propose an algorithm to solve a problem reformulated from the l_0 -norm minimization problem, and provide simulation results to show the superiority of the proposed algorithm compared to other algorithms. All these results included in this chapter were published in [46] as follows:

[46] **Sangjun Park** and Heung-No Lee, "Fast mixed integer quadratic programming for sparse signal estimation," *IEEE Access*, vol. 6, pp. 58439-58449, Oct., 2018.

In Chapter 4, we give conclusions of this dissertation.

Chapter 2: An Information-Theoretic Study for Joint Sparsity

Pattern Recovery with Different Sensing Matrices

2.1. Introduction

Conventionally, signals sensed from sensors such as microphones and imaging devices are sampled following the Shannon and Nyquist sampling theory [1] at a rate higher than twice the maximum frequency for signal reconstruction. As the number of samples decided by this theory is often large, the samples go through a compression stage before being stored. Therefore, taking numerous samples, where most of them will be discarded in this stage, is inefficient. Because compressed sensing (CS) [2]–[7] removes the inefficiency, CS has been applied in various areas such as wireless communications [15], [55], [17]–[19], spectrometers [47], multiple input multiple output (MIMO) radars [20], magnetic resonance imaging (MRI) [16], and imaging/signal processing [48]–[65].

The CS theory states that signals that are sparsely representable in a certain basis are compressively sampled and reconstructed from what we thought is incomplete in information. Let $\mathbf{x} \in \mathbb{R}^N$ be a K -sparse vector with a support set as follows:

$$\mathcal{I} := \{i | x(i) \neq 0\}$$

whose indices indicate the positions of the nonzero coefficients of \mathbf{x} . It is compressively sampled by a model called *single measurement vector* (SMV) as follows:

$$\mathbf{y} = \mathbf{F}\mathbf{x} + \mathbf{n} \quad (11)$$

where $\mathbf{y} \in \mathbb{R}^M$ is a (noisy) measurement vector, $\mathbf{F} \in \mathbb{R}^{M \times N}$ is a sensing matrix, and $\mathbf{n} \in \mathbb{R}^M$ is a noise vector, whose elements are independent and identically distributed (i.i.d) Gaussian with a zero mean and a σ^2 variance. Once the support set is correctly reconstructed, then (11) can be well-posed, which allows us to obtain an accurate estimate of \mathbf{x} using the least square approach. Thus, we consider a support set reconstruction problem.

2.1.1. Information-Theoretic Works for CS with SMV

Works [9]–[14] have studied the support set reconstruction problem from an information-theoretic perspective. For reliable support set reconstruction, sufficient and necessary conditions were established in the linear and sublinear sparsity regimes.

For a support set reconstruction, Wainwright [9] used the union bound to establish a sufficient condition on the number of measurements M for a maximum likelihood (ML) decoder and used Fano’s inequality [51] to obtain a necessary condition on M . This ML decoder was analyzed by Fletcher *et al.* [10] to establish a necessary condition on M . Aeron *et al.* [11] used Fano’s inequality to form necessary conditions on both M and σ^2 . Then, they used the union bound to obtain sufficient conditions on both M and σ^2 for their sub-optimal decoder. Akcakaya and Tarokh [12] used the union and the large deviation bounds based on empirical entropies to get sufficient conditions on M for their joint typical decoder. They used the converse of the channel coding theorem to get necessary conditions on M . Scarlett *et al.* [13] extended this decoder [12] with the assumption that the distribution of the support set is provided. For a uniform distribution case, their necessary and sufficient conditions are equivalent to those of [12]. However, they are better for a non-uniform distribution case. Scarlett and Cevher [14] linked the support set reconstruction with the problem of coding over a mixed channel, where information spectrum methods were used to obtain necessary and sufficient conditions on M .

2.1.2. Information-Theoretic Works for CS with MMV

CS has many applications in wireless sensor networks (WSNs) [15], [55], [17]–[19] and MIMO radars [20]. In these applications, the signals of interest

$$\mathbf{x}^s \in \mathbb{R}^N, s = 1, 2, \dots, S$$

are often modeled as *jointly K -sparse vectors*, implying that

$$\mathcal{I} = \mathcal{I}^1 = \mathcal{I}^2 \dots = \mathcal{I}^S$$

where \mathcal{I}^s is the support set of \mathbf{x}^s and $|\mathcal{I}| = K$, which is referred to as a *joint sparsity structure*.

There are two models for sampling jointly K -sparse vectors. The first model is called *multiple measurement vectors* (MMV) with *the same sensing matrix* [21], in which they are sampled by the same sens-

ing matrix. The second model is named as MMV with *different sensing matrices* [17][18], in which each one is sampled by its own sensing matrix.

The authors of [22]–[24] have conducted information-theoretic research to obtain conditions under which the support set of both the models was reconstructed with a high probability. In noisy MMV with the same sensing matrix, Tang and Nehorai [22] used the hypothesis theory to obtain necessary and sufficient conditions on both the number of measurements M and the number of measurement vectors S , and proved that the success probability of the support set reconstruction increases with S , if $M = \Omega\left(K \log \frac{N}{K}\right)$. Jin and Rao [23] exploited the communication theory to establish necessary and sufficient conditions on M and demonstrated the benefits of the joint sparsity structure based on their conditions. A detailed comparison between the results of our work and [12] will be presented in 2.4. Finally, Duarte *et al.* [24] studied noiseless MMV with different sensing matrices, and formed necessary and sufficient conditions on M . However, it is difficult to apply the conditions to noisy MMV with different sensing matrices.

Meanwhile, works [17][52][53] have presented conditions of practical algorithms for a reliable support set reconstruction. In noiseless MMV with the same sensing matrix, Blanchard and Davies [53] obtained conditions for a reliable reconstruction from rank aware orthogonal matching pursuit (OMP). In noisy MMV with the same sensing matrix, Kim *et al.* [52] created compressive MUSIC, and presented its sufficient condition. In noiseless MMV with different sensing matrices, Baron *et al.* [17] produced trivial pursuit (TP) and distributed compressed sensing-simultaneous OMP (DCS-SOMP). By analyzing TP with the assumption that each sensing matrix contains i.i.d. Gaussian elements and that the nonzero values of each sparse vector are i.i.d. Gaussian variables, they demonstrated that with $M \geq 1$, TP reconstructs the support set as S is sufficiently large. They conjectured that $M \geq K + 1$ suffice for DCS-SOMP to reconstruct the support set as S is sufficiently large, based on its empirical results.

To the best of our knowledge, no information-theoretic study has been published to get necessary and sufficient conditions for a reliable support set reconstruction in noisy MMV with different sensing matrices. Besides, these conditions have not been provided from the practical recovery algorithms for CS with noisy MMV with different sensing matrices.

2.1.3. Motivations

CS with noisy MMV with different sensing matrices has been applied in many applications and the benefits facilitated by the joint sparsity structure have been empirically reported in [15][16]. In WSNs, Caione *et al.* [15] used the joint sparsity structure to reduce the number of transmitted bits per sensor and reported that each sensor can reduce its transmission cost. In MRI, Wu *et al.* [16] modeled multiple diffusion tensor images (DTIs) as jointly sparse vectors. They exploited the joint sparsity structure to reduce the number of samples per DTI, while retaining the reconstruction quality. Using the joint sparsity structure, they also empirically reported that the reconstruction quality of each DTI can be improved for a fixed number of samples per DTI.

To theoretically explain the above empirical benefits facilitated by the joint sparsity structure, theoretical tools are required to measure the performance of CS with noisy MMV with different sensing matrices. Such tools can be useful as guidelines for determining the system parameters in various CS applications with noisy MMV with different sensing matrices. For example, if the number of samples per DTI is fixed in the MRI [16], the theoretical tools may enable us to determine the number of DTIs required for achieving a given reconstruction quality. Thus, the first motivation of this paper is to provide the theoretical tools by establishing sufficient and necessary conditions for a reliable support set reconstruction.

Next, for noiseless MMV with the same sensing matrix, let

$$\mathbf{Y}_A = \mathbf{F} \times [\mathbf{x}^1 \quad \mathbf{x}^2 \quad \dots \quad \mathbf{x}^S] \in \mathbb{R}^{M \times S}.$$

Also, for noiseless MMV with different sensing matrices, let

$$\mathbf{Y}_B = [\mathbf{F}^1 \mathbf{x}^1 \quad \mathbf{F}^2 \mathbf{x}^2 \quad \dots \quad \mathbf{F}^S \mathbf{x}^S] \in \mathbb{R}^{M \times S}.$$

Then, all the elements of \mathbf{Y}_B are uncorrelated because all the sensing matrices are independent. In contrast, those of \mathbf{Y}_A are correlated because they are taken from the same sensing matrix. Now, we consider a case where we set $S > K$ and $M > K$. Then, it is clear that

$$\text{rank}(\mathbf{Y}_B) = \min(S, M)$$

with a high probability and the rank of \mathbf{Y}_B is at most K . Therefore, for this case, we conclude that

$$\text{rank}(\mathbf{Y}_B) > \text{rank}(\mathbf{Y}_A)$$

which implies that a more reliable support set reconstruction can be expected in noiseless MMV with

different sensing matrices for this case. Thus, the second motivation is to verify this perception in the presence of noise, by comparing our results with the existing ones in noisy MMV with the same sensing matrix [23].

2.1.4. Contributions of Chapter 2

The contributions of Chapter 2 are as follows: First, we derive upper and lower bounds of a failure probability of the support set reconstruction from Lemmas 1 and 2, by exploiting Fano's inequality [51] and the Chernoff bound [54]. We believe that these bounds are used for measuring the performance of CS with noisy MMV with different sensing matrices.

Next, we develop necessary and sufficient conditions for a reliable support set reconstruction. Theorem 1 states that

$$M > K \left(1 + \frac{1}{Sf(\text{SNR}_{\min})} \right)$$

suffices to achieve a reliable support set reconstruction in the *linear sparsity* regime, i.e.,

$$\lim_{N \rightarrow \infty} \frac{K}{N} = \beta \in (0, 1/2),$$

and it also states that

$$M > K \left(1 + \frac{1}{Sf(\text{SNR}_{\min})} \log \frac{N}{K} \right)$$

suffices to achieve a reliable support set reconstruction in the *sublinear sparsity* regime, i.e.,

$$\lim_{N \rightarrow \infty} \frac{K}{N} = 0$$

where $f(\text{SNR}_{\min})$ is an increasing function with respect to the minimum signal-to-noise ratio SNR_{\min} defined in (14). Next, for a finite S , N , K , and SNR_{\min} , Theorem 3 states that

$$M < \frac{2K \log \frac{N}{K} - 2 \log 2}{S \log(1 + K \times \text{SNR}_{\min})}$$

is necessary for a reliable support set reconstruction. The necessary and sufficient conditions can be useful as guidelines to determine the system parameters of CS applications with noisy MMV with different sensing matrices. Corollaries 1 and 2 indicate that a reliable support set reconstruction is possible by tak-

ing sufficiently many measurement vectors S for a fixed M with a low SNR_{\min} value. For a fixed N and K , Theorem 2 shows that $M \geq K + 1$ measurements suffice for reconstructing the support set, as S is sufficiently large. Then, for a fixed N , K , and $M = K + 1$, Corollary 3 provides a sufficient condition on S for a reliable support set reconstruction. We then provide theoretical explanations of the benefits of the joint sparsity structure, which confirm the empirical results of CS applications with noisy MMV with different sensing matrices [15][16]. Finally, we compare the sufficient condition (21) with the known one (36) for noisy MMV with the same sensing matrix [23]. Therefore, we demonstrate that if $S \geq K$, noisy MMV with different sensing matrices may require fewer measurements M for a reliable support set reconstruction than noisy MMV with the same sensing matrix under a low noise-level scenario. It confirms the superiority of MMV with different sensing matrices.

2.2. Notations, System Model & Problem Formulation

2.2.1. Notations

The following notations will be used in this chapter.

1. An orthogonal projection matrix which maps an arbitrary vector to the space orthogonal onto the space spanned by the columns of a given matrix \mathbf{F} is defined by

$$\mathbf{Q}(\mathbf{F}) := \mathbf{I}_M - \mathbf{F}(\mathbf{F}^T \mathbf{F})^{-1} \mathbf{F}^T. \quad (12)$$

2. For given sets \mathcal{J} and \mathcal{I} , the relative complements of \mathcal{J} in \mathcal{I} is denoted as $\mathcal{J} \setminus \mathcal{I}$.
3. The *linear sparsity regime* is defined by

$$\lim_{N \rightarrow \infty} \frac{K}{N} = \beta \in (0, 1/2).$$

4. The *sublinear sparsity regime* is defined by

$$\lim_{N \rightarrow \infty} \frac{K}{N} = 0.$$

2.2.2. System Model

Let $\mathbf{x}^1, \mathbf{x}^2, \dots, \mathbf{x}^S$ be jointly K -sparse vectors with a support set \mathcal{I} which belongs to

$$\mathcal{S} := \{\mathcal{H} | \mathcal{H} \subset \{1, 2, \dots, N\}, |\mathcal{H}| = K\}.$$

Thus, the number of nonzero coefficients of each sparse vector is K , the indices of the nonzero coefficients of all the sparse vectors are the same and the indices belong to the support set. In noisy MMV with different sensing matrices, each sparse vector is sampled by its own sensing matrix, i.e.,

$$\mathbf{y}^s = \mathbf{F}^s \mathbf{x}^s + \mathbf{n}^s \quad s = 1, 2, \dots, S \quad (13)$$

where all the sensing matrices have i.i.d. Gaussian elements with a zero mean and a unit variance, and all the noise vectors have i.i.d. Gaussian elements with a zero mean and a σ^2 variance. We assume that all the noise vectors and all the sensing matrices are mutually independent. Then, we let x_{\min} be the smallest nonzero magnitude of all the sparse vectors and SNR_{\min} be the minimum signal-to-noise ratio given by

$$\text{SNR}_{\min} := x_{\min}^2 / \sigma^2. \quad (14)$$

2.2.3. Problem Formulation

We extend Akcakaya and Tarokh [12]'s decoder for noisy MMV with different sensing matrices. It takes all the measurement vectors as its input and yields a support set decision as its output

$$d: \left\{ \forall_s (\mathbf{y}^s, \mathbf{F}^s) \right\} \mapsto \hat{\mathcal{I}} \in \mathcal{S}, \quad s = 1, 2, \dots, S.$$

Its decision rules are given in Definition 1.

Definition 1: All the measurement vectors $\{\mathbf{y}^1, \mathbf{y}^2, \dots, \mathbf{y}^S\}$ and a set $\mathcal{J} \in \mathcal{S}$ are δ jointly typical if the rank of each $\mathbf{F}_{\mathcal{J}}^s$ is K and

$$\left| \left(\sum_{s=1}^S \|\mathbf{Q}(\mathbf{F}_{\mathcal{J}}^s) \mathbf{y}^s\|_2^2 \right) - S(M - K)\sigma^2 \right| < SM\delta. \quad (15)$$

As each sensing matrix contains i.i.d. Gaussian elements, the rank of each $\mathbf{F}_{\mathcal{J}}^s$ is K with a high probability. The decision rule is to find sets that satisfy (15) for all the given measurement vectors and $\delta > 0$. In the entire paper, the support set is denoted by \mathcal{I} and any incorrect support set is denoted by $\bar{\mathcal{I}}$, where their cardinalities are K .

We define the failure events, wherein the joint typical decoder fails to reconstruct the correct support set. First,

$$\mathcal{E}_{\mathcal{I}}^c := \left\{ \left| \left(\sum_{s=1}^S \|\mathbf{Q}(\mathbf{F}_{\mathcal{I}}^s) \mathbf{y}^s\|_2^2 \right) - S(M - K)\sigma^2 \right| \geq SM\delta \right\} \quad (16)$$

implies that the correct support set is not δ jointly typical with all the measurement vectors. For any $\mathcal{J} \in \mathcal{S} \setminus \mathcal{I}$,

$$\mathcal{E}_{\mathcal{J}} := \left\{ \left| \left(\sum_{s=1}^S \left\| \mathbf{Q}(\mathbf{F}_{\mathcal{J}}^s) \mathbf{y}^s \right\|_2^2 \right) - S(M-K)\sigma^2 \right| < SM\delta \right\} \quad (17)$$

implies that an incorrect support set is δ jointly typical with all the measurement vectors. Based on these failure events, we define a failure probability and give its upper bound as follows:

$$\begin{aligned} p_{err} &:= \mathbb{P} \left\{ \hat{\mathcal{I}} \neq \mathcal{I} \mid \mathbf{x}^1, \dots, \mathbf{x}^S \right\} \\ &= \mathbb{P} \left\{ \mathcal{E}_{\mathcal{I}}^c \cup \bigcup_{\mathcal{J} \in \mathcal{S} \setminus \mathcal{I}} \mathcal{E}_{\mathcal{J}} \right\} \\ &\leq \mathbb{P} \left\{ \mathcal{E}_{\mathcal{I}}^c \right\} + \sum_{\mathcal{J} \in \mathcal{S} \setminus \mathcal{I}} \mathbb{P} \left\{ \mathcal{E}_{\mathcal{J}} \right\} \end{aligned} \quad (18)$$

where $\mathbb{P} \left\{ \mathcal{E}_{\mathcal{I}}^c \right\}$ is taken with respect to all the noise vectors and $\mathbb{P} \left\{ \mathcal{E}_{\mathcal{J}} \right\}$ is taken with respect to all the noise vectors and all the sensing matrices. We establish Lemmas 1 and 2 given in 2.6.1 to give upper bounds of the probabilities of the failure events. Combining these lemmas with (18) yields

$$\begin{aligned} p_{err} &\leq \mathbb{P} \left\{ \mathcal{E}_{\mathcal{I}}^c \right\} + \sum_{\mathcal{J} \in \mathcal{S} \setminus \mathcal{I}} \mathbb{P} \left\{ \mathcal{E}_{\mathcal{J}} \right\} \\ &\leq 2p(d_1) + \binom{N}{K} p(d_{2,\alpha^*} - 1) \end{aligned}$$

where p is defined in (41),

$$\begin{aligned} d_1 &= \frac{M\delta}{(M-K)\sigma^2}, \\ d_{2,\alpha^*} &= \frac{(M-K)\sigma^2 + M\delta}{(M-K)\alpha^*}, \\ \alpha^* &= \sigma^2 + x_{\min}^2 \end{aligned}$$

which are defined in (43), (51) and (52), respectively.

It is of interest to examine why $\mathbb{P} \left\{ \mathcal{E}_{\mathcal{I}}^c \right\}$ depends only on the noise vectors. As shown in Lemma 3, the random variable to define the event $\mathcal{E}_{\mathcal{I}}^c$ in (16) is $\sum_{s=1}^S \left\| \mathbf{Q}(\mathbf{F}_{\mathcal{I}}^s) \mathbf{y}^s \right\|_2^2 / \sigma^2$, where the measurement vector in (13) consists of the two parts: the noise part \mathbf{n}^s and the signal part $\mathbf{F}_{\mathcal{I}}^s \mathbf{x}_{\mathcal{I}}^s$. The signal part belongs to the space spanned by the columns of $\mathbf{F}_{\mathcal{I}}^s$. Then, as specified in (12), the orthogonal projection matrix $\mathbf{Q}(\mathbf{F}_{\mathcal{I}}^s)$ maps the measurement vector to the space orthogonal onto the space spanned by the columns of

\mathbf{F}_T^s . Thus, the random variable is a function of the noise vectors only.

2.3. Main Results

As the main contribution of this paper, this section presents sufficient and necessary conditions on M for a reliable support set reconstruction in noisy MMV with different sensing matrices. We interpret the conditions to demonstrate the benefits facilitated by the joint sparsity structure.

2.3.1. Sufficient Conditions on M

In [9][12], the authors have shown that fewer measurements M for a reliable support set reconstruction are required for noisy SMV in the linear sparsity regime, compared to the sublinear sparsity regime. Based on the results of [9][12], we are motivated to examine, if the same result can be observed in noisy MMV with different sensing matrices.

Theorem 1: For any $\rho > 1$, we let $\delta = \rho^{-1}(1 - K/M)x_{\min}^2$. If the number of measurements satisfies

$$M > K + \nu_1 \frac{K}{S} \quad (19)$$

then the failure probability p_{err} defined in (18) converges to zero in the linear sparsity regime where

$$\nu_1 = -\frac{2(1 - \log \beta)}{\log\left(1 - \frac{1 - \rho^{-1}}{1 + \text{SNR}_{\min}^{-1}}\right) + \frac{1 - \rho^{-1}}{1 + \text{SNR}_{\min}^{-1}}} > 0. \quad (20)$$

Also, under the same conditions on ρ and δ , if the number of measurements satisfies

$$M > K + \nu_2 \frac{K}{S} \log \frac{N}{K} \quad (21)$$

then the failure probability p_{err} defined in (18) converges to zero in the sublinear sparsity regime where

$$\nu_2 = -\frac{2}{\log\left(1 - \frac{1 - \rho^{-1}}{1 + \text{SNR}_{\min}^{-1}}\right) + \frac{1 - \rho^{-1}}{1 + \text{SNR}_{\min}^{-1}}} > 0. \quad (22)$$

Proof: The proof is given in Section 2.6.3.

In terms of N , K , and S , the asymptotic order of the sufficient condition on M for the linear sparsity

regime is $\Omega\left(K + \frac{K}{S}\right)$, whereas the order for the sublinear sparsity regime is $\Omega\left(\frac{K}{S} \log \frac{N}{K}\right)$. It can confirm that fewer measurements are required in the linear sparsity regime, compared to the sublinear sparsity regime. Next, from the sufficient conditions, we observe an inverse relationship between M and S , owing to the joint sparsity structure. This relationship implies that taking more measurement vectors S reduces the number of required measurements M for a reliable support set reconstruction. Then, the relationship can be used for explaining the empirical results of Caione *et al.* [15] and Wu *et al.* [16]. In [16], the authors have reported that the number of transmitted bits per sensor could be inversely reduced by the number of sensors, which implies that the transmission cost of each sensor could be saved. The result can be confirmed by our inverse relationship by considering S and M as the number of sensors and the number of transmitted bits per sensor, respectively. In [15], S and M are considered as the number of DTIs and the number of samples of each DTI, respectively. Again, it has been observed from [15] that the joint sparsity structure enabled the number of samples of each DTI to be inversely reduced by the number of DTIs, reducing the acquisition time for each DTI. These results can be confirmed by our inverse relationship.

Theorem 2: For any $\rho > 1$, we let $\delta = \rho^{-1}(1 - K/M)x_{\min}^2$, N and K be fixed. If the number of measurements can satisfy $M \geq K + 1$, the failure probability p_{err} defined in (18) converges to zero as taking infinitely many measurement vectors.

Proof: The proof is given in Section 2.6.3.

Theorem 2 suggests that with $M \geq K + 1$, a reliable support set reconstruction for noisy MMV with different sensing matrices is possible by taking an infinite number of measurement vectors. As the impact of noise can disappear in our sufficient condition, we believe that the support set reconstruction becomes robust against noise by taking sufficiently many measurement vectors.

2.3.2. Discussions on the Sufficient Conditions

We now examine the effect of SNR_{\min} on the sufficient conditions of Theorem 1. The aim is to determine the relationship amongst S , M and SNR_{\min} for a reliable support set reconstruction.

Corollary 1: For any $\rho > 1$, we let $\delta = \rho^{-1}(1 - K/M)x_{\min}^2$. The sufficient conditions of Theorem 1 are

rewritten as

$$M > K + \left(\frac{-\sqrt[3]{S} + (\sqrt{S} \times \text{SNR}_{\min})^{-1}}{1 - \rho^{-1}} \right)^2 4K \log \frac{N}{K} \quad (23)$$

in the sublinear sparsity regime and

$$M > K + \left(\frac{-\sqrt[3]{S} + (\sqrt{S} \times \text{SNR}_{\min})^{-1}}{1 - \rho^{-1}} \right)^2 4K (1 - \log \beta) \quad (24)$$

in the linear sparsity regime.

Proof: The proof is given in Section 2.6.4

Corollary 1 suggests that for a fixed M , a reliable support set reconstruction is possible by taking more measurement vectors S , although SNR_{\min} is low. Namely, we observe a noise reduction effect, which shows that using the joint sparsity structure leads to an increase in SNR_{\min} or a decrease in σ^2 by the square root of S . This effect can explain the improvement in the reconstruction quality of the DTIs, as empirically reported in [16].

We then improve our noise reduction effect by considering that SNR_{\min} is larger than a certain value.

Corollary 2: For any $\rho > 3$, we let $\delta = \rho^{-1}(1 - K/M)x_{\min}^2$ and $\alpha = 2/3$. If

$$\text{SNR}_{\min} \geq \frac{\alpha}{1 - \rho^{-1} - \alpha} = \frac{2\rho}{\rho - 3}, \quad (25)$$

the sufficient conditions of Theorem 1 are rewritten as

$$M > K + \frac{S^{-1} + (S \times \text{SNR}_{\min})^{-1}}{1 - \rho^{-1}} 4K \log \frac{N}{K} \quad (26)$$

in the sublinear sparsity regime, and

$$M > K + \frac{S^{-1} + (S \times \text{SNR}_{\min})^{-1}}{1 - \rho^{-1}} 4K (1 - \log \beta) \quad (27)$$

in the linear sparsity regime.

Proof: The proof is given in Section 2.6.4.

Corollary 2 requires $\rho > 3$ to ensure that the lower bound in (25) is positive. A simple computation shows that Corollary 2 requires fewer measurements in both the regimes compared to Corollary 1 because

$$\begin{aligned}
\left(\frac{\sqrt[3]{S} + (\sqrt{S} \times \text{SNR}_{\min}^{-1})}{1 - \rho^{-1}} \right)^2 &= S^{-1} \left(\frac{1 + \text{SNR}_{\min}^{-1}}{1 - \rho^{-1}} \right)^2 \\
&\geq S^{-1} \left(\frac{1 + \text{SNR}_{\min}^{-1}}{1 - \rho^{-1}} \right) \\
&= \frac{S^{-1} + (S \times \text{SNR}_{\min}^{-1})^{-1}}{1 - \rho^{-1}}
\end{aligned}$$

where the second inequality is owing to

$$\frac{1 + \text{SNR}_{\min}^{-1}}{1 - \rho^{-1}} = \frac{1}{t} > 1$$

for any $\rho > 3$ and t defined in (71). Then, Corollary 2 improves the noise reduction effect observed in Corollary 1 by showing that SNR_{\min} is increased by S for the region of SNR_{\min} in (25).

Theorem 2 suggests, it is to be noted, that $M = K + 1$ is sufficient for a reliable support set reconstruction if S is sufficiently large with a fixed N and K . Then, it would be interesting to determine how large S should be required for achieving the minimum number of measurements at each sensor, i.e., $M = K + 1$. In wireless sensor networks [55], energy sources used in sensors are very limited due to limitation of sensor sizes. Thus, minimizing the energy used for transmission of data at each sensor which often leads to extending the lifetime of the sensor battery is a value of importance. This point is noted in Caione *et. al.* [15] as an advantage of using distributed compressed sensing on joint sparse model-2 signal ensembles (see Section V there). Corollary 3 which aims to provide a sufficient condition on S for achieving $M = K + 1$ thus is motivated.

Corollary 3: Let N and K be fixed and finite. For any $\rho > 1$, we let $\delta = \rho^{-1} (K + 1)^{-1} x_{\min}^2$ and $M = K + 1$.

If the number of measurement vectors satisfies

$$S > \underbrace{\left(\log \binom{N}{K} + 2 \right) - \log \varepsilon}_{:= S^*} \times \max \left[\left| \frac{1}{\log \mu_{\mathcal{I}}} \right|, \left| \frac{1}{\log \mu_{\mathcal{J}}} \right| \right], \quad (28)$$

a reliable support set reconstruction is possible in the sense that $p_{err} < \varepsilon$ for sufficiently small $\varepsilon \in (0, 1)$,

where $\log \mu_{\mathcal{I}}$ and $\log \mu_{\mathcal{J}}$ are defined in (73) and (75), respectively. Then, the sufficient condition on S

is decreasing with respect to SNR_{\min} .

Proof: The proof is given in Section 2.6.4.

To the best of our knowledge, the sufficient conditions on S for a reliable support set reconstruction have not yet been developed. A similar result has been reported by Tang and Nehorai [22], in which they reported that $M = \Omega\left(K \log \frac{N}{K}\right)$ and $S = \frac{\log N}{\log \log N}$ suffice for a reliable support set reconstruction in noisy MMV with the same sensing matrix, as N is sufficiently large.

It is of interest to examine whether the sufficient condition S^* in (28) is good. For this, we implement the joint typical decoder in (15) and conduct experiments for different values of SNR_{\min} and K , for a fixed $N = 50$. We count the number of failure occurrences, wherein the joint typical decoder fails to reconstruct the support set. We obtain the smallest S^{emp} such that the ratio of the failure occurrences is smaller than $\varepsilon = 0.01$. By comparing S^{emp} with S^* in (28), we see that S^* approaches S^{emp} , as SNR_{\min} is sufficiently large. As an example, we see that $S^{\text{emp}} = 8$ and $S^* = 12$ at $\text{SNR}_{\min} = 20[\text{dB}]$, $K = 2$. Then, at $\text{SNR}_{\min} = 30[\text{dB}]$ and $K = 2$, we obtain that $S^{\text{emp}} = 5$ and $S^* = 6$. A similar trend is observed at $K = 5$. As an example, we see that $S^{\text{emp}} = 12$ and $S^* = 19$ at $\text{SNR}_{\min} = 20[\text{dB}]$ and $K = 5$. Then, we see that $S^{\text{emp}} = 7$ and $S^* = 10$ at $\text{SNR}_{\min} = 30[\text{dB}]$ and $K = 5$.

Fletcher *et al.* [10] have reported that the ML decoder requires $M = K + 1$ measurements for a reliable support set reconstruction in noisy SMV, when the signal-to-noise ratio is sufficiently large. This result can be observed from Corollary 3. Specifically, we assume that SNR_{\min} is sufficiently large for a fixed N and K . Then, from (73) and (75), it is easy to see that

$$\begin{aligned} \lim_{\text{SNR}_{\min} \rightarrow \infty} \log \mu_{\mathcal{I}} &= -\infty, \\ \lim_{\text{SNR}_{\min} \rightarrow \infty} \log \mu_{\mathcal{J}} &= 2^{-1} (1 - \rho^{-1} - \log \rho). \end{aligned}$$

Hence, (28) is simplified to

$$S > \left(\log \left(\binom{N}{K} + 2 \right) - \log \varepsilon \right) \times \left| 2 \left(1 - \rho^{-1} - \log \rho \right)^{-1} \right|. \quad (29)$$

Note that N , K , and ε are fixed. Thus, for a large ρ , we have

$$\left| 1 - \rho^{-1} - \log \rho \right| \gg 2 \left(\log \left(\binom{N}{K} + 2 \right) - \log \varepsilon \right), \quad (30)$$

which leads to $S \geq 1$. This result suggests that the joint typical decoder requires $M = K + 1$ measurements for a reliable support set reconstruction in noisy SMV, whenever SNR_{\min} is sufficiently large and

ρ satisfies (30).

2.3.3. Necessary Condition on M

We specify a necessary condition that must be satisfied by a decoder for a reliable support set reconstruction in noisy MMV with different sensing matrices. Unlike the sufficient conditions of Theorem 1, the necessary condition is presented for a finite N and K .

We begin by transforming (13) into

$$\begin{bmatrix} \mathbf{y}^1 \\ \vdots \\ \mathbf{y}^S \end{bmatrix} = \underbrace{\begin{bmatrix} \mathbf{F}^1 & & \\ & \ddots & \\ & & \mathbf{F}^S \end{bmatrix}}_{=: \mathbf{F} \in \mathbb{R}^{SM \times SN}} \begin{bmatrix} \mathbf{x}^1 \\ \vdots \\ \mathbf{x}^S \end{bmatrix} + \begin{bmatrix} \mathbf{n}^1 \\ \vdots \\ \mathbf{n}^S \end{bmatrix} \quad (31)$$

$=: \mathbf{y} \in \mathbb{R}^{SM}$ $=: \mathbf{x} \in \mathbb{R}^{SN}$ $=: \mathbf{n} \in \mathbb{R}^{SM}$

where \mathbf{x} is an SK -sparse vector belonging to an infinite set

$$\mathcal{X}_{x_{\min}} := \left\{ \mathbf{x} \in \mathbb{R}^{SN} \mid |x(i)| \geq x_{\min}, \forall i \in \mathcal{I}, |\mathcal{I}| = SK \right\}$$

where $x(i)$ is the i th element of \mathbf{x} and \mathcal{I} is the support set of \mathbf{x} . Owing to the joint sparsity structure, the number of possible support sets is $\binom{N}{K}$. Then, we define a failure probability as:

$$p_{err} := \mathbb{E}_{\mathbf{F}} \sup_{\mathbf{x} \in \mathcal{X}_{x_{\min}}} \mathbb{P} \left\{ \hat{\mathcal{I}} \neq \mathcal{I} \mid \mathbf{x}, \mathbf{F} \right\} \quad (32)$$

where $\hat{\mathcal{I}}$ is an estimate of the support set based on \mathbf{y} and \mathbf{F} in (31). Then, Lemma III-3 of [11] yields

$$\sup_{\mathbf{x} \in \mathcal{X}_{x_{\min}}} \mathbb{P} \left\{ \hat{\mathcal{I}} \neq \mathcal{I} \mid \mathbf{x}, \mathbf{F} \right\} \geq \min_{\hat{\mathbf{x}} \in \mathcal{X}_{\{x_{\min}\}}} \max_{\mathbf{x} \in \mathcal{X}_{\{x_{\min}\}}} \mathbb{P} \left\{ \hat{\mathbf{x}} \neq \mathbf{x} \mid \mathbf{x}, \mathbf{F} \right\} \quad (33)$$

where $\hat{\mathbf{x}}$ is an estimate for \mathbf{x} based on \mathbf{y} and \mathbf{F} in (31) and

$$\mathcal{X}_{\{x_{\min}\}} := \left\{ \mathbf{x} \in \mathbb{R}^{SN} \mid x(i) = x_{\min}, \forall i \in \mathcal{I}, |\mathcal{I}| = SK \right\}$$

which is a finite set. Assume that \mathbf{x} is uniformly distributed over this finite set. Applying Fano's inequality [51] to (33) yields

$$\begin{aligned} \max_{\mathbf{x} \in \mathcal{X}_{\{x_{\min}\}}} \mathbb{P} \left\{ \hat{\mathbf{x}} \neq \mathbf{x} \mid \mathbf{x}, \mathbf{F} \right\} &\geq \mathbb{P} \left\{ \hat{\mathbf{x}} \neq \mathbf{x} \mid \mathbf{F} \right\} \\ &\geq 1 - \frac{\mathbb{I}(\mathbf{x}; \mathbf{y} \mid \mathbf{F}) + \log 2}{\log \left(\left| \mathcal{X}_{\{x_{\min}\}} \right| - 1 \right)} \end{aligned} \quad (34)$$

where \mathbf{x} and $\hat{\mathbf{x}}$ belong to the finite set $\mathcal{X}_{\{x_{\min}\}}$ and $\mathbb{I}(\mathbf{x}; \mathbf{y})$ is the mutual information between \mathbf{x} and \mathbf{y} . We

| | Our results | Yuzhe and Rao [23] |
|---|---|--|
| Linear sparsity regime $\lim_{N \rightarrow \infty} \frac{K}{N} = \beta \in (0, 1/2)$ | $M = \Omega\left(K + \frac{K}{S}\right)$ | Not presented |
| Sublinear sparsity regime $\lim_{N \rightarrow \infty} \frac{K}{N} = 0$ | $M = \Omega\left(\frac{K}{S} \log \frac{N}{K}\right)$ | $M = \Omega\left(\frac{K \log N}{\min(K, S)}\right)$ |
| N and K are finite $(\text{SNR}_{\min} \rightarrow \infty \text{ or } S \rightarrow \infty)$ | $M \geq K + 1$ | Not presented |

Table 2.4.1: Sufficient conditions on M for support set reconstruction

get a necessary condition on M to ensure that the lower bound in (34) is bounded away from zero, as follows:

Theorem 3: Let N and K are fixed and finite. In (31), if the number of measurements satisfies

$$M < \frac{2K \log \frac{N}{K} - 2 \log 2}{S \log(1 + K \times \text{SNR}_{\min})} \quad (35)$$

then the failure probability p_{err} defined in (32) is bounded away from zero.

Proof: The proof is given in Section 2.6.3.

2.4. Relations to the Existing Information-Theoretic Results

2.4.1. Relations to Noisy MMV with the Same Sensing Matrix [23]

Jin and Rao [23] have exploited the Chernoff bound to obtain a tight sufficient condition on M for a reliable support set reconstruction for noisy MMV with the same sensing matrix in the sublinear sparsity regime. Owing to the complicated form of their sufficient condition, they could not clearly show the benefits facilitated by the joint sparsity structure. Thus, they simplified their condition under scenarios such as: *i)* a low noise-level scenario and *ii)* a scenario with S identical sparse vectors. In Table 2.4.1, we summarize our sufficient conditions on M , and compare them to that of [23] under the low noise-level scenario in the sublinear sparsity regime.

First, in a low noise-level scenario, as shown in Table 2.4.1, the sufficient condition [23] for noisy MMV with the same sensing matrix is

$$M = \Omega\left(\frac{K \log N}{\min(K, S)}\right). \quad (36)$$

If $S < K$, the sufficient conditions (21) and (36) have the same order, implying that there is no significant performance gap in the support set reconstruction between the models. If $S > K$, (36) becomes $M = \Omega(\log N)$, whereas (21) becomes $M = \Omega\left(\frac{K}{S} \log N\right)$.

It implies that noisy MMV with different sensing matrices is superior to noisy MMV with the same sensing matrix or $S > K$, with respect to M for a reliable support set reconstruction. This comparison results support the perception presented in Section 2.1.3, wherein a more reliable support set reconstruction could be expected in a noiseless MMV with different sensing matrices owing to the linear independency of the measurement vectors. Moreover, it validates the perception, even in the presence of noise.

Second, we consider a scenario with S identical sparse vectors. Then, the sufficient condition of [23] is

$$M = \Omega\left(\frac{K \log N}{\log\left(1 + S \|\mathbf{x}\|_2^2 / \sigma^2\right)}\right). \quad (37)$$

From (37), we observe that σ^2 is reduced by a factor of S . However, the noise reduction effect for noisy MMV with the same sensing matrix requires a restriction, where all the sparse vectors should be identical, which can be hardly achieved in practice. In contrast, the noise reduction effect for noisy MMV with different sensing matrices does not require this restriction, as shown in Corollaries 1 and 2.

2.4.2. Relations to Noisy SMV [12]

Akcakaya and Tarokh [12] have used the joint typical decoder to establish the sufficient conditions on M for a reliable support set reconstruction in noisy SMV. They exploited the exponential inequalities [56] to obtain the upper bounds on the sum of the weighted chi-square random variables. In this subsection, we demonstrate that the approaches developed in this paper are superior to the use of the exponential inequalities. Thus, we use the exponential inequalities to generalize their bounds for noisy MMV with different sensing matrices. We give Propositions 1 and 2 to prove that the generalized bounds are worse than the bounds of Lemmas 1 and 2.

Proposition 1: For any positive δ , we have

$$\mathbb{P}\{\mathcal{E}_{\mathcal{I}}^c\} \leq 2p(d_1) \leq 2p_{1,\text{exp}}$$

where both $p(d_1)$ and d_1 are given in Lemma 1, and

$$p_{1,\text{exp}} := \exp\left(-\frac{S\delta^2}{4\sigma^4} \frac{M^2}{M-K+2\delta M/\sigma^2}\right). \quad (38)$$

Proof: The proof is given in Section 2.6.5.

Proposition 2: For any $\mathcal{J} \in \mathcal{S} \setminus \mathcal{I}$ and any $\delta > 0$ such that

$$0 < \delta < (1-K/M)x_{\min,\mathcal{J}}^2, \quad (39)$$

we have

$$\mathbb{P}\{\mathcal{E}_{\mathcal{J}}\} \leq p\left(d_{2,\lambda_{\min}(\mathbf{r}_{\mathcal{J}})} - 1\right) \leq p_{2,\mathcal{J},\text{exp}}$$

where both $p\left(d_{2,\lambda_{\min}(\mathbf{r}_{\mathcal{J}})} - 1\right)$ and $d_{2,\lambda_{\min}(\mathbf{r}_{\mathcal{J}})}$ are given in Lemma 2 and

$$p_{2,\mathcal{J},\text{exp}} := \exp\left(-\frac{S^2(M-K)}{4\sum_{s=1}^S \alpha_{\mathcal{J},s}^2} \left(x_{\min,\mathcal{J}}^2 - \frac{M\delta}{M-K}\right)^2\right) \quad (40)$$

and $\alpha_{\mathcal{J},s}$ is defined in (49) and $x_{\min,\mathcal{J}}^2$ is defined in (53).

Proof: The proof is given in Section 2.6.5.

If $S=1$, we see that $p_{1,\text{exp}}$ and $p_{2,\mathcal{J},\text{exp}}$ are equal to the bounds of Akcakaya and Tarokh [12]. Propositions 1 and 2 state that the bounds on the failure probability of Lemmas 1 and 2 are tighter than the bounds of [12] for noisy SMV.

2.5. Conclusions

We have studied a support set reconstruction problem for CS with noisy MMV with different sensing matrices. The union and Chernoff bounds have been used to obtain the upper bound of the failure probability of the support set reconstruction, and Fano's inequality has been used to obtain the lower bound of this failure probability. As we have obtained the upper bound by analyzing an exhaustive search decoder, the bound is used to measure the performance of CS with noisy MMV with different sensing matrices. We have then developed the necessary and sufficient conditions in terms of the sparsity K , the ambient dimension N , the number of measurements M , the number of measurement vectors S , and the

minimum signal-to-noise ratio SNR_{\min} . They can be useful as guidelines to determine the system parameters in various CS applications with noisy MMV with different sensing matrices.

The conditions are interpreted to provide theoretical explanations for the benefits facilitated by the joint sparsity structure in noisy MMV with different sensing matrices:

- i.* From the sufficient conditions of Theorem 1, we have observed the inverse relationship between M and S . Owing to the inverse relation, we can take fewer measurements M per each measurement vector for a reliable support set reconstruction by taking more measurement vectors S .
- ii.* From the sufficient conditions of Corollaries 1 and 2, we have observed the noise reduction effect, which shows that the usage of the joint sparsity structure results in an increase in SNR_{\min} or a decrease in σ^2 by a factor of S . Therefore, the support set reconstruction can be robust against noise by taking sufficiently many measurement vectors.
- iii.* From Theorem 2, we have shown that $M = K + 1$ is achieved for a fixed N and K , as S is sufficiently large. From Corollary 3, we have provided the sufficient condition on S to reconstruct the support set for a fixed N , K , and $M = K + 1$.

The above theoretical explanations confirm the empirical benefits of the joint sparsity structure, as shown in CS applications with noisy MMV with different sensing matrices [15][16].

We have compared our sufficient conditions for noisy MMV with different sensing matrices with the other existing results [23] for noisy MMV with the same sensing matrix. For a low-level noise scenario with $S \geq K$, we have shown that the number of measurements for a reliable support set reconstruction for noisy MMV with different sensing matrices is lesser than that for noisy MMV with the same sensing matrix. Also, we have observed that noisy MMV with different sensing matrices enjoys the noise reduction effect for arbitrary jointly sparse vectors, whereas, this noise reduction exists in noisy MMV with the same sensing matrix, only if all the sparse vectors are identical.

2.6. Appendices

2.6.1. Appendix A: Lemmas 1 and 2

This section presents Lemmas 1 and 2, which give upper bounds of the probabilities of the failure events defined in (16) and (17), respectively. Also, for simplicity, we define

$$p(x) = \exp\left(-\frac{S(M-K)}{2}x\right)(1+x)^{\frac{S(M-K)}{2}}. \quad (41)$$

Lemma 1: For any positive δ , we have

$$\begin{aligned} \mathbb{P}\{\mathcal{E}_T^c\} &\leq 2\exp\left(-\frac{S(M-K)}{2}d_1\right)(1+d_1)^{\frac{S(M-K)}{2}} \\ &= 2p(d_1) \end{aligned} \quad (42)$$

where the function p is defined in (41), and

$$d_1 := \frac{M\delta}{(M-K)\sigma^2} > 0. \quad (43)$$

Proof: From (16), we have

$$\mathbb{P}\{\mathcal{E}_T^c\} = \mathbb{P}\{Z_T \leq W_1\} + \mathbb{P}\{Z_T \geq W_2\} \quad (44)$$

where Z_T is defined in Lemma 3, and

$$W_i = S(M-K) + (-1)^i SM\delta/\sigma^2, \quad i = 1, 2.$$

Applying the Chernoff bound [54] to (44) yields

$$\begin{aligned} \mathbb{P}\{\mathcal{E}_T^c\} &\leq \sum_{i=1}^2 \exp(-t_i W_i) \mathbb{E}[\exp(t_i Z_T)] \\ &= \sum_{i=1}^2 \underbrace{\exp(-t_i W_i)(1-2t_i)^{-S(M-K)/2}}_{=: f(t_i; W_i)} \end{aligned} \quad (45)$$

where the equality is from Lemma 3, $t_1 < 0$ and $t_2 \in (0, 1/2)$.

As each $f(t_i; W_i)$ is convex, $t_i = t_i^*$ at $f^{(1)}(t_i; W_i) = 0$ yields the minimizer of $f(t_i; W_i)$, where

$$t_i^* = 2^{-1}(1 - W_i^{-1}S(M-K)), \quad i = 1, 2.$$

Thus, $f(t_i; W_i) \geq f(t_i^*; W_i)$ for each i . If $W_1 \leq 0$, it is clear that $\mathbb{P}\{Z_T \leq W_1\} = 0$ because Z_T is quadratic.

Thus, we have

$$\begin{aligned} \mathbb{P}\{\mathcal{E}_T^c\} &= \mathbb{P}\{Z_T \geq W_2\} \\ &\leq f(t_2^*; W_2) \\ &= p(d_1) \end{aligned} \quad (46)$$

where $p(d_1)$ and d_1 are defined in (42) and (43), respectively. If $W_1 > 0$ then $f(t_1^*; W_1) \leq f(t_2^*; W_2)$

because

$$\log f(t_1^*; W_1) - \log f(t_2^*; W_2) = S(M-K)[d_1 + 2\log(1-d_1) - 2\log(1+d_1)] < 0.$$

Thus,

$$\begin{aligned} \mathbb{P}\{\mathcal{E}_{\mathcal{I}}^c\} &= f(t_1^*; W_1) + f(t_2^*; W_2) \\ &\leq 2f(t_2^*; W_2) \\ &= 2\exp\left(-\frac{S(M-K)}{2}d_1\right)(1+d_1)^{\frac{S(M-K)}{2}}. \end{aligned} \quad (47)$$

Finally, combining (46) and (47) leads to (42).

Lemma 2: Let $\mathcal{J} \in \mathcal{S} \setminus \mathcal{I}$ and a matrix $\mathbf{R}_{\mathcal{J}}$ be

$$\mathbf{R}_{\mathcal{J}} = \begin{bmatrix} \alpha_{\mathcal{J},1} \mathbf{I}_{M-K} & & & \\ & \alpha_{\mathcal{J},2} \mathbf{I}_{M-K} & & \\ & & \ddots & \\ & & & \alpha_{\mathcal{J},S} \mathbf{I}_{M-K} \end{bmatrix} \quad (48)$$

where

$$\alpha_{\mathcal{J},s} := \sigma^2 + \|\mathbf{x}_{\mathcal{I} \setminus \mathcal{J}}^s\|_2^2 > 0. \quad (49)$$

Consider any positive δ such that

$$0 < \delta < (1-K/M)(\lambda_{\min}(\mathbf{R}_{\mathcal{J}}) - \sigma^2)$$

where $\lambda_{\min}(\mathbf{R}_{\mathcal{J}})$ is the smallest eigenvalue of $\mathbf{R}_{\mathcal{J}}$. Then, we have

$$\begin{aligned} \mathbb{P}\{\mathcal{E}_{\mathcal{J}}\} &\leq \exp\left(-\frac{S(M-K)}{2}(d_{2,\lambda_{\min}(\mathbf{R}_{\mathcal{J}})} - 1)\right) d_{2,\lambda_{\min}(\mathbf{R}_{\mathcal{J}})}^{\frac{S(M-K)}{2}} \\ &= p(d_{2,\lambda_{\min}(\mathbf{R}_{\mathcal{J}})} - 1) \\ &\leq p(d_{2,\alpha^*} - 1) \end{aligned} \quad (50)$$

where the function p is defined in (41),

$$d_{2,\lambda_{\min}(\mathbf{R}_{\mathcal{J}})} := \frac{(M-K)\sigma^2 + M\delta}{(M-K)\lambda_{\min}(\mathbf{R}_{\mathcal{J}})} \in (0,1), \quad (51)$$

$$\alpha^* := \sigma^2 + x_{\min}^2, \quad (52)$$

and

$$x_{\min}^2 = \min_{\mathcal{J} \in \mathcal{S} \setminus \mathcal{I}} \underbrace{\min_{s \in \{1, 2, \dots, S\}} \|\mathbf{x}_{\mathcal{I} \setminus \mathcal{J}}^s\|_2^2}_{=: x_{\min, \mathcal{J}}^2} \quad (53)$$

Proof: From (17), we have

$$\mathbb{P}\{\mathcal{E}_{\mathcal{J}}\} = \mathbb{P}\{Z_{\mathcal{J}} < W_1\} - \mathbb{P}\{Z_{\mathcal{J}} < W_2\} \leq \mathbb{P}\{Z_{\mathcal{J}} < W_1\} \quad (54)$$

where $Z_{\mathcal{J}}$ is defined in Lemma 4, and

$$W_i = S(M - K)\sigma^2 - (-1)^i SM\delta, \quad i = 1, 2. \quad (55)$$

Applying the Chernoff bound [54] to (54) yields for $t < 0$,

$$\begin{aligned} \mathbb{P}\{\mathcal{E}_{\mathcal{J}}\} &\leq \exp(-tW_1) \mathbb{E}[\exp(tZ_{\mathcal{J}})] \\ &= \exp(-tW_1) \prod_{i=1}^{S(M-K)} (1 - 2t\lambda_i(\mathbf{R}_{\mathcal{J}}))^{-1/2} \\ &\leq \exp(-tW_1) (1 - 2t\lambda_{\min}(\mathbf{R}_{\mathcal{J}}))^{-S(M-K)/2} \\ &=: f(t; W_1) \end{aligned} \quad (56)$$

where the equality is from Lemma 4 and the second inequality is due to that all the eigenvalues are positive. We then define a function $h(t) := \log f(t; W_1)$. Then, we have

$$h^{(2)}(t) = 2S(M - K)\lambda_{\min}^2(\mathbf{R}_{\mathcal{J}}) (1 - 2t\lambda_{\min}(\mathbf{R}_{\mathcal{J}}))^{-2} > 0$$

which implies that h is convex with respect to t . It leads to that f in (56) is logarithmically convex. Thus

$t = t^*$ at $f^{(1)}(t; W_1) = 0$ yields the minimizer of $f(t; W_1)$ where

$$t^* = 2^{-1} (\lambda_{\min}^{-1}(\mathbf{R}_{\mathcal{J}}) - W_1^{-1}S(M - K)) < 0.$$

Substituting t^* in (56) yields

$$\begin{aligned} \mathbb{P}\{\mathcal{E}_{\mathcal{J}}\} &\leq f(t^*; W_1) \\ &= \exp\left(-\frac{S(M - K)}{2} (d_{2, \lambda_{\min}(\mathbf{R}_{\mathcal{J}})} - 1)\right) d_{2, \lambda_{\min}(\mathbf{R}_{\mathcal{J}})}^{\frac{S(M - K)}{2}} \\ &= p(d_{2, \lambda_{\min}(\mathbf{R}_{\mathcal{J}})} - 1). \end{aligned} \quad (57)$$

where $d_{2, \lambda_{\min}(\mathbf{R}_{\mathcal{J}})}$ is defined in (51) and p is defined in (41).

Next, let $\beta = 2^{-1}S(M - K)$ and $x = d_{2, \lambda_{\min}(\mathbf{R}_{\mathcal{J}})}$ in the upper bound (57). Then, we have

$$p(x - 1) = x^\beta \exp(-\beta(x - 1)),$$

where

$$\frac{\partial p(x-1)}{\partial x} = \beta x^\beta \exp(-\beta(x-1))(x^{-1}-1) > 0 \quad (58)$$

and

$$\frac{\partial x}{\partial \lambda_{\min}(\mathbf{R}_{\mathcal{J}})} = -x < 0. \quad (59)$$

Due to (58) and (59), we have

$$\begin{aligned} \frac{\partial p(x-1)}{\partial \lambda_{\min}(\mathbf{R}_{\mathcal{J}})} &= \frac{\partial p(x-1)}{\partial x} \frac{\partial x}{\partial \lambda_{\min}(\mathbf{R}_{\mathcal{J}})} \\ &= -\beta x^{\beta-1} \exp(-\beta(x-1))(x^{-1}-1) < 0 \end{aligned}$$

which shows that the upper bound in (57) is decreasing with respect to $\lambda_{\min}(\mathbf{R}_{\mathcal{J}})$. Then, remind that the matrix in (48) is the covariance matrix of a multivariate Gaussian vector \mathbf{b} in (68). Then for any incorrect support set, its smallest eigenvalue can be easily computed and lower bounded by

$$\lambda_{\min}(\mathbf{R}_{\mathcal{J}}) = \min_{s \in \{1, 2, \dots, S\}} \alpha_{\mathcal{J}, s} = \sigma^2 + x_{\min, \mathcal{J}}^2 \geq \alpha^* \quad (60)$$

where $x_{\min, \mathcal{J}}^2$ is defined in (53) and α^* is defined in (52). Thus, for any incorrect support set $\mathcal{J} \in \mathcal{S} \setminus \mathcal{I}$, we conclude that

$$\begin{aligned} \mathbb{P}\{\mathcal{E}_{\mathcal{J}}\} &\leq p(d_{2, \lambda_{\min}(\mathbf{R}_{\mathcal{J}})} - 1) \\ &\leq p(d_{2, \alpha^*} - 1) \end{aligned}$$

which completes the proof.

2.6.2. Appendix B: Lemmas 3 and 4

First of all, we give the Scharf's theorem [57] to compute the moment generating function of a quadratic random variable. We then make Lemmas 3 and 4 to give the moment generating functions of the random variables of $\mathcal{E}_{\mathcal{I}}^c$ and $\mathcal{E}_{\mathcal{J}}$ that were used in the proofs of Lemmas 1 and 2, respectively.

Scharf's theorem [Page 64, [57]]: Let $\mathbf{b} \in \mathbb{R}^N$ be a multivariate Gaussian vector with a mean \mathbf{m} and a covariance \mathbf{R} . Then, a random variable

$$Q \triangleq (\mathbf{b} - \mathbf{m})^T (\mathbf{b} - \mathbf{m})$$

is quadratic with $\mathbb{E}[Q] = \text{tr}[\mathbf{R}]$, $\mathbb{V}[Q] = 2\text{tr}[\mathbf{R}^T \mathbf{R}]$ and for any t

$$\mathbb{E}[\exp(tQ)] = \prod_{i=1}^N (1 - 2t\lambda_i(\mathbf{R}))^{-1/2}.$$

Lemma 3: In (16), define a quadratic random variable

$$Z_{\mathcal{I}} := \sum_{s=1}^S \|\mathbf{Q}(\mathbf{F}_{\mathcal{I}}^s) \mathbf{y}^s\|_2^2 / \sigma^2. \quad (61)$$

Then, we have

$$\begin{aligned} \mathbb{E}[Z_{\mathcal{I}}] &= S(M - K), \\ \mathbb{V}[Z_{\mathcal{I}}] &= 2S(M - K), \end{aligned}$$

and for any $0 < t < 0.5$,

$$\mathbb{E}[\exp(tZ_{\mathcal{I}})] = (1 - 2t)^{-S(M-K)/2}. \quad (62)$$

Proof: The orthogonal projection matrix is decomposed as

$$\mathbf{Q}(\mathbf{F}_{\mathcal{I}}^s) = \mathbf{U}_{\mathcal{I}}^s \mathbf{D}^s (\mathbf{U}_{\mathcal{I}}^s)^T$$

where \mathbf{D}^s is a diagonal matrix, whose first $M - K$ diagonals are ones and the remains are zeros, and $\mathbf{U}_{\mathcal{I}}^s$ is a unitary matrix. Then, we have

$$\begin{aligned} Z_{\mathcal{I}} &= \sum_{s=1}^S \|\mathbf{Q}(\mathbf{F}_{\mathcal{I}}^s) \mathbf{y}^s\|_2^2 / \sigma^2 \\ &= \sum_{s=1}^S \|\mathbf{Q}(\mathbf{F}_{\mathcal{I}}^s) \mathbf{n}^s\|_2^2 / \sigma^2 \\ &= \sum_{s=1}^S \left\| \mathbf{D}^s \underbrace{(\mathbf{U}_{\mathcal{I}}^s)^T \mathbf{n}^s}_{=\mathbf{w}^s} / \sigma^2 \right\|_2^2 \\ &= \sum_{s=1}^S \|\mathbf{D}^s \mathbf{w}^s\|_2^2 \end{aligned} \quad (63)$$

where \mathbf{w}^s is a multivariate Gaussian vector with mean $\mathbf{0}_M$ and covariance \mathbf{I}_M . Since the first $M - K$ diagonal elements of each diagonal matrix are ones, we have

$$\begin{aligned} Z_{\mathcal{I}} &= \sum_{s=1}^S \|\mathbf{D}^s \mathbf{w}^s\|_2^2 \\ &= \sum_{s=1}^S \sum_{i=1}^{M-K} |w^s(i)|^2 \\ &= \sum_{s=1}^S (\mathbf{w}_p^s)^T \mathbf{w}_p^s \\ &= \mathbf{w}^T \mathbf{w} \end{aligned} \quad (64)$$

which is quadratic, where

$$\mathbf{w}_p^s = \left[w^s(1) \quad w^s(2) \quad \cdots \quad w^s(M-K) \right]^T$$

and

$$\mathbf{w} = \left[(\mathbf{w}_p^1)^T \quad (\mathbf{w}_p^2)^T \quad \cdots \quad (\mathbf{w}_p^S)^T \right]^T. \quad (65)$$

In (63), \mathbf{w}^s is determined by $\mathbf{U}_{\mathcal{I}}^s$ and \mathbf{n}^s . Since the elements of $\mathbf{U}_{\mathcal{I}}^s$ and \mathbf{n}^s are independent, \mathbf{w}^i and \mathbf{w}^j are mutually independent for any $1 \leq i \neq j \leq S$. The covariance matrix of \mathbf{w} is an identity matrix. Thus, applying the Scharf's theorem to $Z_{\mathcal{I}}$ completes the proof.

Lemma 4: In (17), for any $\mathcal{J} \in \mathcal{S} \setminus \mathcal{I}$, define a quadratic random variable

$$Z_{\mathcal{J}} := \sum_{s=1}^S \left\| \mathbf{Q}(\mathbf{F}_{\mathcal{J}}^s) \mathbf{y}^s \right\|_2^2. \quad (66)$$

Then, we have

$$\begin{aligned} \mathbb{E}[Z_{\mathcal{J}}] &= \text{tr}[\mathbf{R}_{\mathcal{J}}], \\ \mathbb{V}[Z_{\mathcal{J}}] &= 2\text{tr}[\mathbf{R}_{\mathcal{J}}^T \mathbf{R}_{\mathcal{J}}], \end{aligned}$$

and for any t ,

$$\mathbb{E}[\exp(tZ_{\mathcal{J}})] = \prod_{i=1}^{S(M-K)} (1 - 2t\lambda_i(\mathbf{R}_{\mathcal{J}}))^{-1/2},$$

where $\mathbf{R}_{\mathcal{J}}$ is given in (48).

Proof: Similar to the proof of Lemma 3,

$$\mathbf{Q}(\mathbf{F}_{\mathcal{J}}^s) = \mathbf{U}_{\mathcal{J}}^s \mathbf{D}^s (\mathbf{U}_{\mathcal{J}}^s)^T$$

where \mathbf{D}^s is a diagonal matrix, whose first $M-K$ diagonals are ones and the remains are zeros, and $\mathbf{U}_{\mathcal{J}}^s$ is a unitary matrix. Then,

$$\begin{aligned} Z_{\mathcal{J}} &= \sum_{s=1}^S \left\| \mathbf{Q}(\mathbf{F}_{\mathcal{J}}^s) \mathbf{y}^s \right\|_2^2 \\ &= \sum_{s=1}^S \left\| \mathbf{Q}(\mathbf{F}_{\mathcal{J}}^s) \mathbf{c}^s \right\|_2^2 \\ &= \sum_{s=1}^S \left\| \mathbf{D}^s \underbrace{(\mathbf{U}_{\mathcal{J}}^s)^T \mathbf{c}^s}_{=\mathbf{b}^s} \right\|_2^2 \\ &= \sum_{s=1}^S \left\| \mathbf{D}^s \mathbf{b}^s \right\|_2^2 \end{aligned} \quad (67)$$

where \mathbf{b}^s is a multivariate Gaussian vector with mean $\mathbf{0}_M$ and

$$\mathbb{V}[\mathbf{b}^s] = \left(\sigma^2 + \|\mathbf{x}_{\mathcal{I} \setminus \mathcal{J}}^s\|_2^2 \right) \mathbf{I}_M$$

and

$$\mathbf{c}^s = \mathbf{n}^s + \sum_{u \in \mathcal{I} \setminus \mathcal{J}} \mathbf{f}_u^s x^s(u).$$

Since the first $M - K$ diagonal elements of each diagonal matrix are ones, we have

$$\begin{aligned} Z_{\mathcal{J}} &= \sum_{s=1}^S \|\mathbf{D}^s \mathbf{b}^s\|_2^2 \\ &= \sum_{s=1}^S \sum_{i=1}^{M-K} |b^s(i)|^2 \\ &= \sum_{s=1}^S (\mathbf{b}_p^s)^T \mathbf{b}_p^s \\ &= \mathbf{b}^T \mathbf{b} \end{aligned} \tag{68}$$

which is quadratic, where

$$\mathbf{b}_p^s = [b^s(1) \quad b^s(2) \quad \cdots \quad b^s(M-K)]^T$$

and

$$\mathbf{b} = [(\mathbf{b}_p^1)^T \quad (\mathbf{b}_p^2)^T \quad \cdots \quad (\mathbf{b}_p^S)^T]^T.$$

In (68), \mathbf{b}^s is determined by $\mathbf{U}_{\mathcal{J}}^s, \mathbf{n}^s$ and $\{\mathbf{f}_u^s : u \in \mathcal{I} \setminus \mathcal{J}\}$. Since the elements of $\mathbf{U}_{\mathcal{J}}^s, \mathbf{n}^s$ and $\{\mathbf{f}_u^s : u \in \mathcal{I} \setminus \mathcal{J}\}$ are independent, \mathbf{b}^i and \mathbf{b}^j are mutually independent for any $1 \leq i \neq j \leq S$. As shown in (48), the covariance matrix of \mathbf{b} is diagonal. Thus, applying the Scharf's theorem to $Z_{\mathcal{J}}$ completes the proof.

2.6.3. Appendix C: Proofs of Theorems 1, 2, and 3

Proof of Theorem 1: It is clear that K goes to infinity as N goes to infinity in the linear sparsity regime.

Then, let $M = cK$ where $c > 1$. From (42), we have

$$\log \mathbb{P}\{\mathcal{E}_T^c\} \leq 2^{-1} SK(c-1) \underbrace{(\log(1+d_1) - d_1)}_{=: A} + \log 2$$

where $A < 0$ due to (43). Thus,

$$\lim_{N \rightarrow \infty} \mathbb{P}\{\mathcal{E}_I^c\} \leq \lim_{K \rightarrow \infty} \exp\left(2^{-1}SK(c-1)A + \log 2\right) = 0$$

implying that the probability that the correct support set is not δ jointly typical with all the measurement vectors vanishes. Then, from (50), we have

$$\begin{aligned} \log \sum_{\mathcal{J} \in \mathcal{S} \setminus \mathcal{I}} \mathbb{P}\{\mathcal{E}_{\mathcal{J}}\} &\leq \log \binom{N}{K} p(d_{2,a^*} - 1) \\ &= \log \binom{N}{K} + 2^{-1}SK(c-1) \underbrace{(\log(1-t) + t)}_{=: \gamma} \\ &\leq K \underbrace{\left(1 + \log \frac{N}{K} + 2^{-1}S(c_1-1)\gamma\right)}_{=: \eta} \end{aligned} \quad (69)$$

where the last inequality is due to

$$\binom{N}{K} \leq \exp\left(K \log \frac{Ne}{K}\right). \quad (70)$$

In (69), $\gamma < 0$ for any t such that

$$t = \frac{1 - \rho^{-1}}{1 + \text{SNR}_{\min}^{-1}} \in (0, 1). \quad (71)$$

If $c > 1 + S^{-1}v_1$, then $\eta < 0$, which yields

$$\lim_{N \rightarrow \infty} \sum_{\mathcal{J} \in \mathcal{S} \setminus \mathcal{I}} \mathbb{P}\{\mathcal{E}_{\mathcal{J}}\} \leq \lim_{K \rightarrow \infty} \exp(K\eta) = 0$$

implying that the probability that all incorrect support sets are δ jointly typical with all the measurement vectors vanishes. Thus the failure probability defined in (18) converges to zero if M satisfies (19).

Next, the remain is to derive (21) in the sublinear sparsity regime. Let $M = K + cK \log \frac{N}{K}$ where $c > 1$.

From, (42), we have

$$\log \mathbb{P}\{\mathcal{E}_I^c\} \leq 2^{-1}ScK \log \frac{N}{K} \underbrace{(\log(1+d_1) - d_1)}_{=: A} + \log 2$$

where $A < 0$ due to (43). Thus, we have

$$\lim_{N \rightarrow \infty} \mathbb{P}\{\mathcal{E}_I^c\} \leq \lim_{N \rightarrow \infty} \exp\left(2^{-1}ScKA \log \frac{N}{K} + \log 2\right) = 0$$

implying that the probability that the correct support set is not δ jointly typical with all the measurement vectors vanishes. Then, from (50), we have

$$\begin{aligned}
\log \sum_{\mathcal{J} \in \mathcal{S} \setminus \mathcal{I}} \mathbb{P}\{\mathcal{E}_{\mathcal{J}}\} &\leq \log \left(\binom{N}{K} p(d_{2,\alpha^*} - 1) \right) \\
&= \log \binom{N}{K} + 2^{-1} ScK \underbrace{(\log(1-t) + t)}_{=: \gamma} \log \frac{N}{K} \\
&\leq K \underbrace{(1 + 2^{-1} Sc\gamma)}_{=: \eta} \log \frac{N}{K} + K
\end{aligned}$$

where the last inequality is due to the bound in (70) and $\gamma < 0$ for any t defined in (71). If $c > S^{-1}v_2$, then $\eta < 0$, which yields

$$\begin{aligned}
\lim_{N \rightarrow \infty} \sum_{\mathcal{J} \in \mathcal{S} \setminus \mathcal{I}} \mathbb{P}\{\mathcal{E}_{\mathcal{J}}\} &\leq \lim_{N \rightarrow \infty} \exp(K\eta \log \frac{N}{K} + K) \\
&= 0
\end{aligned}$$

implying that the probability that all incorrect support sets are δ jointly typical with all the measurement vectors vanishes. Thus, the failure probability defined in (18) converges to zero if M satisfies (21), which completes the proof.

Proof of Theorem 2: From Lemma 1, we have

$$\mathbb{P}\{\mathcal{E}_{\mathcal{I}}^c\} \leq 2 \left(\underbrace{\exp\left(-\frac{M-K}{2}d_1\right)}_{=: \mu_{\mathcal{I}}} (1+d_1)^{\frac{M-K}{2}} \right)^S. \quad (72)$$

If $M \geq K+1$, we have

$$\log \mu_{\mathcal{I}} = 2^{-1} (M-K)(\log(1+d_1) - d_1) < 0 \quad (73)$$

due to (43), which implies $\mu_{\mathcal{I}} < 1$. From Lemma 2,

$$\mathbb{P}\{\mathcal{E}_{\mathcal{J}}\} \leq \left(\underbrace{\exp\left(-\frac{M-K}{2}(d_{2,\alpha^*} - 1)\right)}_{=: \mu_{\mathcal{J}}} d_{2,\alpha^*}^{\frac{M-K}{2}} \right)^S. \quad (74)$$

Similarly, if $M \geq K+1$, we have

$$\log \mu_{\mathcal{J}} = 2^{-1} (M-K)(\log(1-t) + t) < 0 \quad (75)$$

due to (71), which implies $\mu_{\mathcal{J}} < 1$. Thus, we conclude

$$\lim_{S \rightarrow \infty} p_{err} \leq 2 \lim_{S \rightarrow \infty} \mu_{\mathcal{I}}^S + \binom{N}{K} \lim_{S \rightarrow \infty} \mu_{\mathcal{J}}^S = 0$$

for $M \geq K+1$ which completes the proof.

Proof of Theorem 3: The mutual information in (34) is bounded by

$$\begin{aligned}
\mathbb{I}(\mathbf{x}; \mathbf{y} | \mathbf{F}) &= h(\mathbf{y} | \mathbf{F}) - h(\mathbf{y} | \mathbf{x}, \mathbf{F}) \leq h(\mathbf{y}) - h(\mathbf{n}) \\
&\leq \sum_{i=1}^{SM} h(y_i) - h(\mathbf{n}) \\
&\leq 2^{-1} SM \left(\log(2\pi e(Kx_{\min}^2 + \sigma^2)) - \log(2\pi e\sigma^2) \right) \\
&= 2^{-1} SM \log(1 + K \times \text{SNR}_{\min})
\end{aligned}$$

where $h(\mathbf{x})$ is the differential entropy of \mathbf{x} , and $h(\mathbf{x} | \mathbf{y})$ is the conditional entropy of \mathbf{x} given \mathbf{y} . Then, the last inequality is due to that the Gaussian distribution maximizes the differential entropy. The denominator in (34) is bounded by

$$\begin{aligned}
\log\left(\left|\mathcal{X}_{\{x_{\min}\}}\right| - 1\right) &= \log\left(\binom{N}{K} - 1\right) \\
&> K \log \frac{N}{K}
\end{aligned}$$

for sufficiently large N . Then, we have

$$\begin{aligned}
p_{err} &= \mathbb{E}_{\mathbf{F}} \sup_{\mathbf{x} \in \mathcal{X}_{\min}} \mathbb{P}\{\hat{\mathcal{I}} \neq \mathcal{I} | \mathbf{x}, \mathbf{F}\} \\
&\geq \mathbb{E}_{\mathbf{F}} \min_{\hat{\mathbf{x}} \in \mathcal{X}_{\{x_{\min}\}}} \max_{\mathbf{x} \in \mathcal{X}_{\{x_{\min}\}}} \mathbb{P}\{\hat{\mathbf{x}} \neq \mathbf{x} | \mathbf{x}, \mathbf{F}\} \\
&> 1 - \frac{2^{-1} SM \log(1 + K \times \text{SNR}_{\min}) + \log 2}{K \log \frac{N}{K}}.
\end{aligned} \tag{76}$$

From (76), the failure probability is bounded away from zero by zero if (35) is satisfied, which completes the proof.

2.6.4. Appendix D: Proofs of Corollaries 1, 2 and 3

Proof of Corollary 1: From the inequality $\log(1+x) \leq \frac{2x}{2+x}$ for $x \in (-1, 0]$,

$$\begin{aligned}
v_2 &= -\frac{2}{\log(1-t) + t} \\
&< (4-2t)t^{-2} \\
&< 4t^{-2}
\end{aligned} \tag{77}$$

where t is defined in (71). Then, we have

$$\frac{v_2}{S} < \frac{4}{St^2}. \tag{78}$$

From (71),

$$\sqrt{St} = \frac{1 - \rho^{-1}}{\sqrt[3]{S} + (\sqrt{S} \times \text{SNR}_{\min})^{-1}} \quad (79)$$

Combining (21), (78) and (79) leads to (23). This approach is used to get (24) using the following equality

$$\nu_1 = \nu_2 (1 - \log \beta) \quad (80)$$

where $\lim_{N \rightarrow \infty} \frac{K}{N} = \beta \in (0, 1/2)$, which completes the proof.

Proof of Corollary 2: Substituting $\alpha = 2/3$ in (25), and rearranging the result with respect to t can yield, $2/3 \leq t < 1$ where t is defined in (71). Then from (77), a simple computation yields that

$$\begin{aligned} \nu_2 &< (4 - 2t)t^{-2} \\ &\leq 4t^{-1} \end{aligned}$$

which immediately yields that

$$\frac{\nu_2}{S} < \frac{4}{St}. \quad (81)$$

where

$$St = \frac{1 - \rho^{-1}}{S^{-1} + (S \times \text{SNR}_{\min})^{-1}}. \quad (82)$$

Combining (21), (81) and (82) leads to (26). This approach is used to get (27) using (80), which completes the proof.

Proof of Corollary 3: We assume that $\mu_{\mathcal{I}} \geq \mu_{\mathcal{J}}$ and

$$\begin{aligned} p_{err} &\leq \mathbb{P}\{\mathcal{E}_{\mathcal{I}}^c\} + \sum_{\mathcal{J} \in \mathcal{S} \setminus \mathcal{I}} \mathbb{P}\{\mathcal{E}_{\mathcal{J}}\} \\ &\leq \left(\binom{N}{K} + 2 \right) \mu_{\mathcal{I}}^S \\ &< \varepsilon \\ &< 1. \end{aligned} \quad (83)$$

Then, if the number of measurement vectors satisfies

$$S > \frac{\log \varepsilon - \log \left(\binom{N}{K} + 2 \right)}{\log \mu_{\mathcal{I}}} > 0, \quad (84)$$

(83) is achieved for small ε , and hence, a reliable support set reconstruction is possible. If $\mu_{\mathcal{I}} < \mu_{\mathcal{J}}$, we

obtain inequalities similar to (83) and (84) by replacing $\mu_{\mathcal{I}}$ by $\mu_{\mathcal{J}}$, where

$$S > \frac{\log \varepsilon - \log \left(\binom{N}{K} + 2 \right)}{\log \mu_{\mathcal{J}}} > 0. \quad (85)$$

Combining (84) and (85) yields (28).

Next, a simple computation yields that for any d_1 in (43),

$$\frac{\partial \log \mu_{\mathcal{I}}}{\partial d_1} = -\frac{d_1}{2(1+d_1)} < 0$$

where $\log \mu_{\mathcal{I}}$ is given in (73). From (43), we see $d_1 \propto \text{SNR}_{\min}$ that leads to

$$\log \mu_{\mathcal{I}} \propto \text{SNR}_{\min}^{-1}.$$

Also, for any t in (71), we have

$$\frac{\partial \log \mu_{\mathcal{J}}}{\partial t} = -\frac{t}{2(1-t)} < 0$$

where $\log \mu_{\mathcal{J}}$ is given in (75). From (43), we see $t \propto \text{SNR}_{\min}$ that leads to

$$\log \mu_{\mathcal{J}} \propto \text{SNR}_{\min}^{-1}.$$

Thus, the sufficient condition on S in (28) turns out to be a decreasing function with respect to SNR_{\min} , which completes the proof.

2.6.5. Appendix E: Proofs of Propositions 1 and 2

First of all, we introduce the exponential inequalities [56], and use them in the proofs of Propositions 1 and 2.

The exponential inequalities [56]: Let

$$Y_i, i = 1, 2, \dots, D$$

be i.i.d. Gaussian variables with a zero mean and a unit variance. Then, let

$$\alpha_i, i = 1, 2, \dots, D$$

be non-negative. We set

$$\begin{aligned} |\alpha|_{\infty} &= \sup |\alpha_i|, \\ |\alpha|_2^2 &= \sum_{i=1}^D \alpha_i^2, \end{aligned}$$

and let

$$Y = \sum_{i=1}^D \alpha_i (Y_i^2 - 1). \quad (86)$$

Then, the following inequalities hold for any positive x

$$\mathbb{P}\{Y \geq 2|\alpha|_2 \sqrt{x} + 2|\alpha|_\infty x\} \leq \exp(-x), \quad (87)$$

$$\mathbb{P}\{Y \leq -2|\alpha|_2 \sqrt{x}\} \leq \exp(-x). \quad (88)$$

Proof of Proposition 1: In the proof of Lemma 3, $Z_{\mathcal{I}}$ is represented by

$$Z_{\mathcal{I}} = \sum_{s=1}^S \sum_{i=1}^{M-K} w^s(i)^2$$

where $w^s(i)$ is Gaussian with a zero mean and a unit variance. Define a random variable below

$$\begin{aligned} Y &= Z_{\mathcal{I}} - S(M-K) \\ &= \sum_{s=1}^S \sum_{i=1}^{M-K} (w^s(i)^2 - 1) \end{aligned}$$

which is of the form of (86). Then, we have

$$\mathbb{P}\{\mathcal{E}_{\mathcal{I}}^c\} = \underbrace{\mathbb{P}\{Y \leq -SM\delta/\sigma^2\}}_{=:A} + \underbrace{\mathbb{P}\{Y \geq SM\delta/\sigma^2\}}_{=:B}.$$

Combining A with (88) gives

$$\begin{aligned} \mathbb{P}\{Y \leq -SM\delta/\sigma^2\} &= \mathbb{P}\{Y \leq -2\sqrt{S(M-K)x}\} \\ &\leq \underbrace{\exp\left(-\frac{SM^2\delta^2}{4(M-K)\sigma^4}\right)}_{=:C} \end{aligned}$$

and combining B with (87) gives

$$\begin{aligned} \mathbb{P}\{Y \geq SM\delta/\sigma^2\} &= \mathbb{P}\{Y \geq 2\sqrt{S(M-K)x} + 2x\} \\ &\leq p_{1,\text{exp}} \end{aligned}$$

where $p_{1,\text{exp}}$ is defined in (38). It is readily seen that $p_{1,\text{exp}} \geq C$, which leads to $\mathbb{P}\{\mathcal{E}_{\mathcal{I}}^c\} \leq 2p_{1,\text{exp}}$.

Next, from (42) and (38), we have

$$\log p(d_1) = 2^{-1} S(M-K)(\log(1+d_1) - d_1)$$

and

$$\log p_{1,\text{exp}} = -2^{-1} S(M-K)d_1^2(2+4d_1)^{-1}$$

where $d_1 > 0$ is defined in (43). Then, we have

$$\log \frac{p(d_1)}{p_{1,\text{exp}}} = \frac{S(M-K)}{2} \underbrace{\left(\log(1+d_1) - d_1 + d_1^2 (2+4d_1)^{-1} \right)}_{=:g(d_1)}.$$

For any $d_1 > 0$, we have $\max_{d_1 > 0} g(d_1) = 0$ and

$$\frac{\partial g(d_1)}{\partial d_1} = -d_1^2 (2+3d_1)(1+d_1)^{-1} (1+2d_1)^{-2} < 0.$$

Thus, we conclude

$$\log \frac{p(d_1)}{p_{1,\text{exp}}} \leq 0,$$

which completes the proof.

Proof of Proposition 2: In the proof of Lemma 4, $Z_{\mathcal{J}}$ is represented by

$$\begin{aligned} Z_{\mathcal{J}} &= \sum_{s=1}^S \sum_{i=1}^{M-K} b^s(i)^2 \\ &= \sum_{s=1}^S \sum_{i=1}^{M-K} \alpha_{\mathcal{J},s} g^s(i)^2 \end{aligned}$$

where $\alpha_{\mathcal{J},s}$ is defined in (49) and $g^s(i)$ is Gaussian with a zero mean and a unit variance. Then, define a new random variable below

$$\begin{aligned} Y &= Z_{\mathcal{J}} - S(M-K) \\ &= \sum_{s=1}^S \sum_{i=1}^{M-K} \alpha_{\mathcal{J},s} (g^s(i)^2 - 1). \end{aligned}$$

which is of the form of (86). Then, from (54), we have

$$\begin{aligned} \mathbb{P}\{\mathcal{E}_{\mathcal{J}}\} &\leq \mathbb{P}\left\{ Y < SM\delta - (M-K) \sum_{s=1}^S \|\mathbf{x}_{\mathcal{I} \setminus \mathcal{J}}^s\|_2^2 \right\} \\ &\leq \mathbb{P}\left\{ Y < \underbrace{SM\delta - S(M-K) \chi_{\min, \mathcal{J}}^2}_{=:A} \right\} \\ &\leq p_{2, \mathcal{J}, \text{exp}} \end{aligned} \tag{89}$$

where $p_{2, \mathcal{J}, \text{exp}}$ is defined in (40), the last inequality is due to (88). Due to (39), A is negative. Thus the exponential inequality of (88) gives the upper bound $p_{2, \mathcal{J}, \text{exp}}$.

Next, from (50) and (40), we have

$$\log p\left(d_{2, \lambda_{\min}(\mathbf{R}_{\mathcal{J}})} - 1\right) = 2^{-1} S(M-K)(t + \log(1-t))$$

and

$$\begin{aligned}\log p_{2,\mathcal{J},\text{exp}} &\geq -\frac{S(M-K)}{4} \left(\frac{x_{\min,\mathcal{J}}^2 - \frac{M\delta}{M-K}}{x_{\min,\mathcal{J}}^2 + \sigma^2} \right)^2 \\ &= -4^{-1} S(M-K) t^2\end{aligned}$$

where $t \in (0,1)$ is defined in (71) and the inequality is due to (60). Then, we have

$$\log \frac{p\left(d_{2,\lambda_{\min}(\mathbf{R}_{\mathcal{J}})} - 1\right)}{p_{2,\mathcal{J},\text{exp}}} \leq \frac{S(M-K)}{4} \underbrace{\left(t^2 + 2t + 2\log(1-t)\right)}_{=:g(t)}.$$

For any $t \in (0,1)$, we have $\max_{t \in (0,1)} g(t) = 0$ and

$$\frac{\partial g(t)}{\partial t} = -2t^2(1-t)^{-1} < 0.$$

Thus we conclude

$$\log \frac{p\left(d_{2,\lambda_{\min}(\mathbf{R}_{\mathcal{J}})} - 1\right)}{p_{2,\mathcal{J},\text{exp}}} \leq 0$$

which completes the proof.

Chapter 3: Fast Mixed Integer Quadratic Programming for Sparse Signal Estimation

3.1. Introduction

Compressed sensing [6] has attracted attention because it allows for the acquisition of signal samples at a rate lower than the Nyquist rate. The theory of compressed sensing is built under a sparsity assumption that an n -dimensional signal \mathbf{x} can be sparsely represented using a few non-zero coefficients in a basis. This sparse signal is sampled to yield an m -dimensional measurement vector

$$\mathbf{b} = \mathbf{F}\mathbf{x} + \mathbf{n}$$

where \mathbf{n} is a noise vector of size $m \times 1$ and \mathbf{F} is a sensing matrix of size $m \times n$. Since $m < n$, the problem of estimating \mathbf{x} is ill-posed. However, the theory shows that \mathbf{x} is reliably estimated by solving the l_0 -norm problem:

$$\min_{\mathbf{x}} \quad \tau \|\mathbf{x}\|_0 + 2^{-1} \|\mathbf{b} - \mathbf{F}\mathbf{x}\|_2^2 \quad (90)$$

where τ is a positive regularization value. In (90), the l_0 -norm function is non-convex and discontinuous. Indeed, (90) is known to be NP-hard. Instead of solving (90), researches aim to solve an l_1 -norm problem which can be formulated by relaxing the l_0 -norm function in (90) as follows:

$$\min_{\mathbf{x}} \quad \tau \|\mathbf{x}\|_1 + 2^{-1} \|\mathbf{b} - \mathbf{F}\mathbf{x}\|_2^2. \quad (91)$$

Candes [6] has proved that a solution to (91) is equivalent to a solution to (90) if \mathbf{F} satisfies a *restricted isometry constant* (RIC) condition. Many l_1 -norm-based methods have been proposed to solve (91). The earliest method is l_1l_s [58]. This method is based on an interior point technique and can estimate \mathbf{x} from a small number of iterations. In each of iteration, l_1l_s solves a linear equation system expressed in a matrix-vector product form. The matrix in each system changes as the iteration passes. Thus, factorization methods such as the LU decomposition and the QR decomposition can be used to reduce the computations for solving this system. However, solving multiple linear equation systems can be still burdensome. This makes its computational cost too high for high-dimensional \mathbf{x} . Then, *gradient projection sparse recovery* [59], homotopy [60], split-Bregman [61] and *your algorithms for l_1* (YALL1) [62] have been pro-

posed to solve (91). These are first-order-type methods that do not require matrix-inversions in all iterations. This implies that they are computationally tractable to estimate high-dimensional \mathbf{x} . But, there are known problems on (91). First, the l_1 -norm function yields a biased estimation for large non-zero magnitudes, while the l_0 -norm function considers all non-zero magnitudes equally [63]. Second, if \mathbf{F} does not satisfy the RIC condition, – either m is small or the elements of \mathbf{F} are correlated – then a solution to (91) is sub-optimal [64].

In the literature, l_0 -norm-based methods such as *iterative hard thresholding* (IHT) [25], variants of IHT [26]–[28], and *mean doubly augmented Lagrangian* (MDAL) [31] have been proposed to solve (90). Zhu and Dong [28] have shown that their method is superior to homotopy [60]. Dong and Zhang [31] have shown that MDAL restores images with higher quality than those recovered by split-Bregman [61]. These results in [28], [31] suggest that more accurate sparse signal estimation is conducted using the l_0 -norm function rather than the l_1 -norm function.

Recently, Bourguignon *et al.* [32] have proposed a novel approach to solve (90). This approach aims to find an estimate for \mathbf{x} and the positions of the non-zero elements of \mathbf{x} , i.e., the support set. From (90), they have made a mixed integer quadratic programming (MIQP) problem:

$$\begin{aligned} \min_{\mathbf{u} \in \{0,1\}^n, \mathbf{x} \in \mathbb{R}^n} \quad & \tau \mathbf{1}_n^T \mathbf{u} + 2^{-1} \|\mathbf{b} - \mathbf{F}\mathbf{x}\|_2^2 \\ \text{subject to} \quad & |\mathbf{x}| \leq M \mathbf{u} \end{aligned} \quad (92)$$

where the binary vector \mathbf{u} indicates *the support set* and M is a positive value. For (92), M can be known in practical contexts. For example, if \mathbf{x} is an 8-bit greyscale image, M is set to be 255. Bertsimas *et al.* [33] have proposed methods to estimate upper bounds on M if both \mathbf{F} and \mathbf{b} are known. Bourguignon *et al.* [32] used CPLEX [34] to solve (92) and demonstrated that CPLEX is superior to IHT [xx] for sparse signal estimation. According to explanations in [32], this result is because CPLEX exhaustively searches for a whole feasible space to find the global solution to (92) while IHT finds a local solution to (90).

CPLEX [34] is a commercial solver which can be used to solve MIQP problems. Then, CPLEX is implemented based on a branch-and-cut method [66] that is a combination of a cutting plane method [67] with a branch-and-bound method [65]. As noted in [40], the branch-and-cut method has non-polynomial computational costs in the worst-case and can be troublesome to solve MIQP problems with large variables. This implies the computational intractability of using CPLEX in solving integer programming prob-

lems with large variables. In 3.4, we empirically confirm this computational intractability.

In this chapter, we aim to propose a fast method based on the *alternating direction method* (ADM) for solving (92). We analyze the computational cost per iteration of the proposed method, referred to as ADM-MIQP. According to this result, we can show that ADM-MIQP is a first-order-type method. We evaluate the quality of its solution using metrics defined as follows.

First, we define *support set error* (SSE) as

$$d_1(\mathbf{u}, \hat{\mathbf{u}}) := k^{-1} \sum_{i=1}^n \|\mathbf{u}(i) - \hat{\mathbf{u}}(i)\| \quad (93)$$

where $\hat{\mathbf{u}}$ is a solution to (92) and \mathbf{u} is constructed from

$$\begin{aligned} \mathbf{u}(i) &= 0 & \text{if } i \notin \mathcal{I} \\ \mathbf{u}(i) &= 1 & \text{if } i \in \mathcal{I} \end{aligned}$$

where \mathcal{I} is the support set to be detected. Second, we define *mean square error* (MSE) as

$$d_2(\mathbf{x}, \tilde{\mathbf{x}}) := n^{-1} \|\mathbf{x} - \tilde{\mathbf{x}}\|_2^2 \quad (94)$$

where \mathbf{x} is an original signal and $\tilde{\mathbf{x}}$ is an estimate of \mathbf{x} . Then, we compare ADM-MIQP with both YALL1 and MDAL in terms of SSE and MSE. We observe the following:

- ADM-MIQP significantly surpasses both MDAL and YALL1 in terms of both MSE and SSE.
- ADM-MIQP exhibits good estimation performance close to the performance of ORACLE that knows support set *a priori*.
- ADM-MIQP is computationally tractable for solving (92) with the problem dimension up to the order of one million.
- ADM-MIQP exhibits a computational cost given by $O(n^{1.3})$ in our simulations.

The rest of this chapter is organized as follows. Section 3.2 gives a summary about ADM. Section 3.3 elucidates the derivation and computational costs associated with ADM-MIQP. Also, Section 3.3 gives results of comparison between our proposed approach with that of [40] for solving our problem. Section 3.4 gives simulation studies and shows the superiority of ADM-MIQP compared to other ADM-based methods [28], [62]. Section 3.5 gives conclusions of this paper.

3.2. Alternating Direction Method (ADM)

A branch and bound method [65] finds the global solution to a MIQP problem. But, since this method has non-polynomial computational costs, it is computationally intractable for solving MIQP problems with large variables. We turn instead to ADM for solving the MIQP problem (92). In this sub-section, we introduce ADM and provide its recent results.

It is well-known that ADM is a powerful technique for solving a large-scale convex problem. ADM involves the following steps: *i*) ADM splits this problem into sub-problems and *ii*) solves alternatively these sub-problems until conditions are satisfied. ADM is then proven to find the global solution to this problem as the iteration continues [36], [37]. As the number of iterations approaches infinity, the solution generated by ADM converges to an optimal solution which satisfies the *Karush-Kuhn-Tucker* conditions to a convex problem.

Recently, ADM has been empirically shown to be a powerful technique to find accurate solutions to integer programming problems [38]–[40]. Yadav *et al.* [38] have used ADM to solve an image separation problem that can be modeled as a binary quadratic programming. Souto and Dinis [39] have then solved a signal decoding problem modeled as an integer quadratic programming with an equality constraint using ADM. Last, Takapoui *et al.* [40] have solved problems modeled as MIQPs with an equality constraint, and shown that ADM could be greatly faster than a commercial integer programming method. We are motivated to derive a computationally tractable and accurate method to solve (92) using ADM, inspired by these results in [38]–[40].

3.3. Sparse Signal Estimation via MIQP Problem

The MIQP problem (92) has an inequality constraint and this constraint can be formulated into an equality constraint. Thus, we can use the approach of [40] to solve (92) by taking a further formulation. But, no explicit discussion on how this approach can be used to solve a MIQP problem which has an inequality constraint was given in [40]. In Section 3.3.3, we derive an algorithm based on the approach of [40] for solving (92). We call it *Takapoui's Algorithm with Inequality Constraint* (TAIC). We then compare ADM-MIQP with TAIC with respect to the computational cost per iteration. We show that ADM-MIQP requires much less computation per iteration than TAIC does.

3.3.1. Derivation of ADM-MIQP

It is convenient to solve a single minimization problem rather than a joint minimization problem. To this end, we define

$$\mathbf{d} = \begin{bmatrix} \mathbf{x}^T & \mathbf{u}^T \end{bmatrix}^T \in \mathbb{R}^n \times \{0,1\}^n$$

which is nonconvex. Then, (92) is reformulated into

$$\min_{\mathbf{d}} \quad 2^{-1} \mathbf{d}^T \mathbf{Q} \mathbf{d} + \mathbf{q}^T \mathbf{d} \quad \text{subject to} \quad \mathbf{A} \mathbf{d} \leq \mathbf{0}_{2n}$$

where $\mathbf{Q} = \begin{bmatrix} \mathbf{F}^T \mathbf{F} & \mathbf{O}_n \\ \mathbf{O}_n & \mathbf{O}_n \end{bmatrix}$, $\mathbf{q} = \begin{bmatrix} -\mathbf{F}^T \mathbf{b} \\ \tau \mathbf{1}_n \end{bmatrix}$, and $\mathbf{A} = \begin{bmatrix} \mathbf{I}_n & -M \mathbf{I}_n \\ -\mathbf{I}_n & -M \mathbf{I}_n \end{bmatrix}$. We define a nonnegative vector \mathbf{z} . Then,

$$\begin{aligned} \min_{\mathbf{d}, \mathbf{z}} \quad & 2^{-1} \mathbf{d}^T \mathbf{Q} \mathbf{d} + \mathbf{q}^T \mathbf{d} + I_{\mathcal{X}}(\mathbf{z}) \\ \text{subject to} \quad & \mathbf{A} \mathbf{d} + \mathbf{z} = \mathbf{0}_{2n} \end{aligned} \quad (95)$$

where $I_{\mathcal{X}}(\mathbf{z})$ is an indicator function of $\mathcal{X} := \{\mathbf{z} | \mathbf{z} \geq \mathbf{0}_{2n}\}$, i.e., $I_{\mathcal{X}}(\mathbf{z}) = 0$ for $\mathbf{z} \in \mathcal{X}$ and $I_{\mathcal{X}}(\mathbf{z}) = \infty$ for $\mathbf{z} \notin \mathcal{X}$.

We apply ADM into (95) to obtain

$$\begin{aligned} \mathbf{d}_{t+1} &= \arg \min_{\mathbf{d}} \quad 2^{-1} \mathbf{d}^T [\mathbf{Q} + \rho \mathbf{A}^T \mathbf{A}] \mathbf{d} + \mathbf{q}_{1,t}^T \mathbf{d}, \\ \mathbf{z}_{t+1} &= \arg \min_{\mathbf{z}} \quad I_{\mathcal{X}}(\mathbf{z}) + \rho 2^{-1} \mathbf{z}^T \mathbf{z} + (\rho \mathbf{A} \mathbf{d}_{t+1} - \lambda_t)^T \mathbf{z}, \\ \lambda_{t+1} &= \lambda_t - \rho (\mathbf{A} \mathbf{d}_{t+1} + \mathbf{z}_{t+1}), \end{aligned} \quad (96)$$

where $\mathbf{q}_{1,t} = \mathbf{q} - \mathbf{A}^T (\lambda_t - \rho \mathbf{z}_t)$, λ is the dual variable, and $\rho > 0$ is a penalty value. The sub-problem on \mathbf{d} is an MIQP. Thus, solving this problem is difficult, but we separate it into a pair of problems in terms of \mathbf{x} and \mathbf{u} , respectively:

$$\begin{aligned} \mathbf{x}_{t+1} &= \arg \min_{\mathbf{x}} \quad 2^{-1} \mathbf{x}^T (\mathbf{F}^T \mathbf{F} + 2\rho \mathbf{I}_n) \mathbf{x} + \mathbf{q}_{1,t}^T [1:n] \mathbf{x}, \\ \mathbf{u}_{t+1} &= \arg \min_{\mathbf{u}} \quad \rho M^2 \mathbf{u}^T \mathbf{u} + \mathbf{q}_{1,t}^T [n+1:2n] \mathbf{u}. \end{aligned}$$

Since the sub-problem on \mathbf{x} has a quadratic objective function, we have an analytic closed-form solution:

$$\begin{aligned} \mathbf{x}_{t+1} &= -(\mathbf{F}^T \mathbf{F} + 2\rho \mathbf{I}_n)^{-1} \mathbf{q}_{1,t} [1:n] \\ &= (\mathbf{F}^T \mathbf{D} \mathbf{F} \mathbf{q}_{1,t} [1:n] - \mathbf{q}_{1,t} [1:n]) / (2\rho) \end{aligned} \quad (97)$$

where the second equality is due to the Woodbury formula [xx] and $\mathbf{D} := (\mathbf{F}\mathbf{F}^T + 2\rho\mathbf{I}_m)^{-1}$. The sub-problem on \mathbf{u} is a binary quadratic programming. Since $\mathbf{u}^T \mathbf{u} = \mathbf{1}_n^T \mathbf{u}$, we have

$$\mathbf{u}_{t+1} = \arg \min_{\mathbf{u}} \left(\rho M^2 \mathbf{1}_n + \mathbf{q}_{l,t}[n+1:2n] \right)^T \mathbf{u}$$

which has an analytic closed-form solution as follows:

$$\begin{aligned} \mathbf{u}_{t+1}(i) &= 0 & \text{if } \eta_i \geq 0 \\ \mathbf{u}_{t+1}(i) &= 1 & \text{if } \eta_i < 0 \end{aligned} \quad (98)$$

where $\eta_i = \rho M^2 + \mathbf{q}_{l,t}(n+i)$. The sub-problem on \mathbf{z} is solved to yield a solution:

$$\mathbf{z}_{t+1} = \max \left(\mathbf{0}_{2n}, \lambda_t / \rho + \begin{bmatrix} M \mathbf{u}_{t+1} - \mathbf{x}_{t+1} \\ M \mathbf{u}_{t+1} + \mathbf{x}_{t+1} \end{bmatrix} \right) \quad (99)$$

where “max” operation is performed element-wise.

In summary, we have formulated (95) from (92) by adding the non-negative vector and the indicator function. We then have applied ADM into (95) to produce the iterations given in (96). We have provided analytic solutions to these sub-problems. Then, we have summarized ADM-MIQP in Table 3.3.1.

In [36], [37], it has been proved that for any positive penalty value ρ , ADM can find the global solution to a convex problem. The penalty value only affects the convergence speed, not the quality of the solution. Researchers have discussed how this penalty value can be chosen to improve the speed [36], [37]. However, our problem (92) is non-convex due to the non-convex variable \mathbf{d} . In the literature, there are no convergence studies for non-convex problems with non-convex variables, to the best of our knowledge. It is difficult to find convergence conditions for the penalty value in the problem (92) that is being solved using ADM-MIQP. Afonso *et al.* [68] have solved (90) using their own algorithm derived based on ADM. They have set their penalty value as $\rho = \tau/10$ in their simulations. Ghadimi *et al.* [36] have made a tool for setting the penalty value for a strictly convex problem with an inequality constraint. This tool takes a matrix given in the constraint as its input. By inspired by these works, we have relied upon extensive simulations with various penalty values given by a combination of τ and M , i.e.,

$$\rho \in \{ \tau/M, \tau/M^2, \dots, \tau M^2 \},$$

where M is the element of our matrix \mathbf{A} . Based on results of these simulations, we set the penalty value as

$$\rho = \tau/M$$

| | |
|-------------------|--|
| Input parameters: | $\mathbf{x}_0 = \mathbf{0}_n, \mathbf{u}_0 = \mathbf{0}_n, \mathbf{z}_0 = \mathbf{0}_n, \lambda_0 = \mathbf{0}_{2n}$ $\mathbf{F}, \mathbf{b}, \mathbf{A}, \rho, \tau, M, \varepsilon, \text{MaxIter}$ |
|-------------------|--|

| | |
|----------|--|
| Step 1: | set $\mathbf{D} := (\mathbf{F}\mathbf{F}^T + 2\rho\mathbf{I}_m)^{-1}$ |
| Step 2: | for $t = 0, 1, 2, \dots, \text{maxIter}$ |
| Step 3: | update \mathbf{x}_{t+1} by (97). |
| Step 4: | update \mathbf{u}_{t+1} by (98). |
| Step 5: | update \mathbf{z}_{t+1} by (99). |
| Step 6: | update $\mathbf{d}_{t+1} = [\mathbf{x}_{t+1}^T \quad \mathbf{u}_{t+1}^T]^T$. |
| Step 7: | update $\lambda_{t+1} = \lambda_t - \rho(\mathbf{A}\mathbf{d}_{t+1} + \mathbf{z}_{t+1})$. |
| Step 8: | If $\frac{\ \mathbf{d}_{t+1} - \mathbf{d}_t\ _2}{\ \mathbf{d}_{t+1}\ _2} \leq \varepsilon$, then go to Step 10 |
| Step 9: | end for |
| Step 10: | set $\tilde{\mathcal{I}} = \{i \mathbf{u}_t(i) = 1\}$. |
| Step 11: | set $\mathbf{x}_{sol} = \begin{cases} \mathbf{x}(i) = 0 & \text{if } i \notin \tilde{\mathcal{I}} \\ \mathbf{x}_{\tilde{\mathcal{I}}} = \mathbf{F}_{\tilde{\mathcal{I}}}^\dagger \mathbf{b} & \text{o.w.} \end{cases}$. |

Table 3.3.1: The pseudo codes of ADM-MIQP

and use this value in our simulations. In our simulations, we empirically observe that ADM-MIQP with this penalty value can be used to solve (3) for estimating a sparse signal with the accuracy of

$$\frac{\|\mathbf{x} - \tilde{\mathbf{x}}\|_2^2}{\|\mathbf{x}\|_2^2} \leq \varepsilon$$

where \mathbf{x} is an original sparse signal, $\tilde{\mathbf{x}}$ is the estimated sparse signal and ε is sufficiently small.

Any warm-start techniques can be applied into ADM-MIQP for improving its performance. We run ADM-MIQP multiple times with different initial variables randomly generated. Then, we have different solutions, i.e.,

$$\{\mathbf{d}^1, \mathbf{d}^2, \dots, \mathbf{d}^L\}$$

where L is the number of runs of ADM-MIQP. We then select a solution among these multiple solutions via

$$\mathbf{d}_{sol} := \underset{\mathbf{d} \in \{\mathbf{d}^1, \mathbf{d}^2, \dots, \mathbf{d}^L\}}{\text{argmin}} \quad 2^{-1} \mathbf{d}^T \mathbf{Q} \mathbf{d} + \mathbf{q}^T \mathbf{d}.$$

This selected solution is at least guaranteed to be better than the other unselected solutions in terms of the

cost function.

3.3.2. Computation Costs per Iteration

We aim to show that ADM-MIQP is a first-order-type method. The costs of updating \mathbf{z} and \mathbf{u} are both $O(n)$. Then, the cost of updating \mathbf{x} is $O(mn + m^3)$, due to both the matrix inversion and the matrix-vector products. If \mathbf{D} is stored, then this cost can be reduced to $O(mn)$.

Next, in applications such as a single pixel camera [69], [70], a lensless camera, [71], [72] for an image compression [73], a sensing matrix is constructed by randomly taking m rows from an orthogonal matrix. Then, \mathbf{D} becomes a constant value $\frac{1}{1+2\rho}$. As a result, the update on \mathbf{x} is given as

$$\mathbf{x}_{t+1} = \left((1+2\rho)^{-1} \mathbf{F}^T \mathbf{F} \mathbf{q}_{1,t} [1:n] - \mathbf{q}_{1,t} [1:n] \right) / (2\rho). \quad (100)$$

Indeed, if \mathbf{F} is a partial discrete cosine transform (DCT) matrix, all matrix-vector products in (100) can be performed by the fast Fourier transform operation. That is, the update cost for \mathbf{x} can be significantly reduced to $O(n \log n)$.

3.3.3. Comparison with Work [40]

We now derive the algorithm called TAIC (*Takapoui's Algorithm with Inequality Constraint*) by following the approach of [40] for solving the MIQP problem (92) which only has the inequality constraint. As shown in the Section 3.3.1, it is noted that (92) is equal to (95). Then, we define the symbols as follows:

$$\begin{aligned} \tilde{\mathbf{d}} &:= \begin{bmatrix} \mathbf{d} \\ \mathbf{z} \end{bmatrix} \in \mathbb{R}^n \times \{0,1\}^n \times \mathbb{R}_+^{2n}, \\ \tilde{\mathbf{A}} &:= [\mathbf{A} \quad \mathbf{I}_{2n}] \in \mathbb{R}^{2n \times 4n}, \\ \tilde{\mathbf{q}} &:= \begin{bmatrix} \mathbf{q} \\ \mathbf{0}_{2n} \end{bmatrix} \in \mathbb{R}^{4n \times 1}, \\ \tilde{\mathbf{Q}} &:= \begin{bmatrix} \mathbf{Q} & \mathbf{O}_{2n} \\ \mathbf{O}_{2n} & \mathbf{O}_{2n} \end{bmatrix} \in \mathbb{R}^{4n \times 4n}, \end{aligned}$$

where \mathbf{z} is a slack variable. With these symbols, we reformulate (95) into an MIQP problem with an equality constraint

$$\min_{\tilde{\mathbf{d}}} \quad 2^{-1} \tilde{\mathbf{d}}^T \tilde{\mathbf{Q}} \tilde{\mathbf{d}} + \tilde{\mathbf{q}}^T \tilde{\mathbf{d}} \quad \text{subject to} \quad \tilde{\mathbf{A}} \tilde{\mathbf{d}} = \mathbf{0}_{2n}, \tilde{\mathbf{d}} \in \tilde{\mathcal{X}} \quad (101)$$

where $\tilde{\mathcal{X}} := \mathbb{R}^n \times \{0,1\}^n \times \mathbb{R}_+^{2n}$ is a non-convex set. Similar to (95), we also reformulate (101) into a standard form of ADM as follows:

$$\begin{aligned} \min_{\tilde{\mathbf{d}}, \tilde{\mathbf{z}}} \quad & 2^{-1} \tilde{\mathbf{d}}^T \tilde{\mathbf{Q}} \tilde{\mathbf{d}} + \tilde{\mathbf{q}}^T \tilde{\mathbf{d}} + I_{\tilde{\mathcal{X}}}(\tilde{\mathbf{z}}) \\ \text{subject to} \quad & \begin{bmatrix} \tilde{\mathbf{A}} \\ \mathbf{I}_{4n} \end{bmatrix} \tilde{\mathbf{d}} - \begin{bmatrix} \mathbf{O}_{2n \times 4n} \\ \mathbf{I}_{4n} \end{bmatrix} \tilde{\mathbf{z}} = \mathbf{0}_{6n} \end{aligned} \quad (102)$$

where $I_{\tilde{\mathcal{X}}}(\tilde{\mathbf{z}})$ is an indicator function of $\tilde{\mathcal{X}}$ and $\mathbf{O}_{2n \times 4n}$ is the $2n \times 4n$ matrix of zeros.

Then, TAIC is implemented via

$$\begin{aligned} \tilde{\mathbf{d}}_{t+1} &= \arg \min_{\tilde{\mathbf{d}}} \quad 2^{-1} \tilde{\mathbf{d}}^T \tilde{\mathbf{Q}} \tilde{\mathbf{d}}^T + \tilde{\mathbf{q}}^T \tilde{\mathbf{d}}^T + 2^{-1} \rho \left\| g(\tilde{\mathbf{d}}, \tilde{\mathbf{z}}_t, \tilde{\boldsymbol{\lambda}}_t) \right\|_2^2, \\ \tilde{\mathbf{z}}_{t+1} &= \arg \min_{\tilde{\mathbf{z}}} \quad I_{\tilde{\mathcal{X}}}(\tilde{\mathbf{z}}) + 2^{-1} \rho \left\| g(\tilde{\mathbf{d}}_{t+1}, \tilde{\mathbf{z}}, \tilde{\boldsymbol{\lambda}}_t) \right\|_2^2, \\ \tilde{\boldsymbol{\lambda}}_{t+1} &= \tilde{\boldsymbol{\lambda}}_t - \rho g(\tilde{\mathbf{d}}_{t+1}, \tilde{\mathbf{z}}_{t+1}, \mathbf{0}_{6n}), \end{aligned} \quad (103)$$

where $\tilde{\boldsymbol{\lambda}}$ is the dual variable, $\rho > 0$ is a penalty value, and

$$g(\tilde{\mathbf{d}}, \tilde{\mathbf{z}}, \tilde{\boldsymbol{\lambda}}) := \begin{bmatrix} \tilde{\mathbf{A}} \\ \mathbf{I}_{4n} \end{bmatrix} \tilde{\mathbf{d}} - \begin{bmatrix} \mathbf{O}_{2n \times 4n} \\ \mathbf{I}_{4n} \end{bmatrix} \tilde{\mathbf{z}} + \frac{\tilde{\boldsymbol{\lambda}}}{\rho}.$$

It is noted that (95) is formed by adding *one slack variable* to (92). But, (102) is formed by adding *two slack variables* into (92). Thus, there is an intuition that TAIC requires more computational costs per iteration than ADM-MIQP does.

To investigate the validation of our intuition, we restrict our attentions to the sub-problem on $\tilde{\mathbf{d}}$ in (103) that can be simplified to

$$\tilde{\mathbf{d}}_{t+1} = \arg \min_{\tilde{\mathbf{d}}} \quad 2^{-1} \tilde{\mathbf{d}}^T \tilde{\mathbf{D}} \tilde{\mathbf{d}}^T + \mathbf{h}_t^T \tilde{\mathbf{d}} \quad (104)$$

where $\tilde{\mathbf{D}} := \left[\tilde{\mathbf{Q}} + \rho(\tilde{\mathbf{A}}^T \tilde{\mathbf{A}} + \mathbf{I}_{4n}) \right] \in \mathbb{R}^{4n \times 4n}$ and $\mathbf{h}_t := \tilde{\mathbf{q}} - \rho \begin{bmatrix} \tilde{\mathbf{A}} \\ \mathbf{I}_{4n} \end{bmatrix}^T \left(\begin{bmatrix} \mathbf{O}_{2n \times 4n} \\ \mathbf{I}_{4n} \end{bmatrix} \tilde{\mathbf{z}}_t - \tilde{\boldsymbol{\lambda}}_t \right)$.

The sub-problem on $\tilde{\mathbf{d}}$ in (96) has been decomposed into a pair of problems on \mathbf{x} and \mathbf{u} , respectively. But, $\tilde{\mathbf{D}}$ is a non-diagonal matrix that implies that the sub-problem in (104) cannot be decomposed. We then consider an analytic closed form solution to (104) as follows:

$$\tilde{\mathbf{d}}_{t+1} = -\tilde{\mathbf{D}}^{-1} \mathbf{h}_t. \quad (105)$$

For saving computational costs, the inverse matrix in (105) can be stored. Even with this stored matrix,

TAIC takes $O(16n^2)$ computational cost per iteration for conducting (105) due to the matrix-vector product. This cost can be negligible for a small value of n . For a large value of n , it cannot be ignored. On the other hands, ADM-MIQP takes $O(mn)$ computational cost per iteration. It can be seen that TAIC takes more computational costs per iteration for updating the other variables than ADM-MIQP does. Thus, it can be concluded that the cost of ADM-MIQP is greatly less than that of TAIC.

3.4. Simulations Studies

We conduct simulations to show that ADM-MIQP gives a solution to (92). We compare ADM-MIQP with MDAL and YALL1. The reasons for selecting both MDAL and YALL1 as comparative approaches are *a)* these methods are also based on ADM and *b)* are known to be computationally tractable. We define a Gaussian sparse vector ensemble and a Gaussian noise vector ensemble as follows.

Definition 1: The Gaussian sparse vector ensemble is an ensemble of n -dimensional k -sparse vectors, where each vector \mathbf{x} is generated as follows: *a)* the positions of the non-zero values of \mathbf{x} are randomly selected, *b)* the non-zero values are taken from the standard normal distribution and *c)* \mathbf{x} is normalized to produce the l_2 -norm for \mathbf{x} unit.

Definition 2: The Gaussian noise vector ensemble is an ensemble of m -dimensional noise vectors whose elements are independent and identically distributed Gaussian with zero mean and variance σ^2 .

We define the *signal-to-noise ratio* (SNR) as

$$\text{SNR [dB]} := 10 \log_{10} \left(\frac{\|\mathbf{F}\mathbf{x}\|_2^2}{(m\sigma^2)} \right).$$

We then set the parameters of ADM-MIQP, MDAL, and YALL1 as follows. The regularization value is set as $\tau = \sigma\sqrt{2\log n}$ if SNR [dB] is finite and $\tau = 10^{-4}$ if SNR [dB] is infinite. The M value is set as $M = \max_i |\mathbf{x}(i)|$. As we have stated in 3.3.1, our penalty value is set as $\rho = \tau/M$. The penalty value of YALL1 is set as $\rho = \|\mathbf{b}\|_1/m$, used in [62]. But, MDAL with the penalty value used in [31] failed to yield an accurate solution in our simulation. We conducted extensive simulations to find the penalty value for MDAL. Thus, in our simulations, it was set as $\rho = 10\tau$. We terminated these methods either when the number of iterations exceeded 2000 or when $\frac{\|\mathbf{x}_{t+1} - \mathbf{x}_t\|_2}{\|\mathbf{x}_{t+1}\|_2} \leq 10^{-4}$, as was done in [62], for YALL1, and when

$\frac{\|\mathbf{x}_{t+1}-\mathbf{x}_t\|_2}{\|\mathbf{b}\|_2} \leq 10^{-4}$, as in [31] for MDAL and when $\frac{\|\mathbf{d}_{t+1}-\mathbf{d}_t\|_2}{\|\mathbf{d}_{t+1}\|_2} \leq 10^{-4}$ for ADM-MIQP.

We kept in mind that a solution for \mathbf{x} in (92) must satisfy a convex constraint

$$\mathbf{x} \in \left\{ \mathbf{x} \mid -M \leq \mathbf{x}(i) \leq M \right\}$$

where $i = 1, 2, \dots, n$. However, both YALL1 and MDAL are not designed to use this constraint. Therefore, we extended these methods to use the constraint for a fair comparison. Since the constraint is convex, this extension was easily carried out by adding the following codes:

$$\mathbf{x}_t(i) = \min(\max(\mathbf{x}_t(i), M), -M)$$

where $\mathbf{x}_t(i)$ is the i^{th} element of an intermediate solution at the t^{th} iteration. We conduct all simulations using a computer with Intel (R) Core (TM) i7-3820 processor clocked at 3.6 GHz. The codes are in [74].

3.4.1. Convergence Behaviors of ADM-MIQP

We remind that both SSE defined in (93) and MSE defined in (94) can be used to evaluate the quality of a solution given by ADM-MIQP. We use both of the metrics to study how this solution behaves. Since the elements of \mathbf{u} are either 0 or 1, we have

$$\begin{aligned} kd_1(\mathbf{u}, \mathbf{u}_t) + nd_2(\mathbf{x}, \mathbf{x}_t) &= \|\mathbf{u} - \mathbf{u}_t\|_2^2 + \|\mathbf{x} - \mathbf{x}_t\|_2^2 \\ &= \left\| \begin{bmatrix} \mathbf{x} \\ \mathbf{u} \end{bmatrix} - \begin{bmatrix} \mathbf{x}_t \\ \mathbf{u}_t \end{bmatrix} \right\|_2^2 \\ &= \|\mathbf{d} - \mathbf{d}_t\|_2^2 \end{aligned} \tag{106}$$

where \mathbf{d}_t is the t^{th} solution of the ADM-MIQP and \mathbf{d} is a feasible solution to (92). Thus, if both the metrics are small, the l_2 -norm between the t^{th} solution and the \mathbf{d} is also small. Based on this relation, we define the convergence of ADM-MIQP.

Definition 3: A solution $\mathbf{d}_t = \begin{bmatrix} \mathbf{x}_t^T & \mathbf{u}_t^T \end{bmatrix}^T$ of by ADM-MIQP is convergent to a point $\mathbf{d} = \begin{bmatrix} \mathbf{x}^T & \mathbf{u}^T \end{bmatrix}^T$ to (92) if there exists an integer $T > 0$ such that for every positive ε_1 and ε_2 , we then have $d_1(\mathbf{u}, \mathbf{u}_t) < \varepsilon_1$ and $d_2(\mathbf{x}, \mathbf{x}_t) < \varepsilon_2$ for all $T \leq t \leq \text{maxIter}$, where maxIter is the maximum number of iteration.

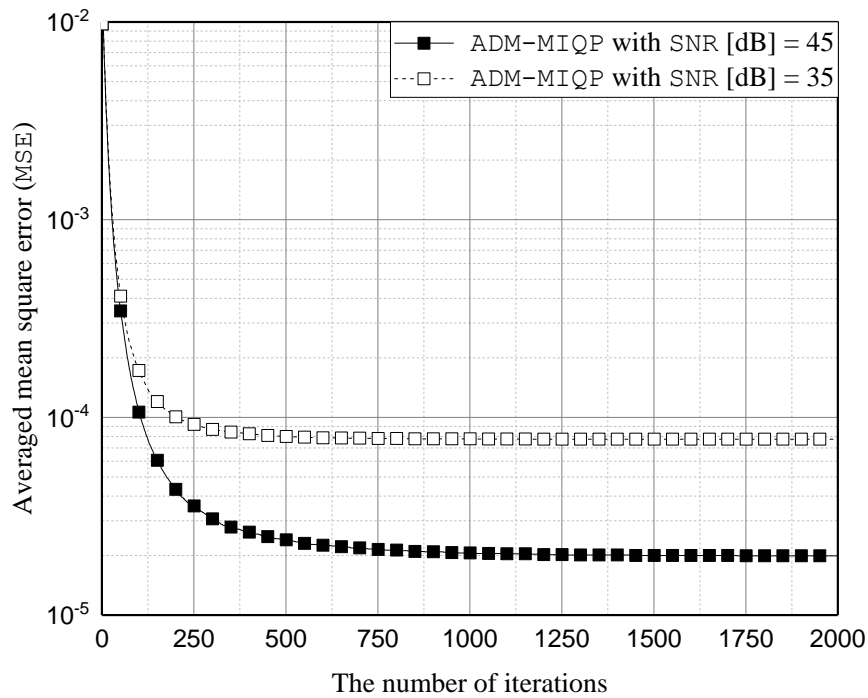


Figure 3.4.1: It plots the average MSE of ADM-MIQP depending on the number of iterations. The problem dimension n , the number of measurements m and the sparsity level k are set to be 1024, 307 and 30, respectively

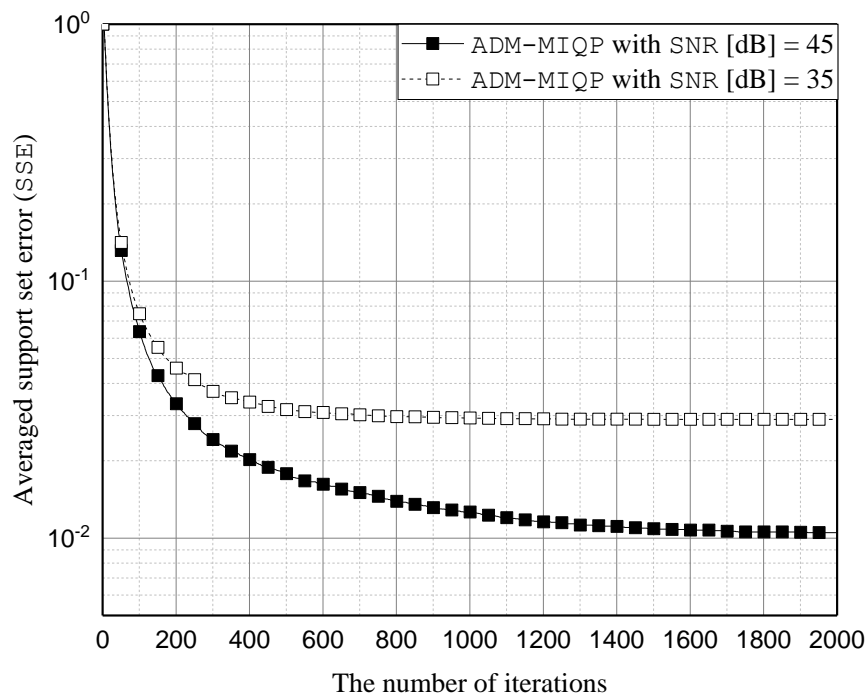


Figure 3.4.2: It plots the average SSE of ADM-MIQP depending on the number of iterations. The problem dimension n , the number of measurements m and the sparsity level k are set to be 1024, 307 and 30, respectively

To show that ADM-MIQP can find a converged solution to the MIQP problem (92), the problem dimension n , the number of measurements m and the sparsity level k were set as 1024, 307 and 30, respectively. Two values for SNR [dB] were considered: 35 and 45, respectively. We generated 1000 independent realizations of the set $(\mathbf{F}, \mathbf{x}, \mathbf{n})$ where \mathbf{F} was made by randomly taking 307 rows of the 1024×1024 DCT matrix, \mathbf{x} was taken from the Gaussian sparse vector ensemble, and \mathbf{n} was taken from the Gaussian noise vector ensemble. We determined average values for both MSE defined in (94) and SSE defined in (93). We then plotted the results in both Figure 3.4.1 and Figure 3.4.2, respectively.

For all the SNRs investigated, both MSE and SSE gradually decreased and were eventually saturated. For SNR [dB] = 45, at the 250th and 500th iterations, MSEs were 3.5×10^{-5} and 2.4×10^{-5} , respectively. Finally, MSE converged to 2×10^{-5} after $O(10^3)$ iterations. This means that an estimate of \mathbf{x} converges to an original sparse signal. Next, we considered SSE at SNR [dB] = 45. At the 250th and 500th iterations, SSEs were 0.041 and 0.031, respectively. Eventually, SSE converged to 0.029 after $O(10^3)$ iterations. This suggests that the detected support set converges to an original support set. Due to (17), after $O(10^3)$ iterations, we observed

$$\|\mathbf{d} - \mathbf{d}_t\|_2^2 < O(10^{-c})$$

where $c \approx 1$. This observation shows the convergence of ADM-MIQP under the definition 3.

3.4.2. Comparison Studies and Discussion

Let $\alpha := m/n$ be an *under-sampling* ratio and $\beta := k/m$ be an *over-sampling* ratio. The phase transition for a given method shows how accurately this method can estimate sparse signals in the (α, β) plane with n . We conducted simulations to study the phase transitions in computations obtained by ADM-MIQP, MDAL and YALL1. The aims of this study include being aware of the overall performance of ADM-MIQP and understanding which of these ADM-based methods, each of which solves different problems to estimate sparse signals, achieves the best performance for this sparse signal estimation.

The problem dimension n was set as 1024. Then, a 15×15 uniformly spaced grid on the (α, β) plane

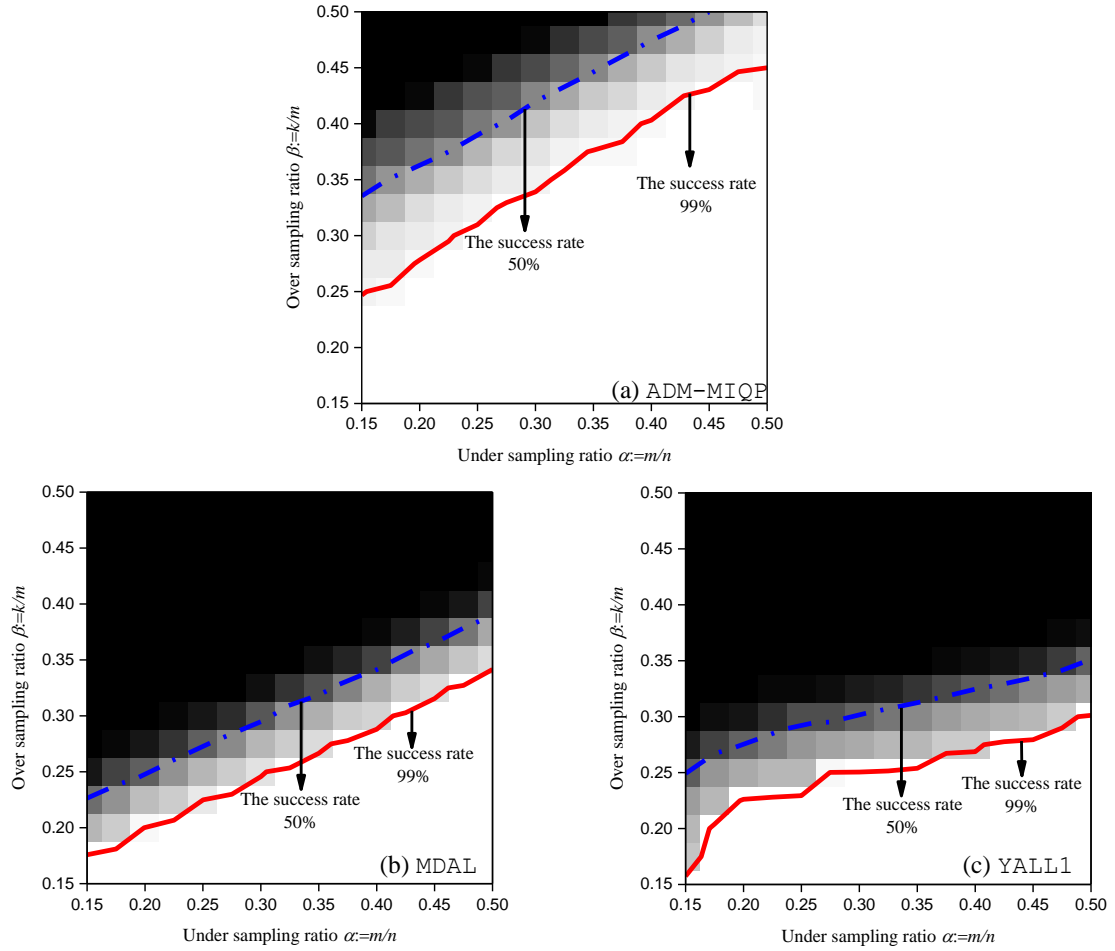


Figure 3.4.3: It plots the empirical phase transitions of the ADM-based methods such as ADM-MIQP, MDAL and YALL1, respectively

was made for $\alpha, \beta \in \{0.15, 0.175, \dots, 0.5\}$. We made 1000 independent realizations of the set (\mathbf{F}, \mathbf{x}) , where \mathbf{F} was derived by randomly taking m rows of the 1024×1024 DCT matrix and \mathbf{x} was taken from the Gaussian sparse vector ensemble. The estimate $\tilde{\mathbf{x}}$ was considered to be successful if $\frac{\|\mathbf{x} - \tilde{\mathbf{x}}\|_2^2}{\|\mathbf{x}\|_2^2} \leq 10^{-4}$.

In Figure 3.4.3, we illustrated the phase transitions for all these methods. The solid line represents a 99% probability of success. That is, for points lying in the graphical area below this line, there was at least 99% probability of success in problem solving. The area beneath the dashed-line then represents a 50% probability of success.

First, we fixed the over-sampling ratio. We then considered the under-sampling ratio to attain a 99% probability of success. The under-sampling ratio for ADM-MIQP was found to be the smallest. As an ex-

ample, for a fixed $\beta = 0.25$, we observed that the under-sampling ratios of ADM-MIQP, MDAL, and YALL1 were 0.25, 0.275, and 0.325, respectively. The under-sampling ratio was proportional to m because n was fixed. This implies that ADM-MIQP requires the smallest value of m for sparse signal estimation, when compared with the other methods.

Second, we fixed the under-sampling ratio and considered the over-sampling ratio to achieve a 99% probability of success. We observed that for ADM-MIQP, the over-sampling ratio was the largest. For a fixed $\alpha = 0.3$, the over-sampling ratios of ADM-MIQP, MDAL and YALL1 were 0.325, 0.25, and 0.225, respectively. The over-sampling ratio was proportional to k for a fixed under-sampling ratio. This shows that ADM-MIQP can estimate \mathbf{x} with the higher value of k in which the other methods cannot.

Next, we conducted simulations to study the performance of all these methods by varying k for a fixed n and m under noisy cases. To this end, $\text{SNR}[\text{dB}]$, n and m were set as 35, 1024, and 307, respectively and k was varied between 30 and 100. We generated 1000 independent realizations of the set $(\mathbf{F}, \mathbf{x}, \mathbf{n})$ in which \mathbf{F} , \mathbf{x} , and \mathbf{n} were obtained through the manner discussed in Section 3.4.1. Then, we obtained the average MSE for each method and plotted these values in Figure 3.4.4

For any k , ADM-MIQP can achieve the lowest MSE when compared with MDAL and YALL1. This means that ADM-MIQP can more accurately estimate \mathbf{x} than the other methods can. The MSE gap between ADM-MIQP and ORACLE is small. At $k = 40$, as an example, we see that MSEs of ADM-MIQP and ORACLE are 7×10^{-6} and 4×10^{-6} , respectively. This suggests that ADM-MIQP can achieve a performance close to that achieved by ORACLE.

Since both MDAL and YALL1 are originally designed to find an estimate of \mathbf{x} , not the support set, we needed to construct the support set based on the estimate $\tilde{\mathbf{x}}$ in order to measure SSEs for these methods. For this purpose, we set a threshold value

$$\zeta = 0.8 \min_i |\mathbf{x}(i)|$$

and constructed the support set $\hat{\mathbf{u}}$ by

$$\begin{aligned} \hat{\mathbf{u}}(i) &= 0 & \text{if } |\tilde{\mathbf{x}}(i)| < \zeta, \\ \hat{\mathbf{u}}(i) &= 1 & \text{if } |\tilde{\mathbf{x}}(i)| \geq \zeta. \end{aligned}$$

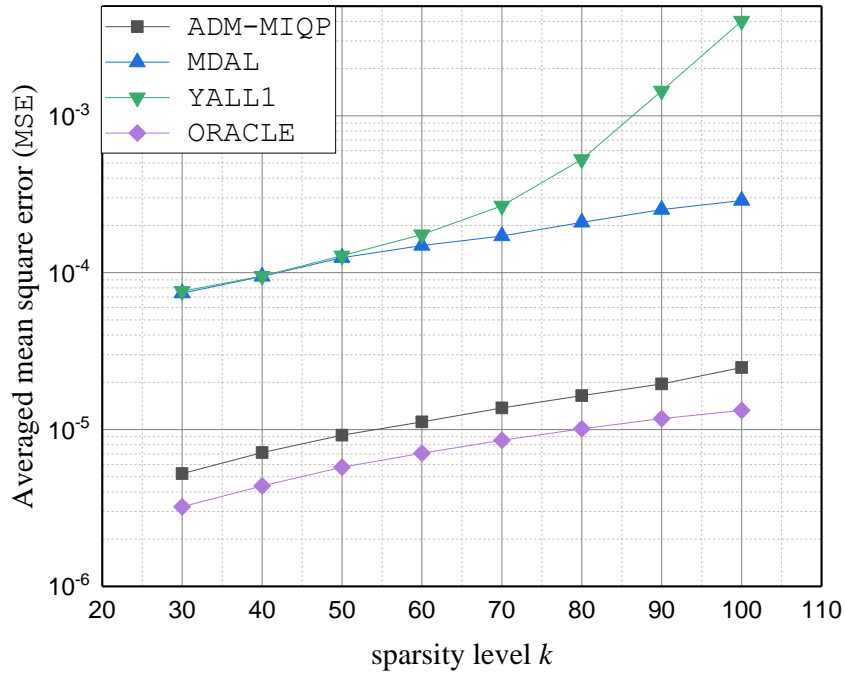


Figure 3.4.4: It plots the average MSEs of ADM-MIQP, MDAL, YALL1 and ORACLE depending on the sparsity level k . The problem dimension n , the number of measurements m and SNR[dB] are set to be 1024, 307 and 35, respectively

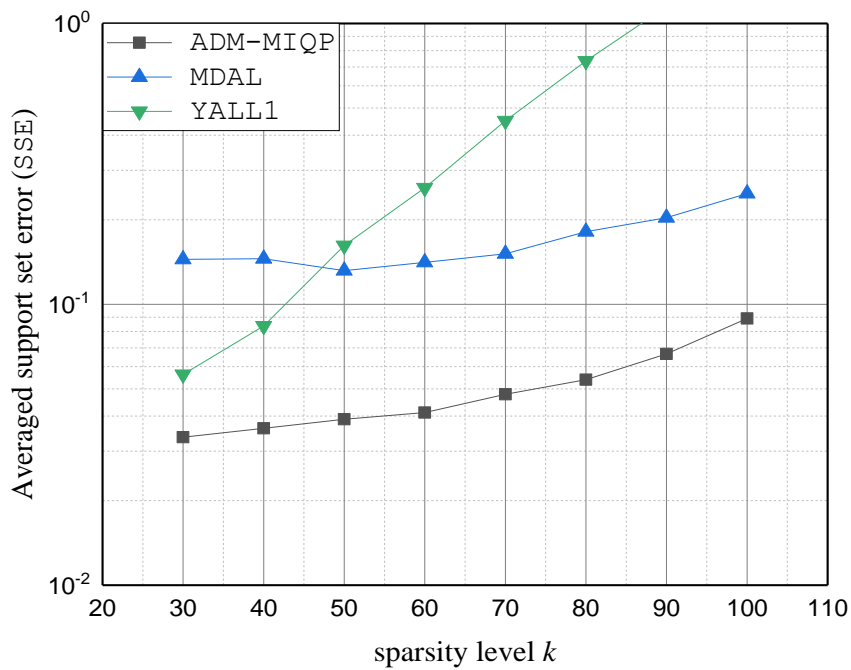


Figure 3.4.5: It plots the average SSEs of ADM-MIQP, MDAL and YALL1 depending on the sparsity level k . The problem dimension n , the number of measurements m and SNR[dB] are set to be 1024, 307 and 35, respectively

Under the same conditions used in the experiment depicted in Figure 3.4.4, we independently generated 1000 realizations of the set $(\mathbf{F}, \mathbf{x}, \mathbf{n})$. We then determined the average SSE for each of the methods and plotted the results in Figure 3.4.5. As with MSE, for any k , ADM-MIQP was found to achieve the lowest SSE. As an example, at $k = 80$, SSEs of ADM-MIQP, MDAL, and YALL1 were 0.04, 0.14, and 0.26, respectively. This means that ADM-MIQP can more accurately detect the support set than the other methods can. Next, at $k = 60$, we counted the number of events for which $\sum_{i=1}^n \|\mathbf{u}(i) - \hat{\mathbf{u}}(i)\|_1 \leq 6$, i.e., for which the support set error could occur within 10%. The results for ADM-MIQP, MDAL, and YALL1 were 962, 227, and 349 events respectively. This suggests that ADM-MIQP surpasses the other methods.

Thus far, we have shown that ADM-MIQP is superior to other ADM-based methods in terms of MSE and SSE. There are multiple reasons for why this is the case.

First, ADM-MIQP is designed to solve (92). The binary vector \mathbf{u} in (92) indicates the support set and $\mathbf{1}_n^T \mathbf{u}$ counts the number of ones in \mathbf{u} . This means that ADM-MIQP aims to find a solution that both the cardinality of the support set and the data-fidelity are jointly minimized. Minimizing the cardinality of the support set is a characteristic of l_0 -norm based methods. This is the reason for the superiority of our method over YALL1.

Second, Dong and Zhang [31] have empirically reported that MDAL finds a local solution to the l_0 -norm problem. By contrast, methods based on ADM tend to find the global solution to a MIQP problem, as reported in [38]–[40]. Then, as reported in [32], CPLEX is capable of finding the global solution to (92). To understand whether ADM-MIQP finds the global solution or not, we compared the solution of ADM-MIQP and that of CPLEX. We independently made 100 realizations of the set (\mathbf{F}, \mathbf{x}) by assuming that n , m , and k were 200, 80, and 10 respectively, where \mathbf{F} was a partial orthogonal sensing matrix and \mathbf{x} was taken from the Gaussian sparse vector ensemble. We determined the average of the objective function

$$\tau \mathbf{1}_n^T \mathbf{u} + 2^{-1} \|\mathbf{b} - \mathbf{F}\mathbf{x}\|_2^2$$

for each method, as well as the average for *normalized MSE*,

$$\|\mathbf{x}_C - \mathbf{x}_A\|_2^2 / \|\mathbf{x}_C\|_2^2$$

where \mathbf{x}_A is an estimate of \mathbf{x} obtained by ADM-MIQP and \mathbf{x}_C is an estimate of \mathbf{x} obtained by CPLEX.

The value of the objective function of CPLEX, and that of ADM-MIQP, were 0.0099 and 0.0094, respec-

tively, and the *normalized* MSE was 0.0033. The gap between these values and the *normalized* MSE were both small. This indicates that ADM-MIQP indeed finds the global solution to (92). This makes ADM-MIQP a superior approach to MDAL.

We observed that ADM-MIQP is computationally tractable for solving (92) up to the problem dimension n of the order of one million. To this end, SNR [dB] was set as 45 and n was varied from 1024 to 1048576. For a fixed n , we altered m and k to $m = \lfloor 0.3n \rfloor$ and $k = \lfloor 0.3m \rfloor$. The number of iterations was set as 1000. At each point $(n, m, k, \text{SNR}[\text{dB}])$, we generated 500 independent realizations of the set $(\mathbf{F}, \mathbf{x}, \mathbf{n})$, where \mathbf{F} , \mathbf{x} , and \mathbf{n} are obtained by the approach given in Section 3.4.1. We determined the average running time for each method and plotted the results in Figure 3.4.6.

In Figure 3.4.6, the average running times for each method grow linearly with n . We calculated the order of the average running times for ADM-MIQP, MDAL and YALL1 with respect to n . The orders are roughly $O(n^{1.3})$, $O(n^{1.3})$, and $O(n^{1.13})$ respectively.

These orders show that ADM-MIQP has polynomial computation costs, leading to that ADM-MIQP is still computationally tractable for solving (92) with the large problem dimension. Finally, YALL1 was found to be a faster method than ADM-MIQP. This is because the l_1 -norm problem (91), solved by YALL1, is easier to solve than (92). Despite this, if the running time for ADM-MIQP is acceptable, ADM-MIQP gains significant improvements on sparse signal estimation.

We conducted simulations to compare ADM-MIQP with CPLEX in terms of the running time. MaxIter was set as 1000. SNR [dB] was set as 45 and n was varied from 128 to 224. Both m and k were altered to $m = \lfloor 0.3n \rfloor$ and $k = \lfloor 0.2m \rfloor$. At each point, we made 50 independent realizations of the set $(\mathbf{F}, \mathbf{x}, \mathbf{n})$, where \mathbf{x} and \mathbf{n} are obtained by the approach given in Section 3.4.1 and \mathbf{F} is a partial orthogonal matrix.

In Figure 3.4.7, the average running time of CPLEX rapidly grows with n . Even n was roughly doubled, the time rapidly increased. At $n = 128$ and $n = 224$, the times are 6.7 secs and 2113 secs, respectively. This observation can be in accordance with the statement in Section 3.1 that CPLEX has the computational intractability in solving (92) with large variables. On the other hands, the average running time of ADM-MIQP does not rapidly grow with n . This observation shows that ADM-MIQP is faster than CPLEX.

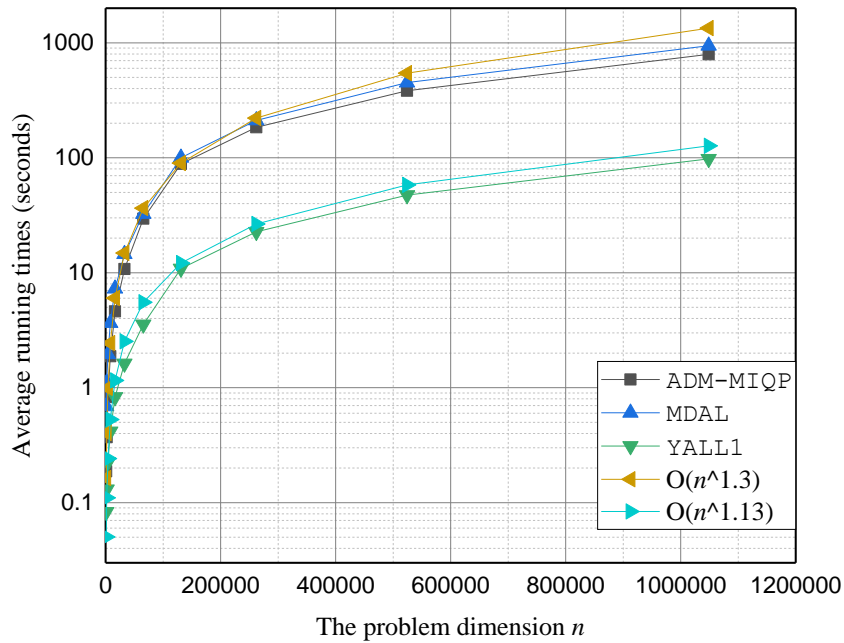


Figure 3.4.6: It plots the average running times of ADM-MIQP, MDAL, YALL1 and CPLEX depending on the problem dimension n with $m = \lfloor 0.3n \rfloor$, $k = \lfloor 0.3m \rfloor$ and SNR [dB] = 45. ADM-MIQP, MDAL and YALL1 have the polynomial computational order

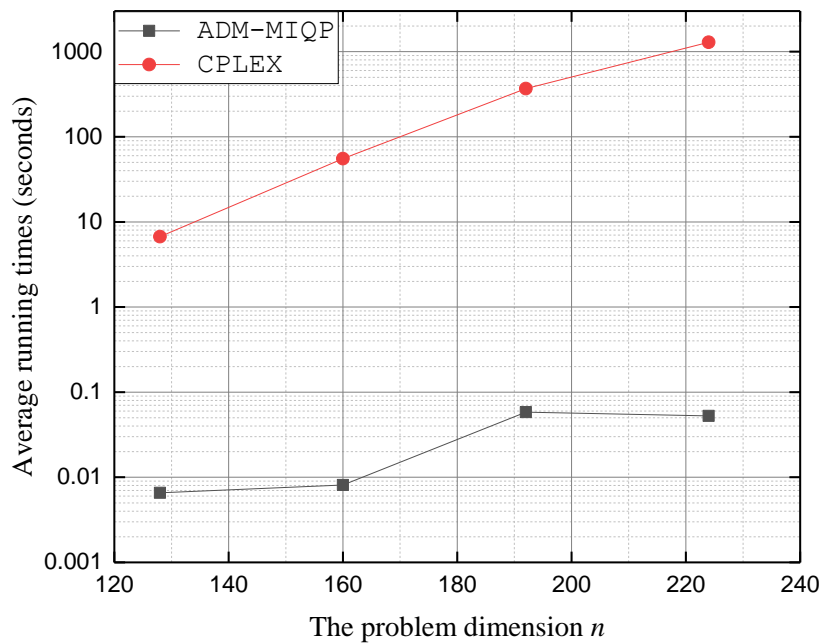


Figure 3.4.7: It plots the average running times of ADM-MIQP and CPLEX depending on the problem dimension n with $m = \lfloor 0.3n \rfloor$, $k = \lfloor 0.2m \rfloor$ and SNR [dB] = 45. This figure shows that ADM-MIQP is significantly faster than CPLEX



Figure 3.4.8: The original grayscale images of size 512×512 are shown in the first row. The images recovered by ADM-MIQP are shown in the second row. The images recovered by MDAL are shown in the third row. Then, the PSNR value of each recovered image is averaged 10 trials at $m = \lfloor 0.15n \rfloor$ and $k = \lfloor 0.05n \rfloor$

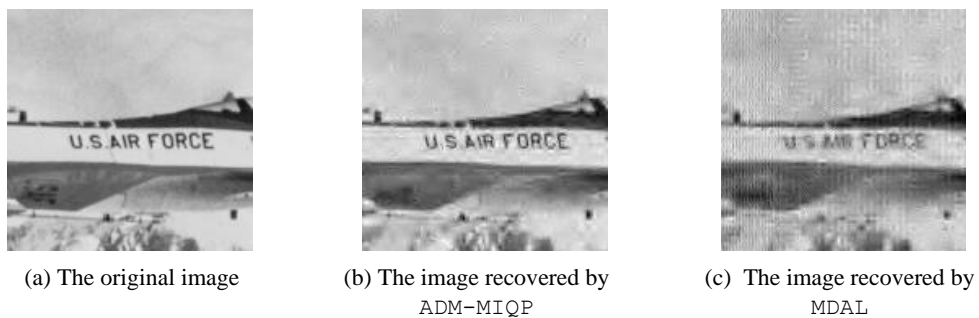


Figure 3.4.9: The images are corresponding to the part of the original and each recovered airplane images

3.4.3. An Image Recovery Example

We conducted an image recovery experiment to demonstrate the successful application of ADM-MIQP. For this study, the discrete wavelet transform was applied onto each image. The k largest magnitude values of the transformed image were retained. For each image, k non-zero values were stacked to form a sparse vector, to be compressed to get an m -dimensional measurement vector using a partial DCT matrix. Both MDAL and ADM-MIQP were used to recover the image. To evaluate the qualities of the recovered images, we used the following *peak-signal-to-noise ratio* (PSNR):

$$\text{PSNR [dB]} := 10 \log_{10} \left(n \times 255^2 / \|\mathbf{x} - \tilde{\mathbf{x}}\|_2^2 \right), \quad (107)$$

where \mathbf{x} is an original image and $\tilde{\mathbf{x}}$ is the recovered image.

In Figure 3.4.8, we illustrate the original greyscale images of size 512×512 with a problem dimension $n = 262144$. We have also showed the images recovered by each method and their PSNRs. These PSNR values were the averages of results from 10 trials where $m = \lfloor 0.15n \rfloor$ and $k = \lfloor 0.05n \rfloor$.

It is immediately observed that ADM-MIQP recovers images with higher quality than MDAL in terms of PSNR. ADM-MIQP then preserves the detailed information in the original images. For example, let us consider the text part “*US AIR Force*” of the recovered airplane image. As shown in Figure 3.4.9, we clearly see this text in (b), recovered by ADM-MIQP, we cannot make out it in (c), recovered by MDAL. This result shows that ADM-MIQP surpasses MDAL in this image recovery example.

3.5. Conclusion

We proposed a fast method referred to as ADM-MIQP to solve the mixed integer quadratic programming problem (92) formulated in [32] from the l_0 -norm problem (90). We derived ADM-MIQP using the alternating direction method, which has been recently used to solve integer programming problems in [38]–[40]. We then showed that ADM-MIQP is a first-order-type method. That is, matrix-vector products are only used to implement ADM-MIQP. We selected MDAL [31] and YALL1 [62] as competitors to ADM-MIQP because these methods are based on ADM to solve the l_0 -norm and the l_1 -norm problems, respectively. We compared ADM-MIQP with ORACLE, an approach which involved *a priori* knowledge of the support set. We used both *support set error* (SSE) (93) and *mean square error* (MSE) (94) to

assess the quality of a solution obtained by each method.

We empirically demonstrated that ADM-MIQP could achieve a significantly better performance than MDAL and YALL1 in terms of both SSE and MSE. We also showed that ADM-MIQP eventually achieved a performance close to that of ORACLE in terms of MSE. We showed that ADM-MIQP is computationally tractable for solving (92) up to the order of one million in the problem dimension. We confirmed that the computational cost of ADM-MIQP is $O(n^{1.3})$ in our simulations. We concluded that ADM-MIQP is efficient in finding an accurate solution to (92) when the problem dimension n is large.

The next step is to conduct convergence analysis for ADM-MIQP. Specifically, it will be interesting to prove that a solution of ADM-MIQP is convergent. Also, this work can be extended to determine the appropriate penalty value that would guarantee the convergence of ADM-MIQP.

Chapter 4: Conclusions Remarks of this Dissertation

In Chapter 1, the author began to introduce the compressed sensing (CS) [2][7] framework where high-dimensional signals can be sampled and reconstructed at a rate below the Nyquist sampling rate using the sparsity structure. The author explained how the signal acquisition and reconstruction in this framework can be conducted. The author compared this framework with the conventional framework supported by the Nyquist-sampling rate. The aim of this comparison is to show that the CS framework can be used to remove an inefficient aspect of the conventional framework, in which the sampling and compression are separately conducted. The author introduced a problem of support set reconstruction in which it aims to reconstruct the support set of an original sparse signal from the knowledge of its corresponding measurements. The author presented motivations to conduct both an information-theoretic work and a construction of a practical algorithm for a reliable support set reconstruction.

In Chapter 2, the author began to review information-theoretic works [9]–[14], [22]–[24] that provide necessary and sufficient conditions for a reliable support set reconstruction under three different models called as noisy single measurement vector (SMV), noisy multiple measurement vectors (MMV) with the same sensing matrix [21] and noiseless MMV with different sensing matrices [17][18], respectively. Then, the author contributed to the signal processing and information theory community by conducting the information-theoretic work which firstly aims to give necessary and sufficient conditions for a reliable support set reconstruction under noisy MMV with the different sensing matrices. The author used these conditions to theoretically confirm benefits, which have not been theoretically verified but only empirically reported in [15], [16]. Last, the author discussed relations between our works with [23] which considers noisy MMV with the same sensing matrix.

In Chapter 3, the author began to review practical algorithms [25]–[28], [31], [58]–[62] to solve either a l_0 -norm minimization problem or a l_1 -norm minimization problem. The author showed recent results in the signal processing community, demonstrating that *i*) the l_0 -norm minimization problem can be recast as an mixed integer quadratic programming problem [32] and *ii*) an alternating direction method can be an useful technique for solving integer programming problems [38]–[40]. These results motivated the author to propose an algorithm to solve the l_0 -norm minimization problem. The author empirically verified the superiority of the proposed algorithm over other algorithms [28], [62] which solve either the l_0 -norm min-

imization problem or the l_1 -norm minimization problem using the alternating direction method.

References

- [1] C. E. Shannon, "A mathematical theory of communication," *The Bell System Technical Journal*, vol. 27, pp. 379-423, 623-656, Jul. Oct. 1948.
- [2] D. Donoho, "Compressed sensing," *IEEE Trans. Inf. Theory*, vol. 52, no. 4, pp. 1289-1306, Apr. 2006.
- [3] E. J. Candes and T. Tao, "Decoding by linear programming," *IEEE Trans. Inf. Theory*, vol. 51, no. 12, pp. 4203-4215, Dec. 2005.
- [4] E. J. Candes, J. Romberg, and T. Tao, "Robust uncertainty principle: Exact signal recovery from highly incomplete frequency information," *IEEE Trans. Inf. Theory*, vol. 52, no. 2, pp. 489-509, Feb. 2006.
- [5] E. J. Candes and T. Tao, "Near optimal signal recovery from random projections : Universal encoding strategies," *IEEE Trans. Inf. Theory*, vol. 52, no. 12, pp. 5406-5425, Dec. 2006.
- [6] E. J. Candes and T. Tao, "Stable signal recovery from incomplete and inaccurate measurements," *Comm. Pure Appl. Math.*, vol. 59, no. 8, pp. 1207-1223, Aug. 2006.
- [7] E. J. Candes and M. Wakin, "An introduction to compressive sensing," *IEEE Sig. Process. Mag.*, vol. 25, no. 2, pp. 21-30, Mar. 2008.
- [8] R. G. Baraniuk, "Compressive Sensing," *IEEE Sig. Process. Mag.*, vol. 24, no. 4, pp. 118-121, Aug. 2007.
- [9] M. J. Wainwright, "Information-theoretic limits on sparsity recovery in the high-dimensional and noisy setting," *IEEE Trans. Inf. Theory*, vol. 55, no. 12, pp. 5728-5741, Dec. 2009.
- [10] A. K. Fletcher, S. Rangan and V. K Goyal, "Necessary and sufficient conditions for sparsity pattern recovery," *IEEE Trans. Inf. Theory*, vol. 55, no. 12, pp. 5758-5772, Dec. 2009.
- [11] S. Aeron, V. Saligrama, and M. Zhao, "Information-theoretic bounds for compressed sensing," *IEEE Trans. Inf. Theory*, vol. 56, no. 10, pp. 5111-5130, Oct. 2010.
- [12] M. Akcakaya and V. Tarokh, "Shannon-theoretic limits on noisy compressive sampling," *IEEE Trans. Inf. Theory*, vol. 56, no. 1, pp. 492-504, Jan. 2010.

- [13] J. Scarlett, J. Evans and S. Dey, "Compressed sensing with prior information: information-theoretic limits and practical decoders," *IEEE Trans. Signal Process.*, vol. 61, no. 2, pp. 427-439, Jan. 2013.
- [14] J. Scarlett and V. Cevher, "Limits on support recovery with probabilistic models: an information-theoretic framework," *IEEE Trans. Inf. Theory*, vol. 63, no. 1, pp. 593-620, Jan. 2017.
- [15] C. Caione, D. Brunelli, and L. Benini, "Compressive sensing optimization for signal ensembles in WSNs," *IEEE Trans. Ind. Inform.*, vol. 10, no. 1, pp. 382-392, Feb. 2014.
- [16] Y. Wu, Y. Zhu, Q. Tang, C. Zou, W. Liu, R. Dai, X. Liu, E. X. Xu, L. Ying, and D. Liang, "Accelerated MR diffusion tensor imaging using distributed compressed sensing," *Magn. Reson. Med.*, vol. 71, no. 2, pp. 763-772, 2014.
- [17] D. Baron, M. F. Duarte, M. B. Wakin, S. Sarvotham, and R. G. Baraniuk, "Distributed compressed sensing," Arxiv preprint arXiv:0901.3403, 2009.
- [18] M. F. Duarte, S. Sarvotham, D. Baron, M. B. Wakin and R. G. Baraniuk, "Distributed compressed sensing of jointly sparse signals," *Conference Record of the Thirty-Ninth Asilomar Conference on Signals, Systems and Computers, 2005.*, Pacific Grove, CA, 2005, pp. 1537-1541.
- [19] W. Chen, R. D. Rodrigues, and I. J. Wassell, "Distributed compressive sensing reconstruction via common support discovery," *2011 IEEE International Conference on Communications (ICC)*, Kyoto, 2011, pp. 1-5.
- [20] S. Gogineni and A. Nehorai, "Target estimation using sparse modeling for distributed MIMO radar," *IEEE Trans. Signal Process.*, vol. 59, no. 11, pp. 5315-5325, Nov. 2011.
- [21] J. Chen and X. Huo, "Theoretical results on sparse representations of multiple-measurement vectors," *IEEE Trans. Signal Process.*, vol. 56, no. 12, pp. 4634-4643, Dec. 2006.
- [22] G. Tang and A. Nehorai, "Performance analysis for sparse support recovery," *IEEE Trans. Inf. Theory*, vol. 56, no. 3, pp. 1383-1399, Mar. 2010.
- [23] Y. Jin and B. D. Rao, "Support recovery of sparse signals in the presence of multiple measurement Vectors," *IEEE Trans. Inf. Theory*, vol. 59, no. 5, pp. 3139-3157, May. 2013.
- [24] M. F. Duarte, M. B. Wakin, D. Braon, S. Sarvotham, and R. G. Baraniuk, "Measurement bounds for sparse signal ensembles via graphical models," *IEEE Trans. Inf. Theory*, vol. 59, no. 7, pp. 4280-4289, Jul. 2013.

- [25] T. Blumensath, M. E. Davies, "Iterative hard thresholding for compressed sensing," *Appl. Comp. Harmon. Anal.*, vol. 27, no. 3, pp. 265-274, Nov. 2009.
- [26] T. Blumensath and M. E. Davies, "Normalized iterative hard thresholding: guaranteed stability and performance," *IEEE J. Sel. Topics Signal Process.*, vol. 4, no. 2, pp. 298-309, Apr. 2010.
- [27] T. Blumensath, "Accelerated iterative hard thresholding," *Signal Process.*, vol. 92, no. 3, pp. 752-756, Mar. 2012.
- [28] Z. Dong and W. Zhu, "Homotopy methods based on l_0 -norm for compressed sensing," *IEEE Trans. on Neural Netw. Learn Sys.*, vol. 29, no. 4, pp. 1132-1146, Apr. 2017.
- [29] H. Mohimani, M. Babaie-Zadeh, C. Jutten, "A fast approach for overcomplete sparse decomposition based on smoothed l_0 norm," *IEEE Trans. Signal Process.*, vol. 57, no. 1, pp. 289-301, Jan. 2009.
- [30] H. Wang, Q. Guo, G. Zhang, G. Li and W. Xiang, "Thresholded smoothed l_0 norm for accelerated sparse recovery," *IEEE Commun. Lett.*, vol. 19, no. 6, pp. 953-956, Jun. 2015.
- [31] B. Dong and Y. Zhang, "An efficient algorithm for l_0 minimization in wavelet frame based image restoration," *J. Sci. Comput.*, vol. 54, pp. 350-368, Feb. 2013.
- [32] S. Bourguignon, J. Ninin, H. Carfantan and M. Mongeau, "Exact sparse approximation problems via mixed-integer programming: formulations and computational performance," *IEEE Trans. on Signal Process.*, vol. 64, no. 6, pp. 1405-1419, Oct. 2016.
- [33] D. Bertsimas, A. King and R. Mazumder, "Best subset selection via a modern optimization lens," *Ann. Statist.*, vol. 44, no. 2, pp. 813-852, 2016.
- [34] IBM ILOG CPLEX V12.8.0, <https://www.ibm.com/products/ilog-cplex-optimization-studio>
- [35] J. E. Mitchell, *Branch-and-Cut Algorithms for Combinatorial Optimization Problems*, Handbook of Applied Optimizations, Oxford Univ. Press, 2000.
- [36] E. Ghadimi, A. Teixeira, I. Shames, and M. Johansson, "Optimal parameter selection for the alternating direction method of multipliers (ADMM): quadratic problems," *IEEE. Trans. on Automatic Control*, vol. 60, no. 3, pp. 644-658, Sep. 2015.
- [37] W. Deng and W. Yin, "On the global and linear convergence of the generalized alternating direction method of multipliers," *J. Sci. Comput.*, vol. 66, no. 3, pp. 889-916, Mar. 2016.

- [38] A. K. Yadav, R. Ranjan, U. Mahbub and M. C. Rotkowitz,, “New methods for handling binary constraints,” *2016 54th Annual Allerton Conference on Communication, Control, and Computing (Allerton)*, Monticello, IL, 2016, pp. 1074-1080.
- [39] N. Souto and R. Dinis, “MIMO detection and equalization for single-carrier systems using the alternating direction method of multipliers,” *IEEE Signal Process. Lett.*, vol. 23, no. 12, pp. 1751-1755, Oct. 2016.
- [40] R. Takapoui, N. Moehle, S. Boyd and A. Bemporad, “A simple effective heuristic for embedded mixed-integer quadratic programming,” *Int. J. Control* , Apr. 2017.
- [41] Sangjun Park, Nam Yul Yu, Heung-No Lee, “An Information-Theoretic Study for Joint Sparsity Pattern Recovery with Different Sensing Matrices,” *IEEE Trans. Inf. Theory*, vol. 63, no. 9, pp. 5559-5571, May. 2017.
- [42] Heung-No Lee, Junho Lee, Sangjun Park, “Signal Acquisition and Method for Distributed Compressive Sensing and Joint Signal Recovery,” application number: 13/250,082, application date: Sep., 30th, 2011, registration number: 8391800, registered date: Mar. 5th, 2013.
- [43] Sangjun Park and Heung-No Lee, “Number of Compressed Measurements Needed for Noisy Distributed Compressed Sensing,” *2012 IEEE International Symposium on Information Theory Proceedings*, Cambridge, MA, 2012, pp. 1648-1651.
- [44] Sangjun Park, Hwanchol Jang and Heung-No Lee, “Study on performance behavior of the compressive sensing measurements for multiple sensor system,” *2011 Conference Record of the Forty Fifth Asilomar Conference on Signals, Systems and Computers (ASILOMAR)*, Pacific Grove, CA, 2011, pp. 1980-1983.
- [45] Sangjun Park, Junho Lee and Heung-No Lee, “Per-sensor measurements behavior of compressive sensing system for multiple measurements,” *2010 Conference Record of the Forty Fourth Asilomar Conference on Signals, Systems and Computers*, Pacific Grove, CA, 2010, pp. 240-242.
- [46] Sangjun Park and Heung-No Lee, “Fast mixed integer quadratic programming for sparse signal estimation,” *IEEE Access*, vol. 6, pp. 58439-58449, Oct., 2018.
- [47] J. Oliver, Woong-Bi Lee, and Heung-No Lee, “Filters with random transmittance for improving resolution in filter-array-based spectrometers,” *Opt. Express*, vol. 21, no. 4, pp. 3969-3989, Feb. 2013.

- [48] M. Elad, *Sparse and Redundant Representations: From Theory to Applications in Signal and Image Processing*, Springer, 2010.
- [49] Y. C. Eldar and G. Kutyniok, *Compressed Sensing: Theory and Applications*, Cambridge University Press, May. 2012.
- [50] Y. C. Eldar, *Sampling Theory: Beyond Bandlimited Systems*, Cambridge University Press, Apr. 2015.
- [51] T. Cover and J. Thomas, *Elements of Information Theory*, New York, USA: Wiley, 2006.
- [52] J. Kim, O. Lee, and J. Ye, "Compressive MUSIC: revisiting the link between compressive sensing and array signal processing," *IEEE Trans. Inf. Theory*, vol. 58, no. 1, pp. 278-301, Jan. 2012.
- [53] J. D. Blanchard and M. E. Davies, "Recovery guarantees for rank aware pursuits," *IEEE Signal Process. Lett.*, vol. 19, no. 7, pp. 427-430, Jul. 2012.
- [54] H. L. Van Trees, *Detection, Estimation, and Modulation Theory, Part I*, New York, USA: Wiley-Interscience, 2001.
- [55] R. Rajagopalan and P. K. Varsheny, "Data-aggregation techniques in sensor networks: A survey," *IEEE Commun. Surveys Tutor.*, vol. 8, no. 4, pp. 48-63, Fourth Quarter 2006.
- [56] B. Laurent and P. Massart, "Adaptive estimation of a quadratic functional by model selection," *Ann. Statist.*, vol. 28, no. 5, pp. 1303-1338, Oct. 2000.
- [57] L. L. Scharf, *Statistical Signal Processing: Detection, Estimation, and Time Series Analysis*, Addison-Wesley Publishing Company, 1991.
- [58] S. J. Kim, K. Koh, M. Lustig, S. Boyd, D. Gorinevsky, "An interior-point method for large-scale l_1 -regularized least square," *IEEE J. Sel. Topics Signal Process.*, vol.1, no. 4, pp. 607-617, Dec. 2007.
- [59] M. Figueriedo, R. Nowak and S. Wright, "Gradient projection for sparse reconstruction: application to compressed sensing and other inverse problems," *IEEE J. Sel. Topics Signal Process.*, vol. 1, no. 4, pp. 586-597, Dec. 2007.
- [60] L. Xiao and T. Zhang, "A proximal-gradient homotopy method for the sparse least-squares problem," *SIAM J. Optim.*, vol. 23, no. 2, pp. 1062-1091, 2013.
- [61] T. Goldstein and S. Osher, "The split Bregman algorithm for l_1 regularized problems," *SIAM J. Imaging Sci.*, vol. 2, no. 2, pp. 323-343, 2009.
- [62] F. Yang and Y. Zhang, "Alternating direction algorithms for l_1 -problems in compressive sensing," *SIAM J. Sci. Comput.*, vol. 33, no. 1, pp. 250- 278, 2011.

- [63] F. Wen, L. Pei, Y. Yang, W. Yu and P. Liu, "Efficient and robust recovery of sparse signal and image using generalized nonconvex regularization," *IEEE Trans. on Comput. Imaging*, vol. 3, no. 4, pp. 566–579, Dec. 2017.
- [64] R. Chartrand and V. Staneva, "Restricted isometry properties and nonconvex compressive sensing," *Inverse Prob.*, vol. 24, no. 3, May. 2008.
- [65] S. Boyd and J. Mattingley, "Branch and bound methods," Stanford University, Stanford, CA, 2018 [Online]. Available: https://stanford.edu/class/ee364b/lectures/bb_notes.pdf
- [66] J. E. Mitchell, *Branch-and-Cut Algorithms for Combinatorial Optimization Problems*, Handbook of Applied Optimizations, Oxford Univ. Press, 2000.
- [67] S. Boyd and L. Vandenberghe, "Localization and cutting-plane method," Stanford University, Stanford, CA, 2008 [Online]. Available: https://see.stanford.edu/materials/lsocoe364b/05-localization_methods_notes.pdf
- [68] M. V. Afonso, J. M. Bioucas-Dias and M. A. T. Figueiredo, "Fast image recovery using variable splitting and constrained optimization," *IEEE Trans. on Img. Process.*, vol. 19, no. 9, pp. 2345-2356, Sep. 2010.
- [69] M. F. Duarte, M. A. Davenport, D. Takhar, J. N. Laska, T. Sun, K. F. Kelly and R. G. Baraniuk, "Single-pixel imaging via compressive sampling," *IEEE Sig. Process. Mag.*, vol. 25, no. 2, pp. 83-91, Mar. 2008.
- [70] D. B. Phillips, M-J. Sun, J. M. Taylor, M. P. Edgar, S. M. Barnett, G. Gibson and M. J. Padgett, "Adaptive foveated single-pixel imaging with dynamic super-sampling," *Sci. Adv.*, vol. 3, no. 4, Apr. 2017.
- [71] G. Satat, M. Tancik and R. Raskar, "Lensless imaging with compressive ultrafast sensing," *IEEE Trans. on Comput. Imaging.*, vol.3, no. 3, pp. 398-407, Sep. 2017.
- [72] G. Huang, H. Jiang, K. Matthews and P. Wilford, "Lensless imaging by compressive sensing," *2013 IEEE International Conference on Image Processing*, Melbourne, VIC, 2013, pp. 2101-2105.
- [73] M. W. Marcellin, M. J. Gormish, A. Bilgin and M. P. Boliek, "An overview of JPEG-2000", *Proceedings, Data Compression Conference*, Snowbird, UT, USA, Mar. 2000, pp. 523-541.
- [74] <https://github.com/infonetGIST/infonetcompressedensing>

Curriculum Vitae

Name : Sangjun Park
Birth Date : March. 26. 1986.
Birth Place : Republic of Korea
Permanent Address : 123 Cheomdangwagi-ro (Oryong-dong), Buk-gu, Gwangju
E-mail : sjpark1@gist.ac.kr; sinjimua@gmail.com

Research Interests

1. Compressed Sensing
2. Convex/Non-Convex Optimization Techniques
3. Channel Codes and Information Theory

Education

2009.9 – 2019.8 School of Electrical Engineering and Computer Science, Gwangju Institute of Science and Technology (Ms/Ph.D Integrated)
2005.3 – 2009.8 Computer Engineering, Chungnam National University (B.S)

Awards

1. 한국전자공학회 하계종합학술대회, Best paper award (우수학생논문상): 다중 측정 벡터 모델에 관한 최신 분석 결과 소개, 7 월 1 일, 2017 년.

International Patent

1. Heung-No Lee, **Sangjun Park**, J. Oliver, Woongbi Lee, “Method and Apparatus for Processing Optical Signal Of Spectrometer Using Sparse Nature of Signals”, US 9,030,662, registration date: May 12th, 2015
2. Heung-No Lee, Junho Lee, **Sangjun Park**, “Signal Acquisition and Method for Distributed Compressive Sensing and Joint Signal Recovery”, application ber: 13/250,082, application date: Sep. 30th, 2011, registration number: 8391800, registered date: Mar. 05th, 2013.

Domestic Patent

1. 이흥노, **박상준**, 제임스올리버, 이웅비, “분광계의 광 신호 처리 방법 및 그 장치”, application number: 10-2012-0079171, application date: July. 20th, 2012, registration number: 10-1423964 , registered data: Jul. 16th. 2014.

- 이흥노, 이준호, **박상준**, “분산적 압축 센싱 및 협력 복구를 수행하는 신호취득 장치 및 그 방법”, application number: 10-2010-0096128, application date: Oct. 1st, 2010 / registration number: 10-1112746, registered date: Jan. 30th, 2012.

International Journal Papers (SCI)

- Sangjun Park** and Heung-No Lee, “Fast mixed integer quadratic programming for sparse signal estimation,” *IEEE Access*, vol. 6, pp. 58439-58449, Oct., 2018.
- Muhammad Asif Raza, **Sangjun Park** and Heung-No Lee, “Evolutionary Channel Sharing Algorithm for Heterogeneous Unlicensed Networks,” *IEEE Trans. Wirel. Commun.*, vol. 16, no. 7, pp. 4378-4389, Jul. 2017.
- Sangjun Park**, Nam Yul Yu, Heung-No Lee, “An Information-Theoretic Study for Joint Sparsity Pattern Recovery with Different Sensing Matrices,” *IEEE Trans. Inf. Theory*, vol. 63, no. 9, pp. 5559-5571, May. 2017.
- Woong-Bi Lee, Hwanchol Jang, **Sangjun Park**, Young Min Song, and Heung-No Lee “COM-PU-EYE: a high resolution computational compound eye,” *Opt. Express*, vol. 24, No. 3, pp. 2013-2026, Feb. 2016
- J. Oliver, WoongBi Lee, **SangJun Park**, and Heung-No Lee, “Improving resolution of miniature spectrometers by exploiting sparse nature of signals,” *Opt. Express*, vol. 20, no. 3, pp. 2613-2625, Jan. 2012.

International Conference

- Pavel S. Ni, **Sangjun Park**, and Heung-No Lee, “Design of Unfocused Ultrasound Imaging System using Compressive Sensing”, 37th Annual International Conference of the IEEE Engineering in Medicine and Biology Society, Milan, Italy, August 24-29, 2015.
- Sangjun Park**, Jeong-Min Ryu, and Heung-No Lee, “A study for establishing a sufficient condition for successful joint support set reconstruction”, ITC-CSCC 2013, June, 2013
- Sangjun Park** and Heung-No Lee, “Number of Compressed Measurements Needed for Noisy Distributed Compressed Sensing”, *2012 IEEE International Symposium on Information Theory Proceedings*, Cambridge, MA, 2012, pp. 1648-1651.
- Sangjun Park** and Heung-No Lee, “On the Derivation of RIP for Random Gaussian Matrices and Binary Sparse Signals”, International Conference on ICT Convergence, Seoul, Korea, September 28 ~ 30, 2011
- Sangjun Park**, Hwanchol Jang and Heung-No Lee, “Study on Performance Behavior of the Compressive Sensing Measurements for Multiple Sensor System”, *2011 Conference Record of the Forty Fifth Asilomar Conference on Signals, Systems and Computers (ASILOMAR)*, Pacific Grove, CA, 2011, pp. 1980-1983.
- Hwanchol Jang, Saeid Nooshabadi, **Sangjun Park** and Heung-No Lee, “Sorted Orthotope Sphere Decoding for MIMO Detection,” The 5th Joint Conference on Information and Com-

- munication Technology & the 1st Yellow Sea International Conference on ubiquitous Computing (JCITCT & YES-ICuC), Shandong University at Weihai, China, Aug 17-20, 2011
7. **Sangjun Park**, Hwanchol Jang and Heung-No Lee, "Performance Limits of the Measurements on Compressive Sensing for Multiple Sensor System", Signal Processing with Adaptive Sparse Structured Representation, Edinburgh, Scotland, June 27-30, 2011.
 8. **Sangjun Park**, Junho Lee and Heung-No Lee, "Per-sensor measurements behavior of compressive sensing system for multiple measurements," *2010 Conference Record of the Forty Fourth Asilomar Conference on Signals, Systems and Computers*, Pacific Grove, CA, 2010, pp. 240-242.

Domestic Journal

1. J. Oliver, Woong-Bi Lee, **Sangjun Park**, and Heung-No Lee, "Evaluation of resolution improvement ability of a DSP technique for filter-array-based spectrometers" KICS (한국통신학회), vol. 38C, no. 6, pp. 497-502, July, 2th, 2013.
2. 이흥노, **박상준**, 박순철, "Introduction to Compressive Sensing (압축센싱 소개)," 대한전자공학회지, 전자공학회지, Vol. 38, No. 1, pp. 19 – 30, Jan. 2011.

Domestic Conference

1. **Sangjun Park**, Haeung Choi, Woong-Bi Lee, Cheolsun Kim, Jusung Kang and Heung-No Lee, "다중 측정 벡터 모델에 관한 최신 분석 결과 소개," 대한전자공학회 학술대회, vol. 2017, no. 6, pp. 771-773, 2017.
2. Pavel S. Ni, **Sangjun Park**, Hwanchol Jang, Seungchan Lee, Jusung Kang, Heung-No Lee, "최소표현을 통한 비디오 기록으로부터의 고해상도 이미지 복원," 한국통신학회 학술대회논문집, vol. 2015, no. 6, pp. 852-853, 2015.
3. Pavel Ni, Jin-Taek Seong, Hwanchol Jang, **Sangjun Park**, Jeong-Min Ryu, Heung-No Lee, "압축 센싱을 이용한 초음파 이미지의 신호 복원" 하계종합학술대회, Jul. 03-05, 2013.
4. J. Oliver, WoongBi Lee, **SangJun Park**, and Heung-No Lee, "A new signal processing technique for improving resolution of spectrometers," 한국통신학회 학술대회논문집, vol. 2013, no. 1, pp. 62-63, 2013.
5. Jeong-Min Ryu, **Sangjun Park**, and Heung-No Lee, "Gallager 코드의 Stopping Set 분석", 한국통신학회 학술대회논문집, vol. 2012, no. 11, pp. 123-124, 2012.
6. **Sangjun Park**, and Heung-No Lee, "다중 압축 센싱 시스템 분석", 제 25 회 신호처리 합동 학술대회, 2012.
7. Jae-Gun Choi, **Sangjun Park** and Heung-No Lee, "무선 센서 네트워크에서 압축 센싱 기술의 활용과 상관 신호를 이용하는 복구 시스템의 성능 분석," vol. 2012, no. 6, pp. 182-183, 2012.

8. Jeong-Min Ryu, **Sangjun Park** and Heung-No Lee, “Regular LDPC Code 의 향상된 Stopping Set 분석,” vol. 2011, no. 6, pp. 610-611, 2011.
9. Junho Lee, **Sangjun Park** and Heung-No Lee, “New Compressive Sensing Model for Multiple Sensor System”, 제 23 회 신호처리합동학술대회, pp.58-61, 2010.
10. **Sangjun Park**, Junho Lee and Heung-No Lee, “Information-Theoretical Analysis for Multiple Sensor System based on Compressive Sensing”, 제 23 회 신호처리합동학술대회, pp.55-57, 2010.
11. **Sangjun Park**, Junho Lee and Heung-No Lee, “Analysis of Joint Typicality Based Information-theoretic Limits on Multiple Sensor System Based on Compressive Sensing”, 대한전자공학회 2010 하계종합학술대회, pp. 1005-1007, 2010.

Book/Book Chapters

1. Jae-Gun Choi, **Sang-Jun Park**, and Heung-No Lee, Intelligent Sensor Networks: Across Sensing, Signal Processing, and Machine Learning (Chapter 15), Taylor & Francis LLC, CRC Press, 2012.

Acknowledgement

석사/박사 학위과정 동안 광주과학기술원(GIST)에서 보낸 약 10 년의 기간은 남은 생에서 잊지 못할 것입니다. 이 기간 동안 다양한 생각을 가진 사람들을 만나는 것과 다른 문화를 가진 사람들을 만나 생활하는 귀중한 시간을 보냈고, 이런 시간은 돈을 주고도 살 수 없는 귀중한 삶의 자산이 되었다고 생각합니다. 무엇보다, 주위 사람들과 서로 소통하고, 의지 및 격려함으로써, 학위 과정을 무사히 마칠 수 있었고, 이에 대해 대단히 감사 드립니다.

다양한 경험들을 할 수 있도록 자리를 마련해주시고, 자유롭게 연구에 대해 끊임없이 토론할 수 있는 분위기를 마련해주신 저의 지도교수인 이흥노 교수님께 감사의 말씀을 드립니다. 교수님께서 말씀하신 3 가지 원칙 “읽고”, “생각하고”, “쓰고”은 귀중한 가르침이었습니다. 학위논문 심사위원을 맡아주신, 황의석 교수님, 신종원 교수님, 오승훈 박사님, Gonnguo Tang 교수님 모든 분들께 감사 드립니다. 또한 단순히 심사위원으로써 역할이 아닌 연장자로서 삶에서 나아가야 하는 방향을 제시해주신 황의석 교수님과 오승훈 박사님께 감사 드립니다.

학위과정 동안 함께한 INFONET 연구실 구성원들께 감사 말씀을 드립니다. 누구보다도 이용비형과 장환철형 그리고 우수길에게 감사 드립니다. 힘들 때마다 많은 조언을 해주었고, 여러 가지 고민을 들어주고, 같이 고민해준 고마운 사람들입니다. 다른 연구실 소속이지만 많은 경험을 같이 해주고 고민해준 강재욱형에게도 감사의 말씀을 드립니다. 이 외에도 연구실에서 졸업해서 나간 분들께 다시 한번 감사의 말씀을 드리고, 일일이 열거하지 못함에 대해 양해 부탁드립니다. 또한, 아직 박사 학위과정 중인 해웅이, 주성이, 재혁이, 철순이 모두 하루 빨리 좋은 결과를 얻어서 졸업하고 원하는 목표를 이룰 수 있었으면 좋겠습니다.

학위 과정 동안 응원해주신 아버지, 어머니, 누나, 매형 그리고 소현이에게도 고맙습니다. 이들의 지속적 지원과 헌신 없이는 무사히 학위 과정을 마칠 수가 없었을 것입니다. 다시 한번 감사의 말씀을 드리고 정직하고 원칙을 지키는 한 사람의 인간으로서 사회에서 활동을 할 것을 약속 드리겠습니다. 감사합니다.

2019 년 6 월 INFONET 연구실 박상준 드림